Étude
comparative

Les oreilles d’ Headgan ©

face à la recommandation ITU-T p.57 Type 3.3

BERNARD LAGNEL
Ingénieur du son Radio France

Août 2018

https://www.lesonbinaural.fr

« Headgar© »

Tour de tête : 53 cm

Photos Bernard Lagnel

Égalisation en champ diffus :

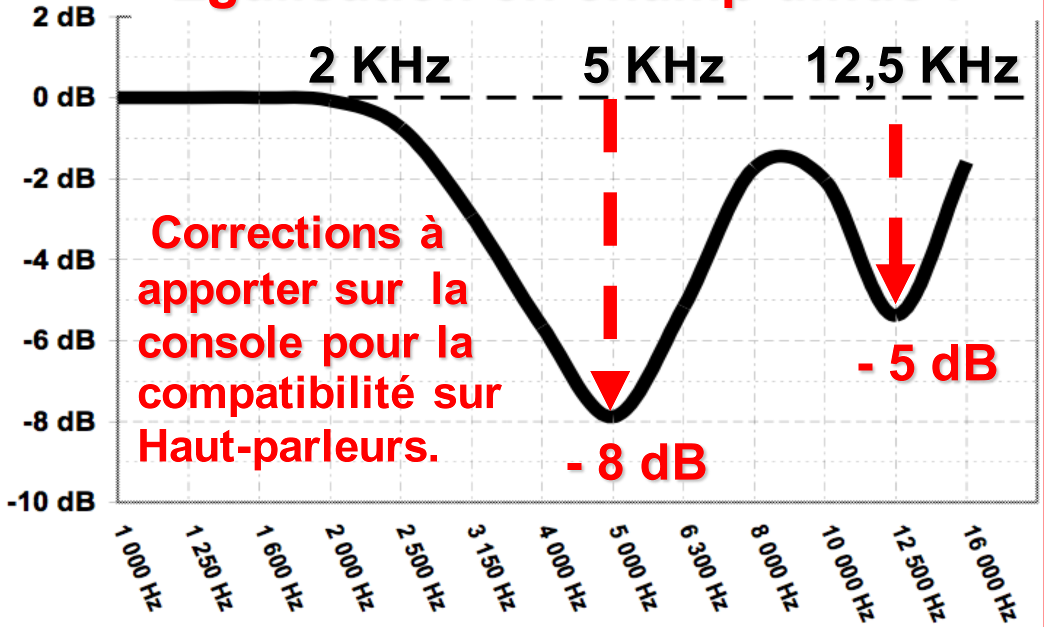

. **2** **Micros-Oreilles** →

. **1** **Genelec type 8020**

. **2** **DPA 4060** ***placés à l'entrée du conduit auditif et du Velcro…***

Note: ***la 8020 peut aussi servir de retour d'ordre !!***

POSE DU VELCRO SUR LA GENELEC TYPE 8020 :

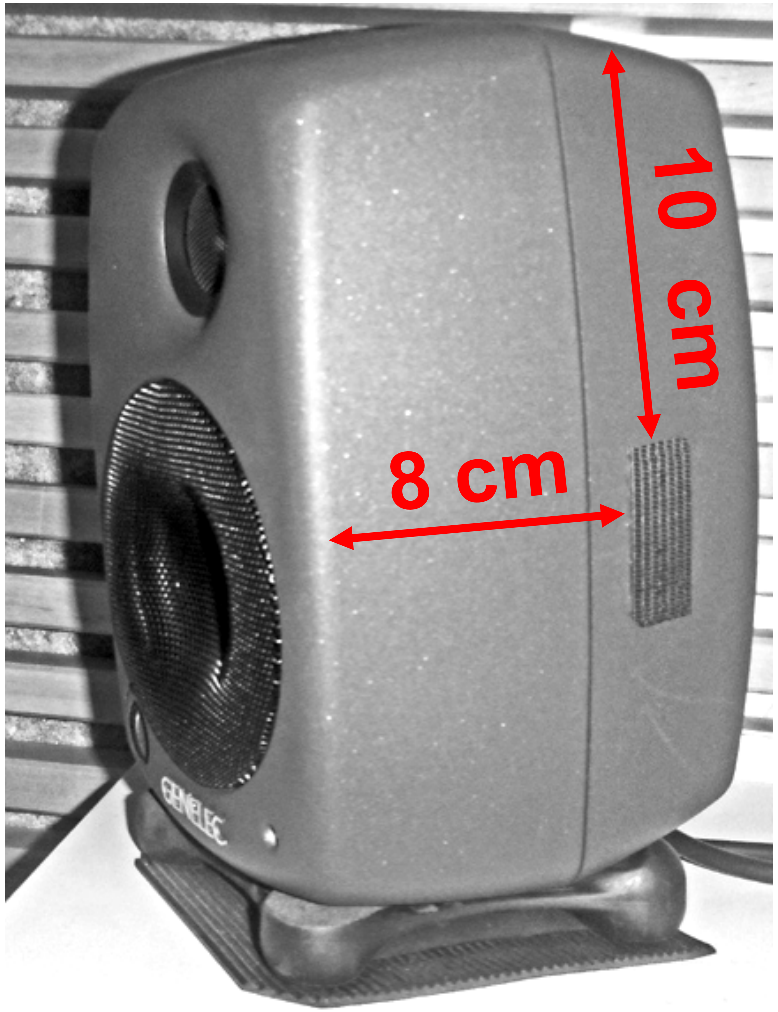

Photos Bernard Lagnel

Personnaliser vos enceintes en leurs rajoutant des Oreilles !!

La structure de la Genelec 8020 permet d'être suspendue et peut être revêtue d'un bas noir, pour plus de discrétion…

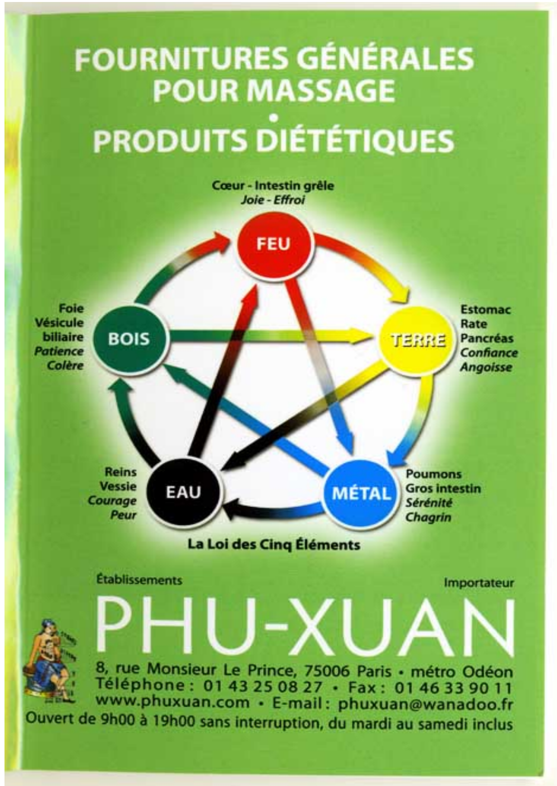

« Les Micros-Oreilles »

… à l'aide d'un modèle d'oreille <u>anthropométrique</u> pour auriculothérapeute !!

Chez :

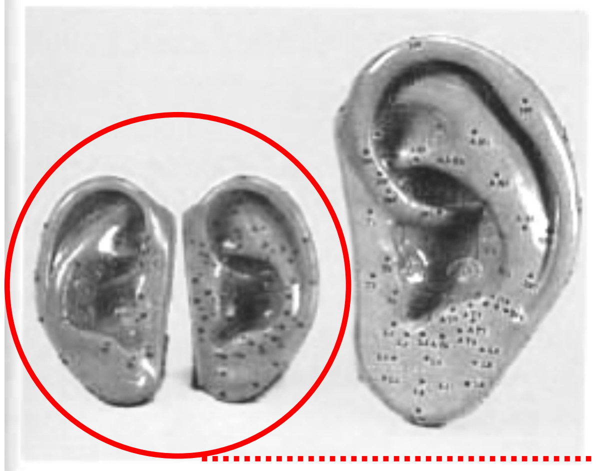

MODÈLES D'OREILLES AVEC LES POINTS D'ACUPUNCTURE

En matière plastique avec la nomenclature internationale et avec un fascicule indiquant les points d'acupuncture (anglais-chinois).

~~Grand modèle, en plastique dur : 12,5 x 7 cm. La pièce **9,90 €**.~~

Petit modèle, en plastique souple : 7,3 x 4 cm. La paire **7,90 €**.

BL 2012

Agrandir les trous et peindre à l'acrylique…

UNION INTERNATIONALE DES TÉLÉCOMMUNICATIONS

UIT-T

P.57

(08/96)

SECTEUR DE LA NORMALISATION
DES TÉLÉCOMMUNICATIONS
DE L'UIT

SÉRIE P: QUALITÉ DE TRANSMISSION TÉLÉPHONIQUE

Appareils de mesures objectives

Recommandation UIT-T P.57

(Antérieurement «Recommandation du CCITT»)

Oreilles artificielles

Type 3.3 – Simulateur de pavillon

L'oreille artificielle de type 3.3 est réalisée en ajoutant au prolongateur de conduit auditif le simulateur de pavillon décrit dans la Publication 959 de la CEI [6] (voir la Figure 7). Les points de la Figure 7b sont situés sur un axe vertical passant par le point d'entrée du canal auditif. La matière du simulateur de pavillon doit être un élastomère de haute qualité, de dureté Shore (A), mesurée en surface à 15 mm en avant de l'orifice du conduit auditif, normalement fixée à 25 ± 3 à 20°C ± 2°C (conformément à l'ISO 868).

Il est recommandé d'utiliser l'oreille artificielle de type 3.3 pour les mesures sur écouteurs supraconques qui, en raison de leur forme particulière, ne s'adaptent pas aux contours circulaires des oreilles artificielles de type 1 ou de type 3.2, selon le cas. Il convient également d'utiliser l'oreille artificielle de type 3.3 pour mesurer les écouteurs intraconques non destinés à reposer au bas de la conque.

La pression acoustique mesurée par l'oreille artificielle de type 3.3 est rapportée au point de référence tympan (DRP). La fonction de correction indiquée aux Tableaux 2a (mesures au 1/3 d'octave) ou 2b (mesures au 1/12 d'octave et mesures sinusoïdales) doit être utilisée pour rapporter les données au point de référence oreille (ERP), lorsqu'il est nécessaire de calculer les équivalents pour la sonie ou de vérifier les résultats par rapport à des spécifications fondées sur des mesures rapportées à l'ERP.

NOTES

1 Pour les calculs d'équivalent pour la sonie à la réception selon les indications de la Recommandation P.79, la correction d'affaiblissement au niveau de l'oreille réelle L_E est nulle.

2 La force d'application des pavillons rigides d'écouteur contre le simulateur de pavillon de type 3.3 doit être 10 fois plus importante que la force d'application en usage réel. Il est recommandé d'utiliser une force d'application de 10 à 20 N. La valeur de la force appliquée lors des mesures doit toujours être relevée.

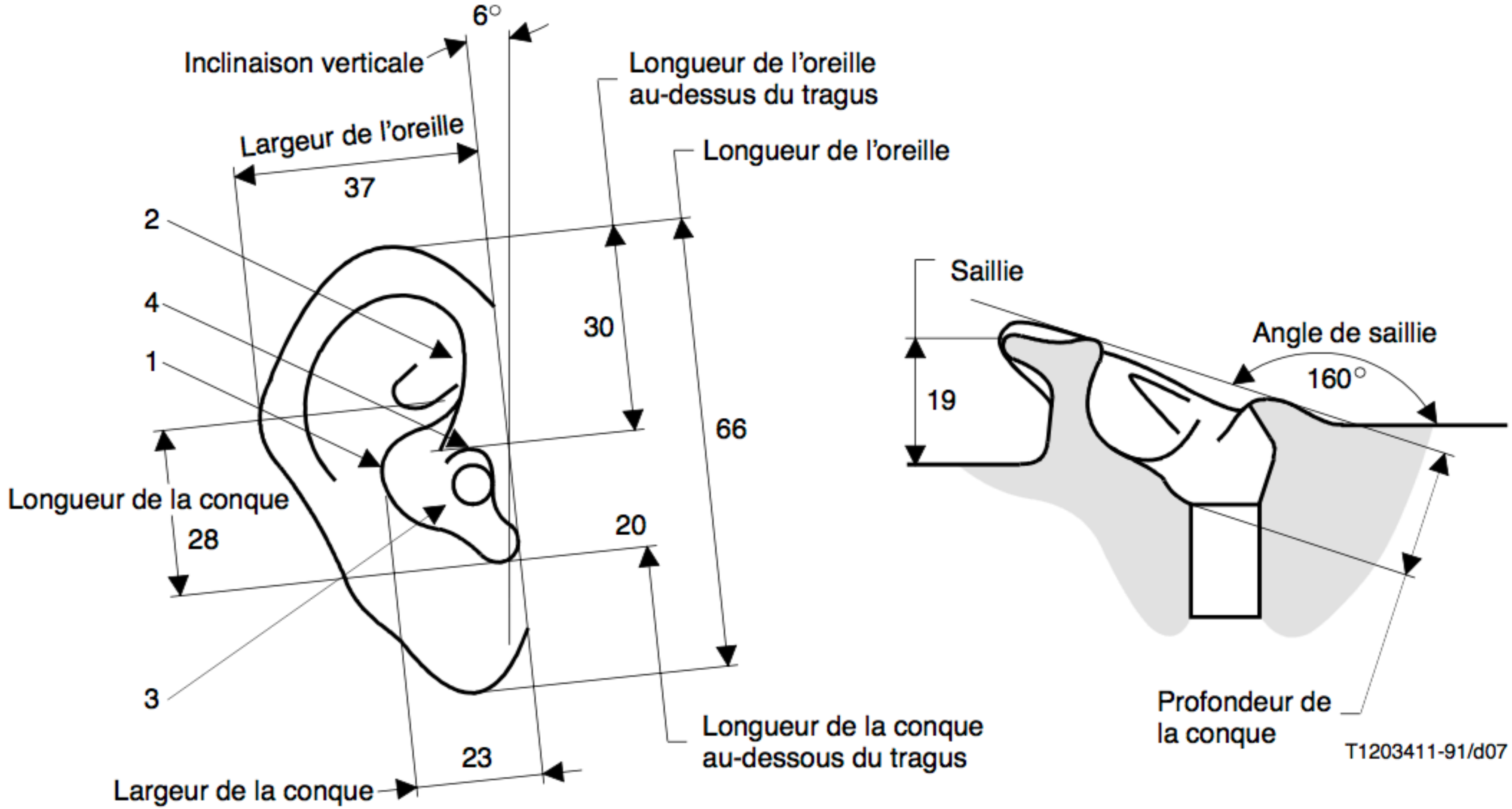

a) Vue de côté

b) Vue en coupe

1 Anthélix 2 Fossette naviculaire 3 Conque 4 Tragus

FIGURE 7a/P.57

Simulateur de pavillon de forme anatomique (échelle quelconque, en millimètres)

« Les Micros-Oreilles »

Vue de face, de l’oreille Gauche :

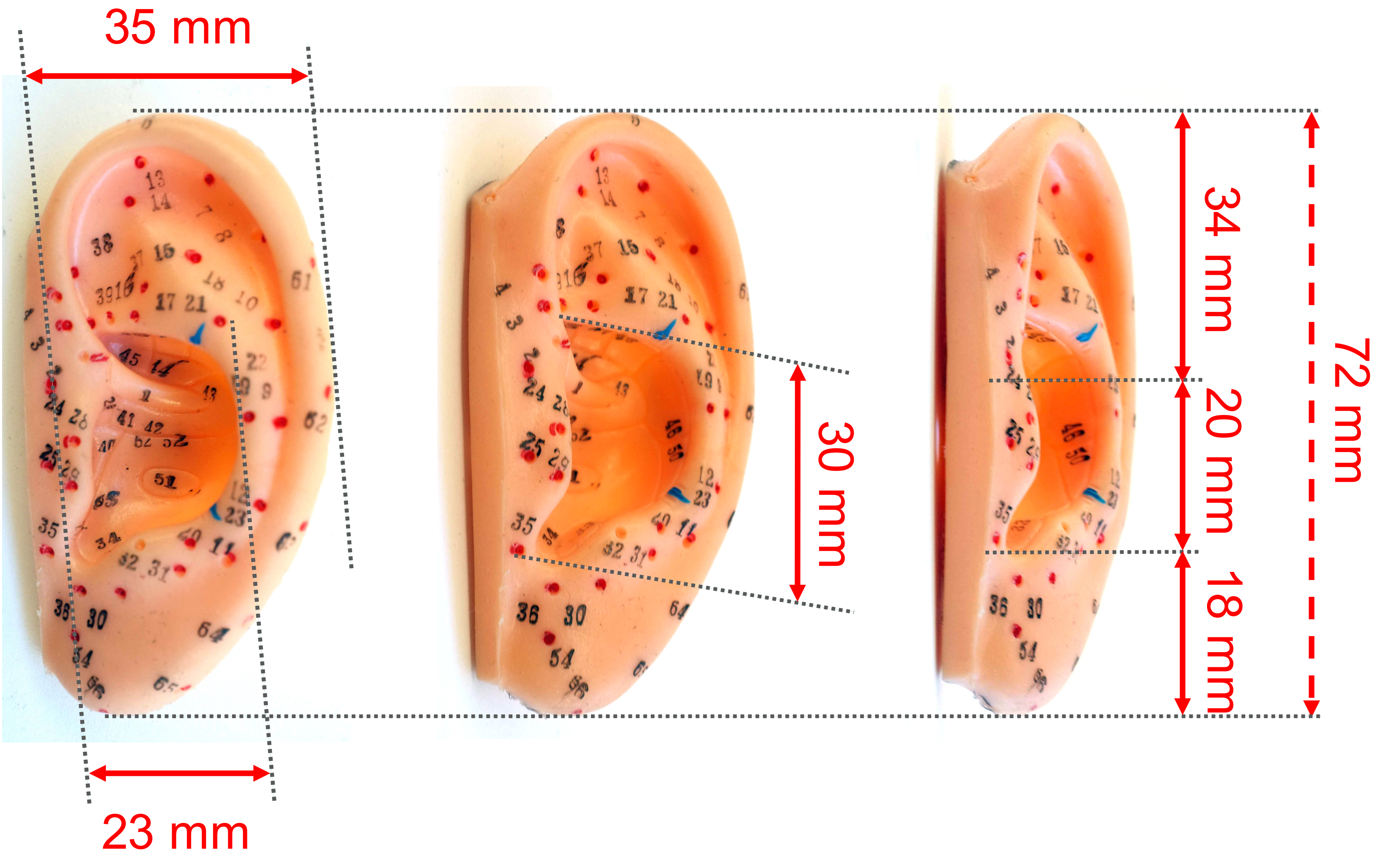

« Les Micros-Oreilles »

Vue de derrière et de côté, de l'oreille Gauche :

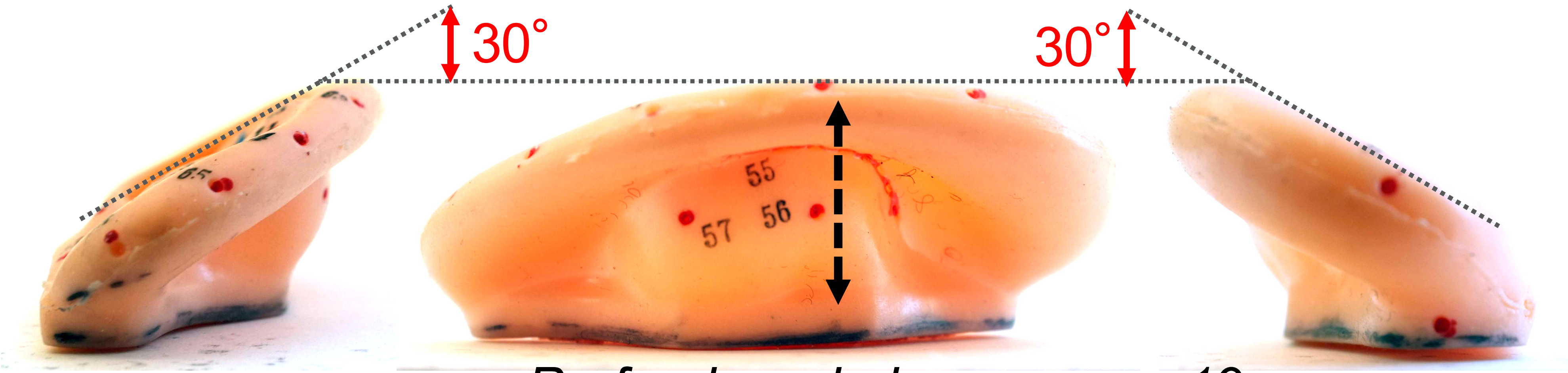

Profondeur de la conque = 19 mm

GENELEC 8020
Vue de dessus

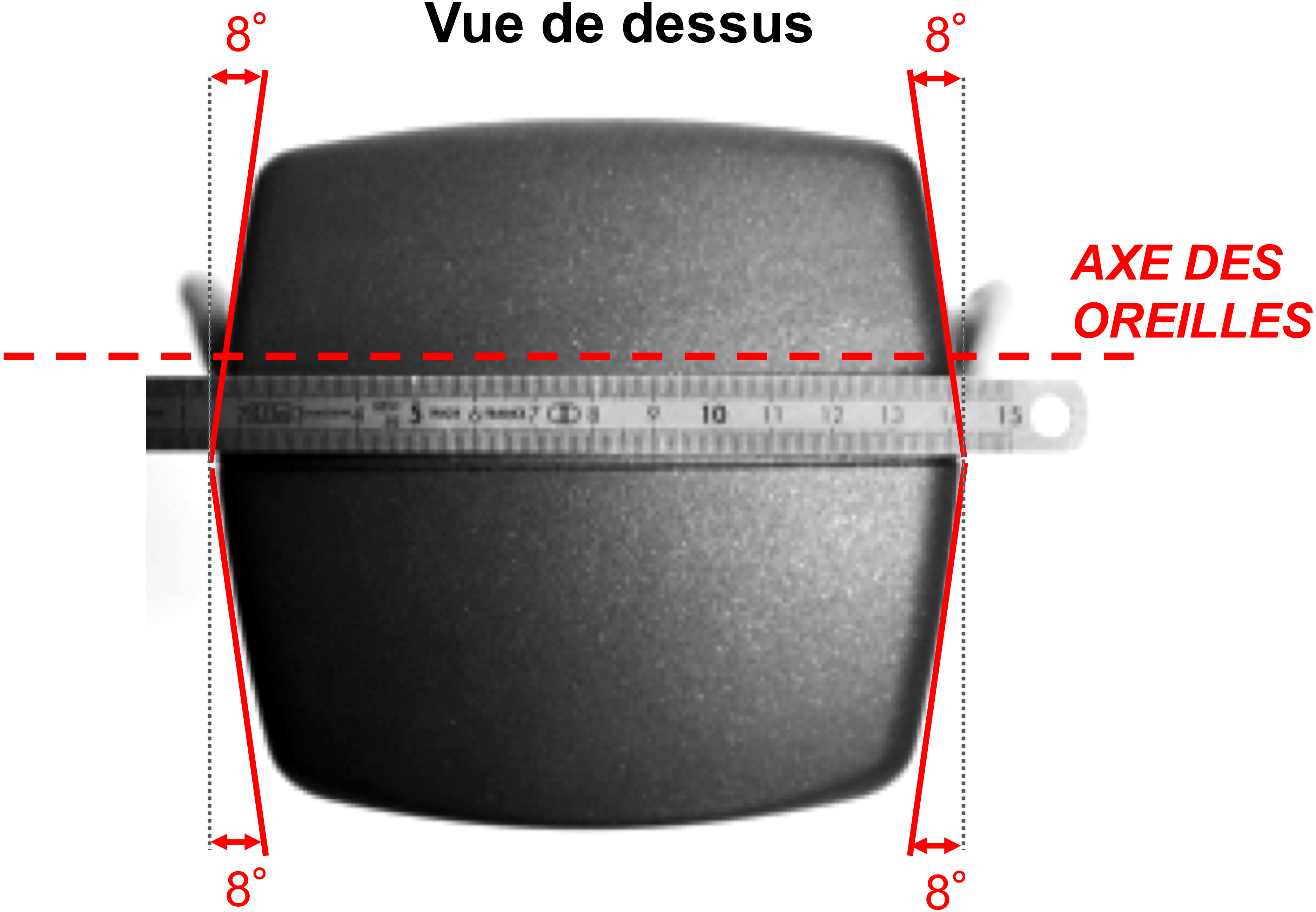

En 1972 : **Kemar** *(mannequin anthropométrique)*

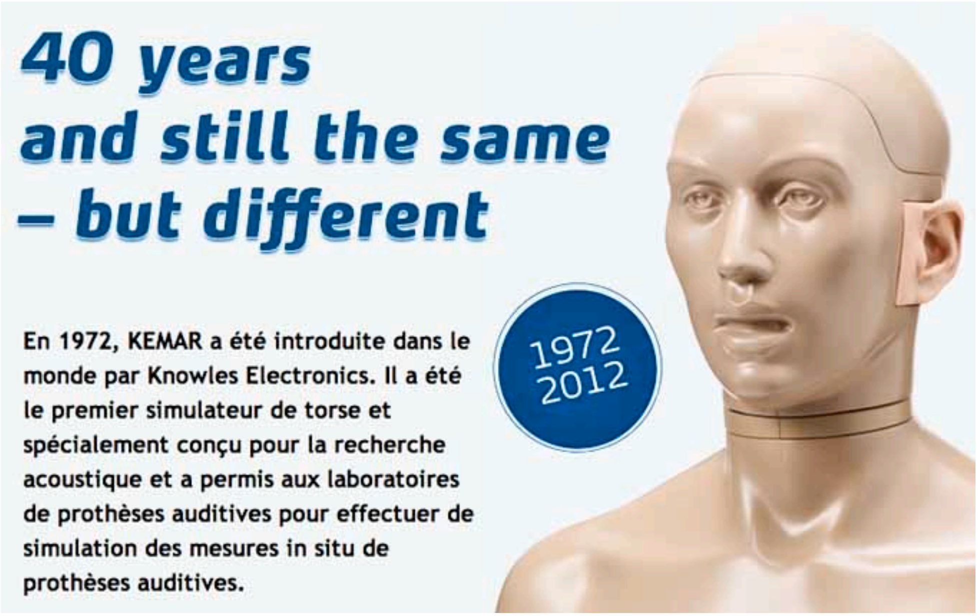

http://kemar.us/KEMAR_Book.pdf

MANIKIN MEASUREMENTS - KEMAR by *GRAS*

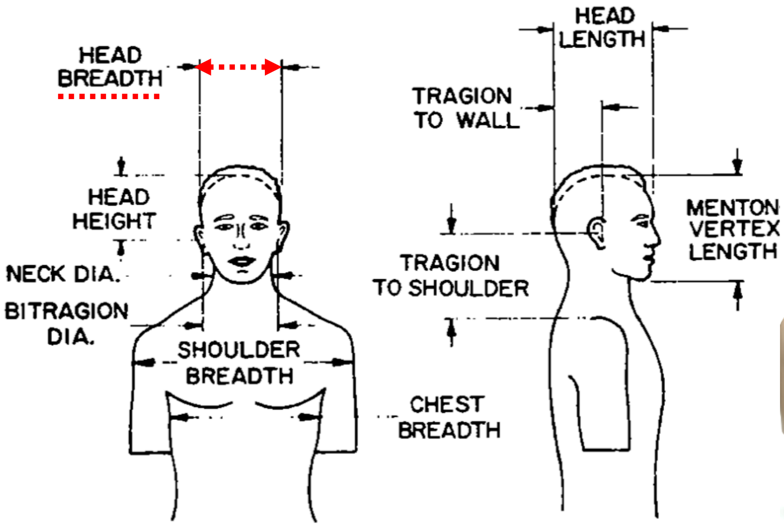

FIG. 1. Anthropometric measures used in design of KEMAR.

TABLE I. Dimensions for KEMAR and average human adults, in centimeters.

	Median male	Median female	Average human	KEMAR
Head breadth	15.5	14.7	15.1	15.2
Head length	19.6	18.0	18.8	19.1
Head height	13.0	13.0	13.0	12.5
Bitragion diameter	14.2	13.5	13.85	14.3
Tragion to wall	10.2	9.4	9.8	9.65
Tragion to shoulder	18.8	16.3	17.55	17.5[a]
Neck diameter	12.1	10.3	11.2	11.3
Shoulder breadth	45.5	39.9	42.7	44.0
Chest breadth	30.5	27.7	29.1	28.2
Menton vertex length	23.2	21.1	22.15	22.4

[a]Adjustable over ±1.27 cm.

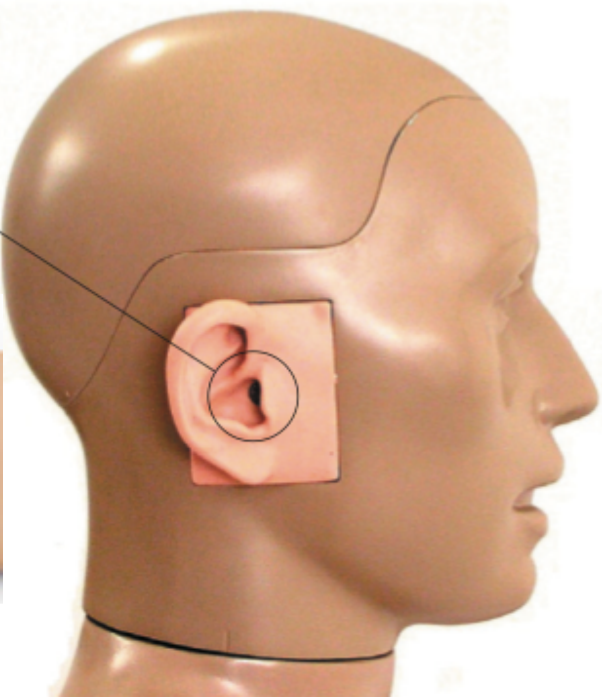

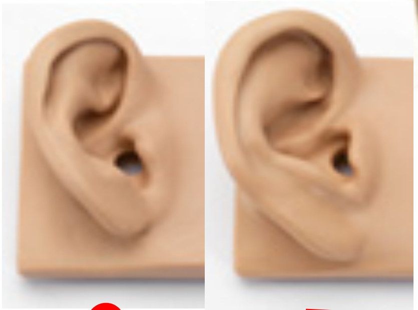

♀ ♂

Photos : www.gras.dk

GRAS Sound & Vibration

KEMAR Type 45BM

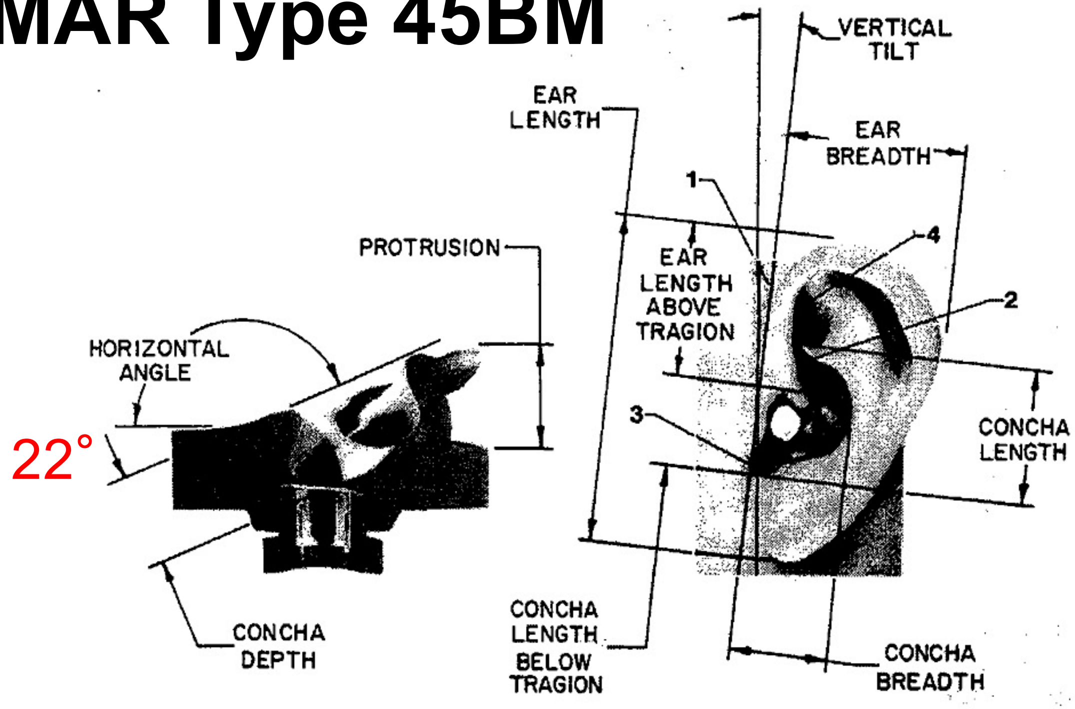

Dimension		Averages			Standard deviation						
		12 Male	12 Female	Overall	12 Male	12 Female	Overall	KEMAR	50% Male[a]	50% Female[a]	Average
Ear length	cm	6.85	6.24	6.55	0.59	0.38	0.58	5.89	6.35	5.84	6.10
Ear length above tragion	cm	3.30	3.07	3.19	0.41	0.20	0.34	2.7	3.04		
Ear breadth	cm	3.77	3.36	3.57	0.24	0.27	0.33	3.1	3.55	3.3	3.42
Ear protrusion	cm	2.28	2.03	2.16	0.22	0.23	0.26	1.85	2.10		
Ear protrusion angle	deg	156.7	155.1	155.9	8.6	9.7	9.0	158			
Vertical tilt front view[b]	deg	3.0	2.7	2.9	3.2	3.6	3.1	7			
Vertical tilt side view[b]	deg	7.6	4.7	6.2	2.8	3.4	2.8	6			
Concha volume	cm^3	4.65	3.94	4.30	0.76	0.81	0.85	4.0			
Concha length	cm	2.73	2.53	2.63	0.23	0.20	0.24	2.45			
Concha length, tragion to lower notch	cm	1.74	1.62	1.68	0.16	0.16	0.17	1.82			
Concha breadth	cm	1.88	1.72	1.80	0.21	0.21	0.22	1.57			
Concha breadth tragion to helix	cm	1.82	1.65	1.73	0.27	0.22	0.25	1.39			
Concha depth	cm	1.29	1.29	1.29	0.12	0.08	0.10	1.33			

[a]Dreyfus (1967).

[b]Four males and four females.

Dimensions externes de l'oreille

Oreille Gauche selon ***ITU-T P.57 Type 3.3***

Brüel & Kjær

Tête et torse Type 4128 c HATS

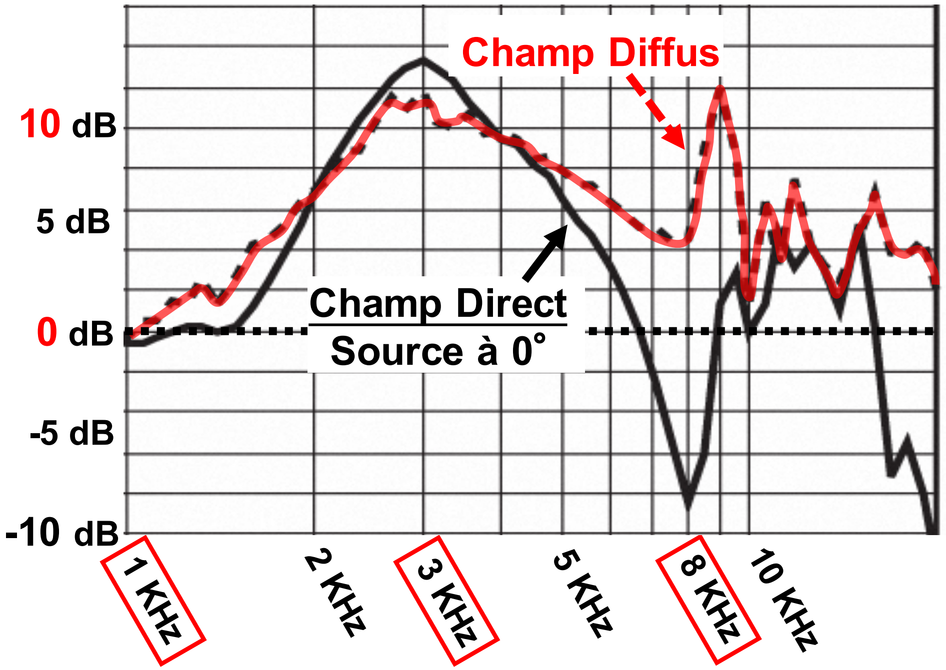

*Oreille Gauche selon **ITU-T P.57 Type 3.3***

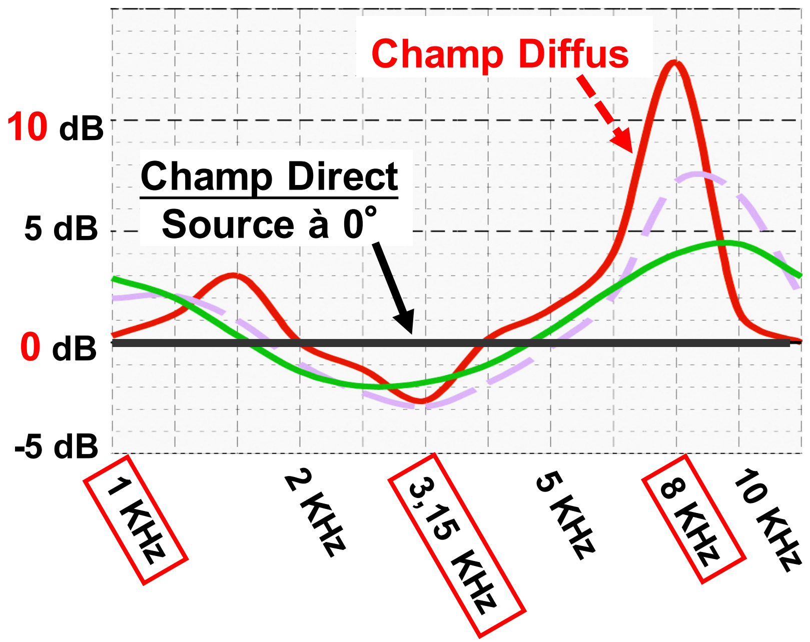

Différence en niveau entre le champ diffus et le champ direct à incidence frontale, pour la tête et torse B&K type 4128 c…

Différence en niveau entre le champ diffus et le champ direct à incidence frontale, pour les résultats polynomiaux…

Norme *ISO 454 de 1975*

« Relation entre les niveaux de pression acoustique de bandes étroites de bruit en champ diffus et en champ libre à incidence frontale pour des sonies égales. »

HEAD Acoustics HMS II.3

Oreille Droite selon ***ITU-T P.57 Type 3.3***
(forme anatomique)

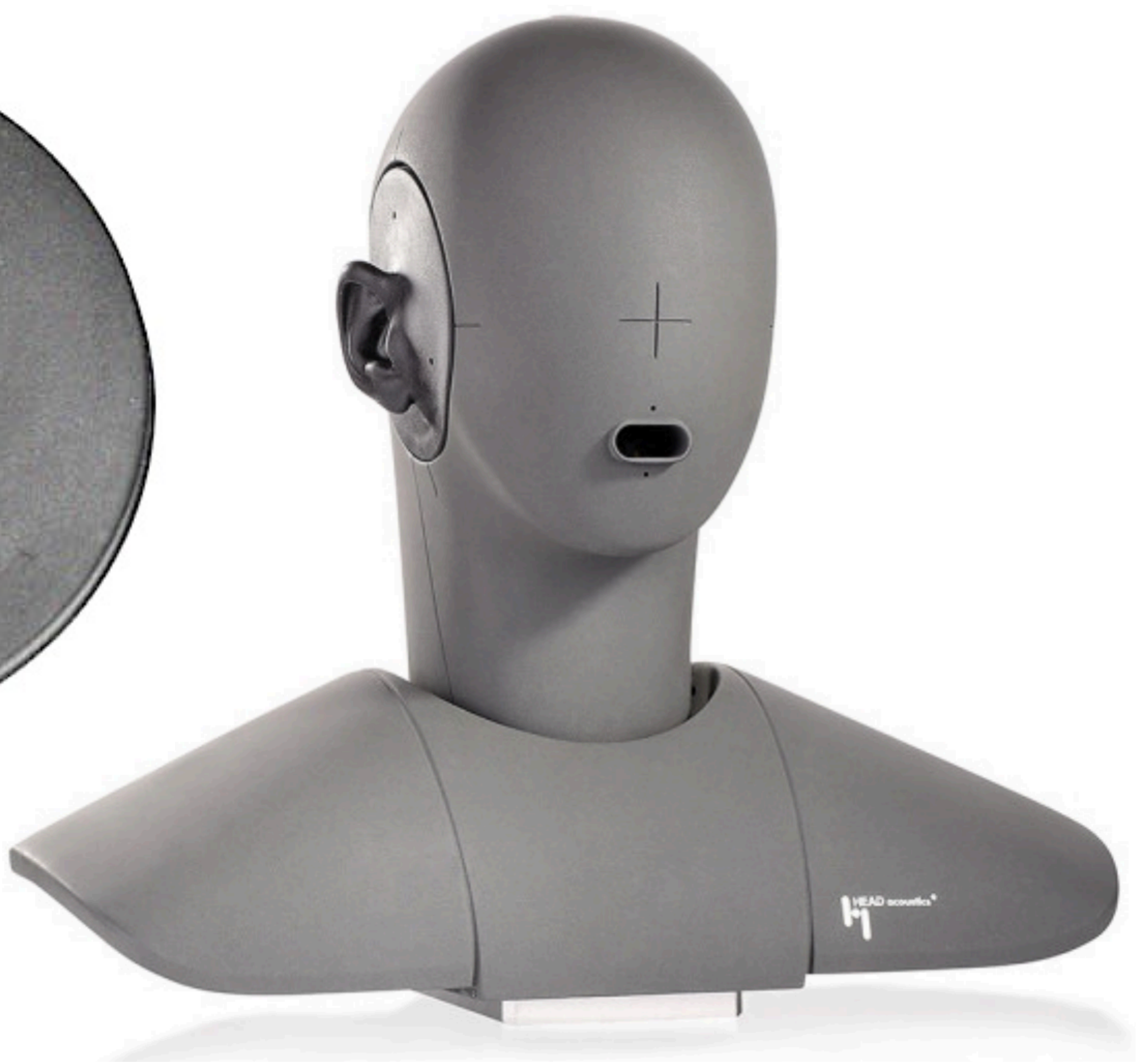

Measuring HRTFs of Brüel & Kjær Type 4128-C, G.R.A.S. KEMAR Type 45BM, and Head Acoustics HMS II.3 Head and Torso Simulators

Snaidero, Thomas; Jacobsen, Finn; Buchholz, Jörg

Publication date:
2011

HRTFs in the diffuse field

Figure 32 shows HRTF measurements in the diffuse field, for all manikins, made with pink noise. The solid curve represents the HRTF, while the dotted lines are tolerances set by ITU-T Rec. P.58[8]. All measurements and tolerances are shown in 1/3rd octave bands. The HRTFs are also an average of the five measured positions.

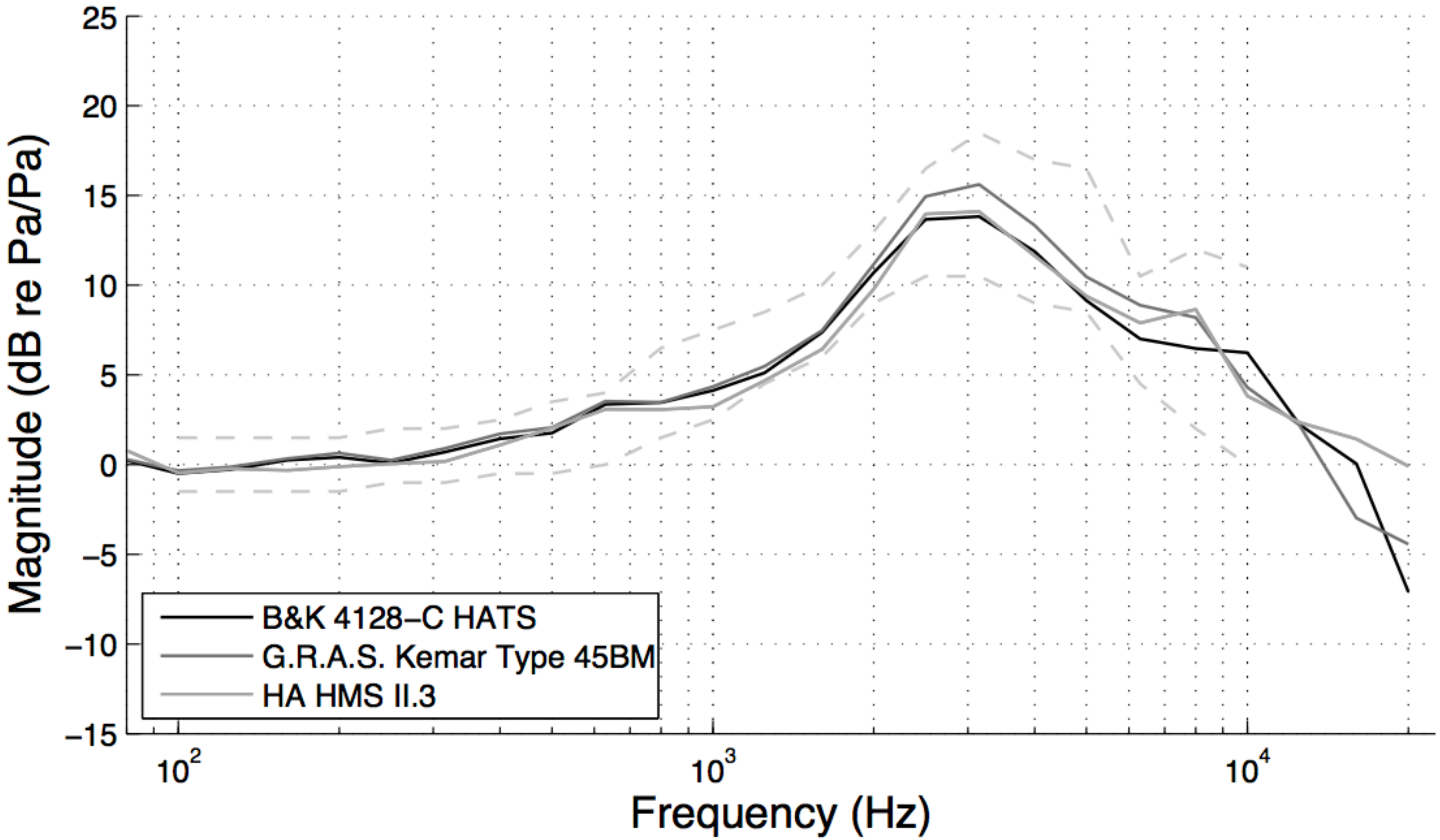

Average of five positions for diffuse-field HRTF. ITU-T Rec. P.58 Tolerances in dashed lines. Right ear is presented. 1/3rd octave bands.

All HATS presented in same plots

Results are shown from the sine sweep method, in 1/12th octave bands.

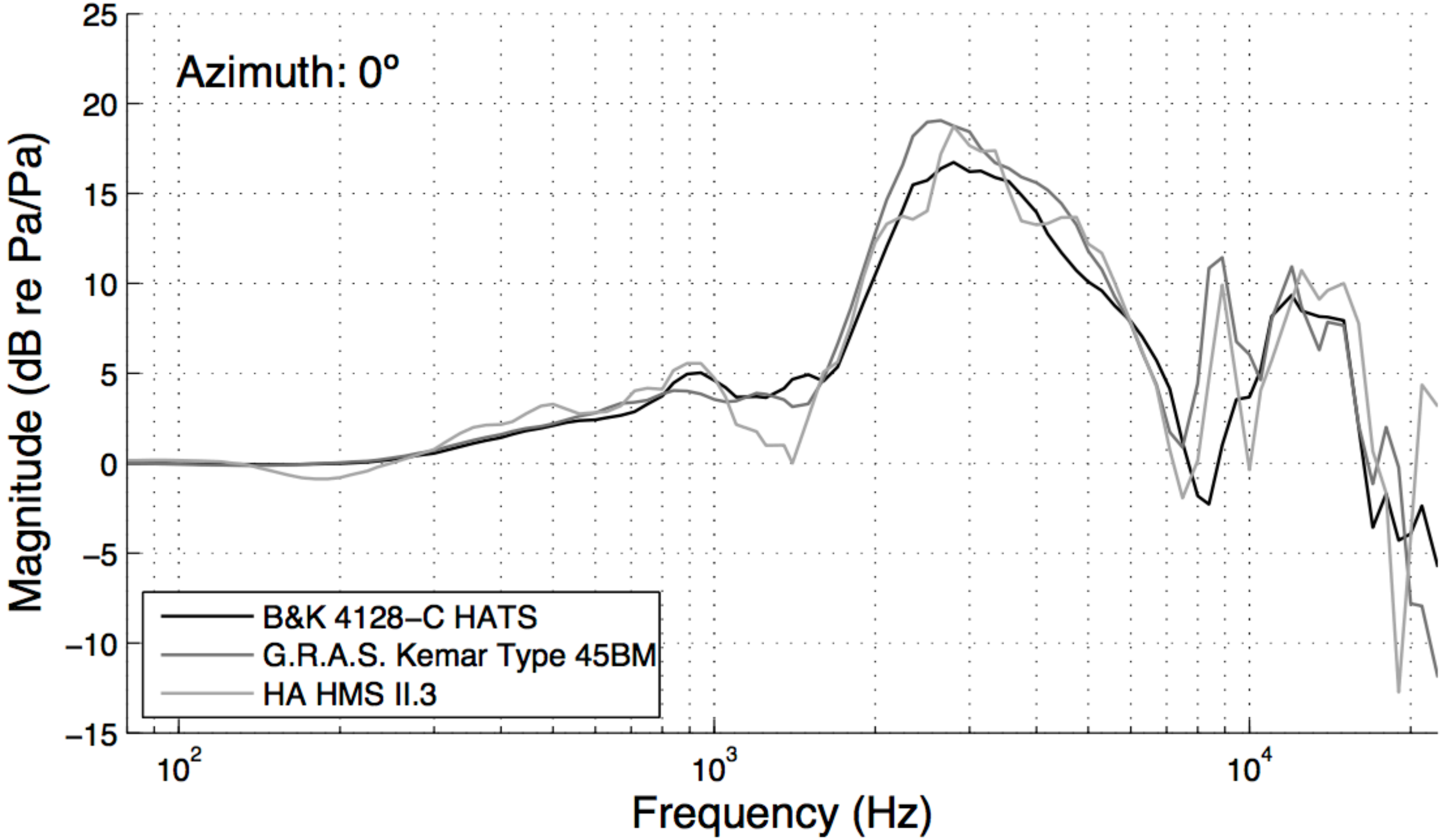

Free-field HRTF of all HATS at 0° azimuth. Left ear is presented.

PLUG-IN **KEMAR** du MIT Oreilles Larges

Oreille Ipsilatéral
Oreille Contralatéral

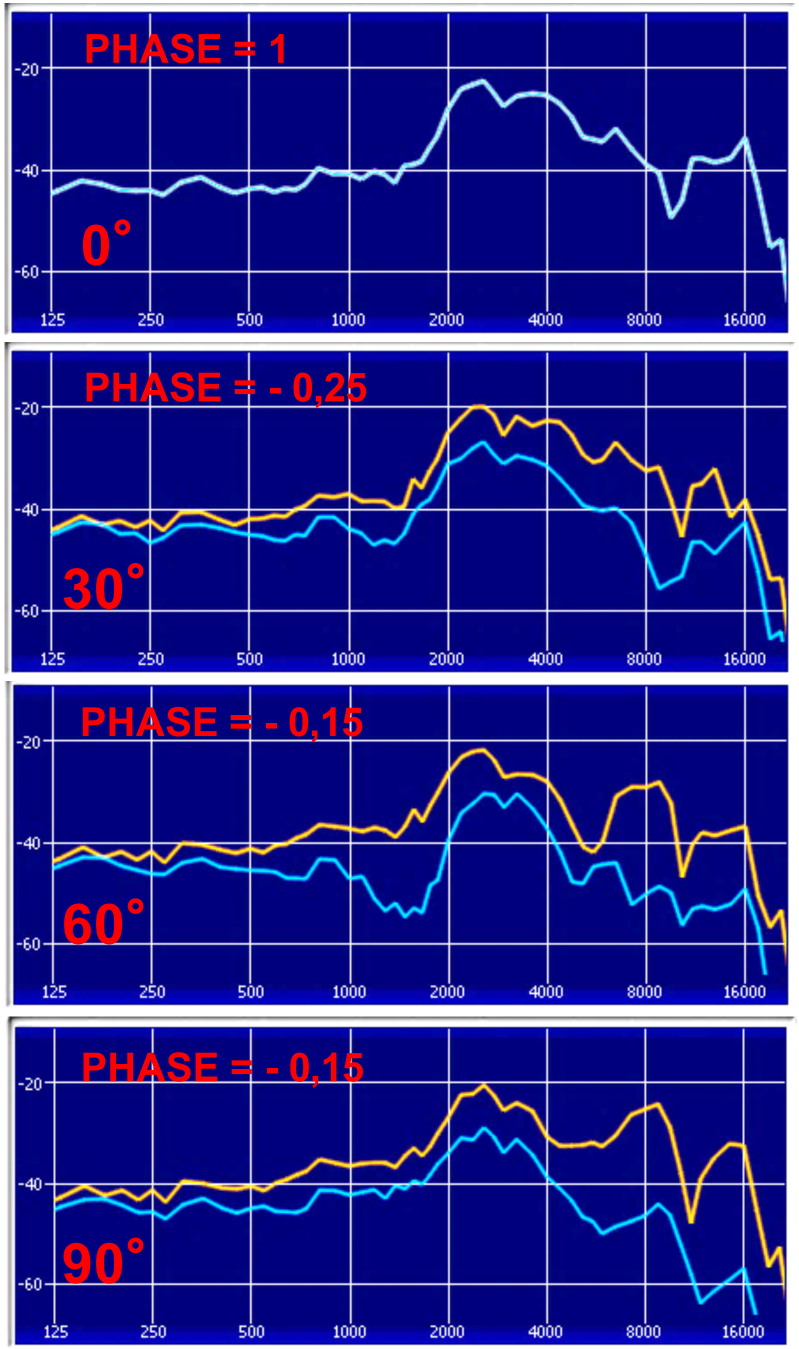

mit_kemar_large_pinna.sofa

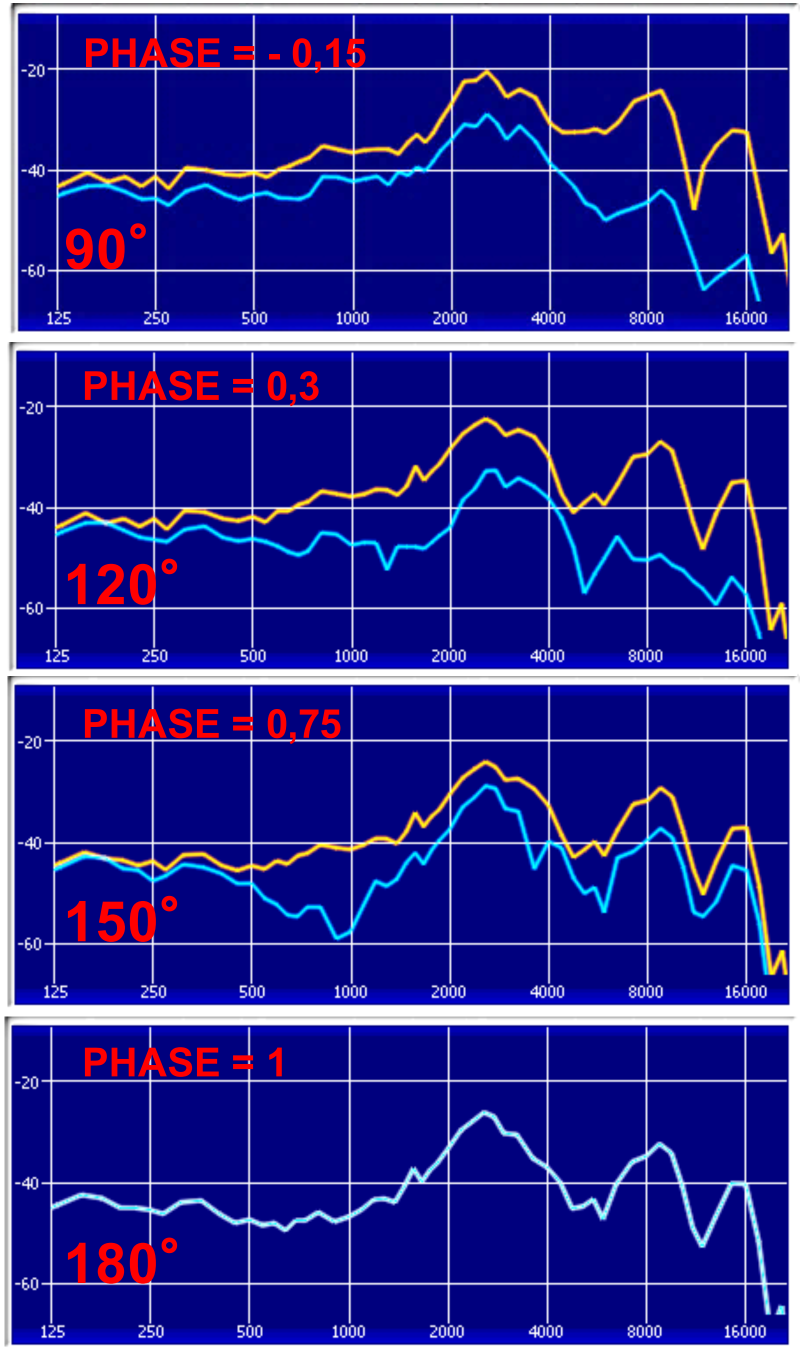

PLUG-IN **KEMAR** du MIT Oreilles Normales

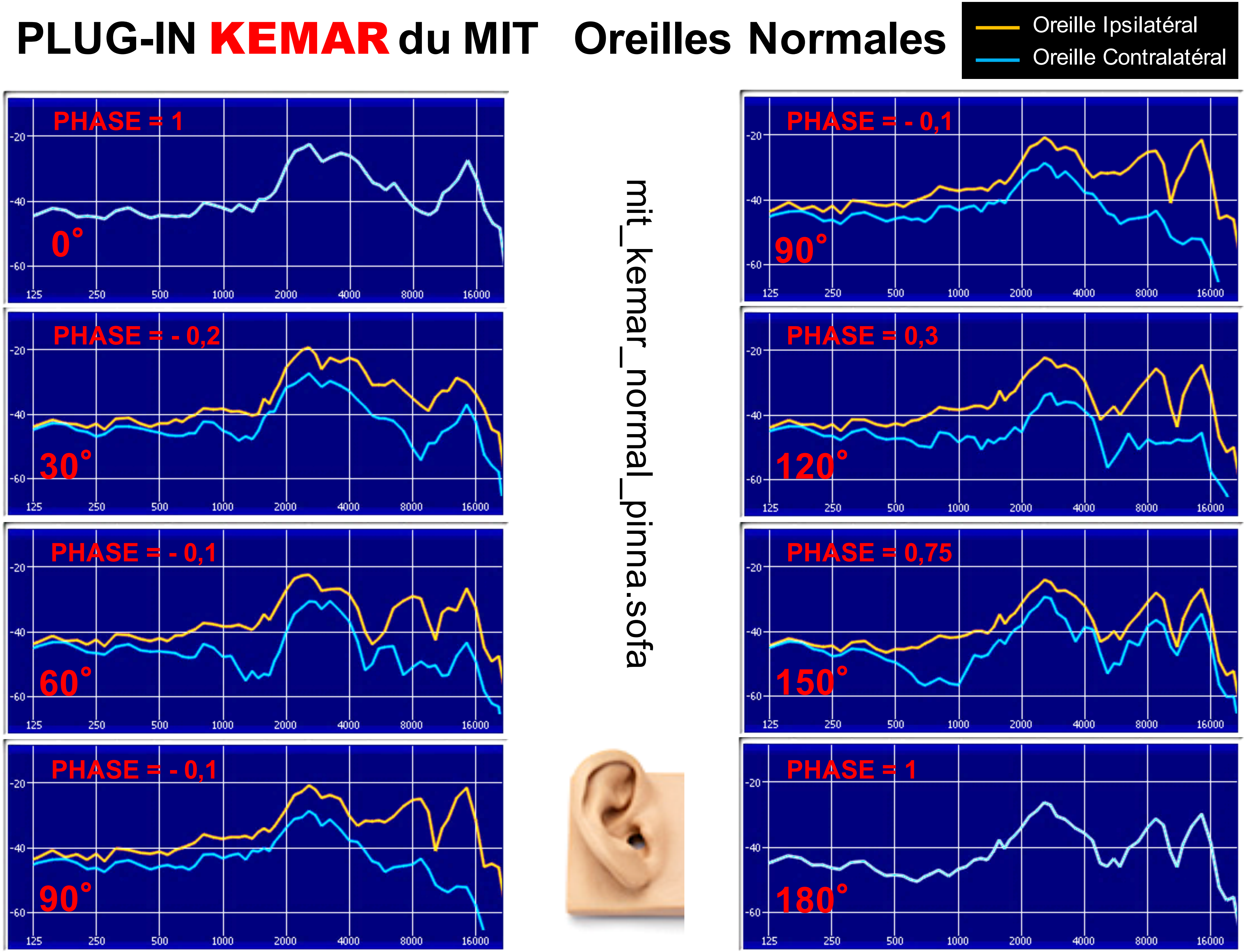

Technical University of Denmark

Measuring HRTFs of Brüel & Kjær Type 4128-C, G.R.A.S. KEMAR Type 45BM, and Head Acoustics HMS II.3 Head and Torso Simulators

Snaidero, Thomas; Jacobsen, Finn; Buchholz, Jörg

Publication date:
2011

Document Version
Publisher's PDF, also known as Version of record

Technical University of Denmark

Measuring HRTFs of Brüel & Kjær Type 4128-C, G.R.A.S. KEMAR Type 45BM, and Head Acoustics HMS II.3 Head and Torso Simulators

Author:

Thomas Snaidero
B.Eng. in Electrical Engineering
Technical University of Denmark

Co-authors:

Finn Jacobsen
DTU Electrical Engineering
Department of Electrical Engineering
Technical University of Denmark
DK-2800 Kgs. Lyngby
Denmark

Jörg Buchholz
National Acoustic Laboratories
126 Greville Street
Chatswood, NSW 2067
Australia

March 29, 2011

Contents

1 Introduction

The purpose of this project is to conduct a set of head related transfer function (HRTF) measurements on three head and torso simulators (HATS), namely Brüel & Kjær Type 4128-C HATS, G.R.A.S. KEMAR Type 45BM, and Head Acoustics HMS II.3.
With regards to standardization, the results will be compared to the current consensus, as per IEC 60318-7[1] for free-field measurements, and ITU-T Rec. P.58[8], for diffuse field measurements. Neither IEC 60318-7 nor ITU-T Rec. P.58 describe a method of deriving HRTFs from measurements, even though there can be differences in results dependent on the method and excitation signal used. The current standards also lack further specifications of the details of the diffuse field measurements, e.g. number of spatial locations to be used.
For free field measurements, some investigations show that a sine sweep can be a better excitation signal than random noise due to its immunity to non-linear distortion of the loudspeaker and the better signal-to-noise ratio in the resulting head related impulse responses (HRIR). The current study will present results of both noise and sine excitation in 1/12th or 1/3rd octave bands.
The aim of the report is primarily to describe the measurement setup and report the results of the HRTF measurements. In a later study, the different measurement methods will be more carefully examined and compared.
The measurements are made at the Technical University of Denmark. Four different azimuth angles are measured in an anechoic chamber for free-field conditions, and diffuse-field measurements are made at five different positions in a reverberation chamber.

1.1 A note about head related transfer functions

A head related transfer function is a function that describes how a signal is filtered by diffraction, scattering and reflection of the head, pinna, and torso before it reaches the eardrum. To determine the sound pressure at the eardrum that an arbitrary source $x(t)$ produces, the impulse response $h(t)$ from the source to the eardrum is needed. It is called the head related impulse response (HRIR), and its Fourier transform H(f) is the HRTF. A method to obtain the HRTF from a source location is to measure the impulse response $h(t)$ at the eardrum, and at the center the listener's head (with the listener absent), for the impulse $\Delta(t)$, of the sound source.

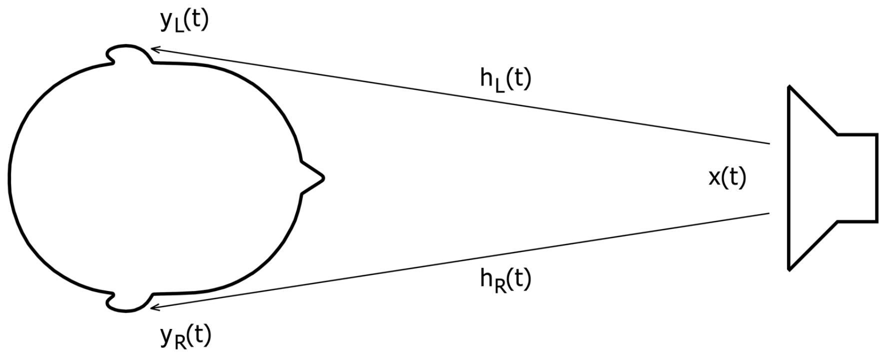

Figure 1: *The filtering of a sound source x(t) through h(t) resulting in the impulse responses at the eardrum of both ears y(t)*

A model of the transmission from a free sound field to the ear canal is described by Møller et al. [7]. The HRTF can be calculated using eq. 1, consisting of the sound transmission from the free-field sound pressure P_1 at the center of head, but with the listener absent, to the sound pressure P_2 at the eardrum.

$$\frac{P_2(\phi, \theta, f)}{P_1(f)} = \frac{sound\ pressure\ at\ eardrum\ reference\ point}{sound\ pressure\ at\ the\ HATS\ reference\ point} \tag{1}$$

The ϕ and θ parameters are elevation and azimuth angles respectively. The eardrum reference point (DRP), and the HATS reference point (HRP, sound pressure at the center of head) are defined by ITU-T Rec. P.58[8].

1.2 Impulse response function measurements

Any linear, time-invariant system can be described by the impulse response, and the Fourier transform of the latter. They describe the linear transmission properties of the system. A signal that is fed to the input of the system is convolved with the system's impulse response. Figure 2 shows how a room can be seen as a single-input, single-output linear time-invariant (LTI) system where $h(t)$ is the impulse response, driven by an input signal $x(t)$ and producing the output signal $y(t)$. The estimation of $h(t)$ can be made, given the input/output signals $x(t)$ and $y(t)$ are known.

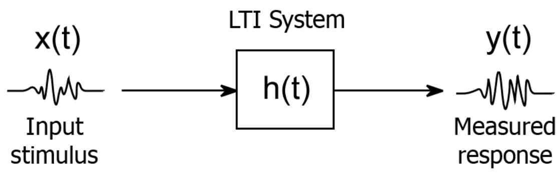

Figure 2: *Linear system to be measured*

This corresponds to multiplying the signal's spectrum with the system's complex transfer function:

$$y(f) = h(f) \cdot x(f) \tag{2}$$

Therefore, to obtain the transfer function, equation 2 can be used by dividing the output spectrum of the system by the input spectrum:

$$h(f) = \frac{Y(f)}{X(f)} \tag{3}$$

where $X(f)$ and $Y(f)$ are the Fourier transforms of the input and output signals.

1.2.1 Excitation signals

To determine the impulse response of an LTI system, one has to use an excitation signal that contains enough energy at all frequencies of interest, to overcome the noise floor, and to achieve a sufficient SNR in the entire spectrum. Random noise, or a logarithmic sine sweep are examples of such signals. But in measurements using noise as the excitation signal, distortion which occurs mainly in the electro-mechanical transducer spreads out over the deconvolved impulse response [9]. It is possible to reduce the effect of distortion by using longer excitation signals with lower level, but this reduces the signal-to-noise-ratio, contaminating the results.

A study by Swen Müller et al. from 2001 [9] has shown that transfer function measurement done with a swept sine wave has a significant number of advantages over other techniques. It allows feeding the device under test with a louder signal, while staying relatively tolerant of time variance and distortion. This has the consequence of increasing the dynamic range of the measurement, i.e. reducing the SNR.

The mathematical description of the sine sweep is given as:

$$x(t) = sin\left[\frac{\omega_1 \cdot T}{ln\left(\frac{\omega_2}{\omega_1}\right)} \cdot \left(e^{\frac{t}{T} * ln\left(\frac{\omega_2}{\omega_1}\right)} - 1\right)\right] \tag{4}$$

where ω_1 is the start frequency, ω_2 the end frequency, and the length of the signal being T seconds. The sweep described here is also exponential, which means that the frequency is increasing a certain amount of decades per second. A property of $x(n)$ shows that the time delay Δt_N between any sample n_0 and a later point with instantaneous frequency N times larger than the instantaneous frequency at $x(n_0)$ is constant:

$$\Delta t_n = T\frac{ln(N)}{ln\frac{\omega_2}{\omega_1}} \tag{5}$$

In other words, Δt_N ensures that each harmonic order will always be at a specific time lead from the linear response, the linear contribution to the response is therefore proportional to $h(n)$, and can be separated from the other nonlinear terms [4].

2 Materials and Methods

This section describes all the steps of the experiment used to measure HRTFs on the manikins. The following equipment was at disposal:

- Brüel & Kjær Type 4128-C HATS model nr. 1 (year model 2010)
- Brüel & Kjær Type 4128-C HATS model nr. 2 (year model 2009)
- Two sets of Type DZ-9769 and DZ-9770 pinnae, shore OO hardness 35, for the Brüel & Kjær HATS
- G.R.A.S. KEMAR Type 45BM with Type KB0065 and KB0066 pinnae (year model 2010)
- Head Acoustics HMS II.3 with Right/Left Pinna according to ITU-T P.57 Type 3.3, anatomically shaped, shore OO hardness 35 (year model 2011)
- Brüel & Kjær 4192 Pressure-field microphone
- Four Brüel & Kjær 4938 Pressure-field microphones mounted as an array, each microphone 15 cm from the center
- Brüel & Kjær 2692-C 4-channel NEXUS Conditioning Amplifier
- Computer running Brüel & Kjær PULSE Data Recorder Type 7701
- Vifa PL11MH09-08 loudspeaker driver mounted on a rigid plastic ball (Ø = 20 cm)
- Tannoy Power-V active loudspeaker
- Brüel & Kjær WB-1463 Controllable motor
- Brüel & Kjær WB-1477 Motion Controller Unit
- Brüel & Kjær Type 2716-C Measuring power amplifier
- Brüel & Kjær Type 4228 Pistonphone
- A plumb line for positioning
- A laser projecting a line
- Two lasers projecting a dot
- Sound absorbing material
- Various BNC and Lemo cables

2.1 Free-field measurements

2.1.1 P_2 measurement at eardrum reference point DRP

The free-field measurements were made in DTU's large anechoic chamber, having a free space of about $1000m^3$ and a lower limiting frequency of about 50 Hz[6]. Prior to the measurements, it was verified that the atmospheric conditions of ambient pressure, temperature and relative humidity was within the tolerances specified in sec. 5 of IEC 60318-7[1]. Four different azimuth angles (0°, 90°, 180° and 270°) were measured for each manikin.

A manikin was mounted vertically on a pole, and connected to a controllable motor. The motor was able to rotate the dummy-head 360° around itself, and was therefore used to rotate counterclockwise to a desired azimuth angle. The measurements were controlled outside of the anechoic chamber in a control room, in order to reduce noise and reflections. A computer running PULSE was connected to the motion controller unit, to which the motor had to be connected to in order to run. The dummy head's microphones where connected to the PULSE Data Recorder through the B&K 4-channel NEXUS Conditioning Amplifier. PULSE was used to generate a stimulus, record the sound from the dummy head, control its rotation, and trigger the measurement itself. It was initially set to produce random noise with a frequency span of 20 Hz to 25.6 kHz at an amplitude of 1 Vrms, and the sampling frequency for the recording was set to 65.535 kHz. The signal was fed into the power amplifier, which was set to a gain of 18 dB, and routed further to the loudspeaker, which was placed 2 m away from the center of head (center of head reference, from IEC-959[2]). Before measurement of each manikin, both microphones in the ears were calibrated using PULSE and the Brüel & Kjær Type 4228 Pistonphone. Measurements were also carried out using a 16 seconds long swept sine, going from 20 Hz to 25.6 kHz at an amplitude of 5 Vrms, for later comparison. The excitation signals were also equalized to compensate for the frequency response of the loudspeaker having lower energy below 200 Hz and above 10 kHz, in order to improve the SNR at these frequencies.

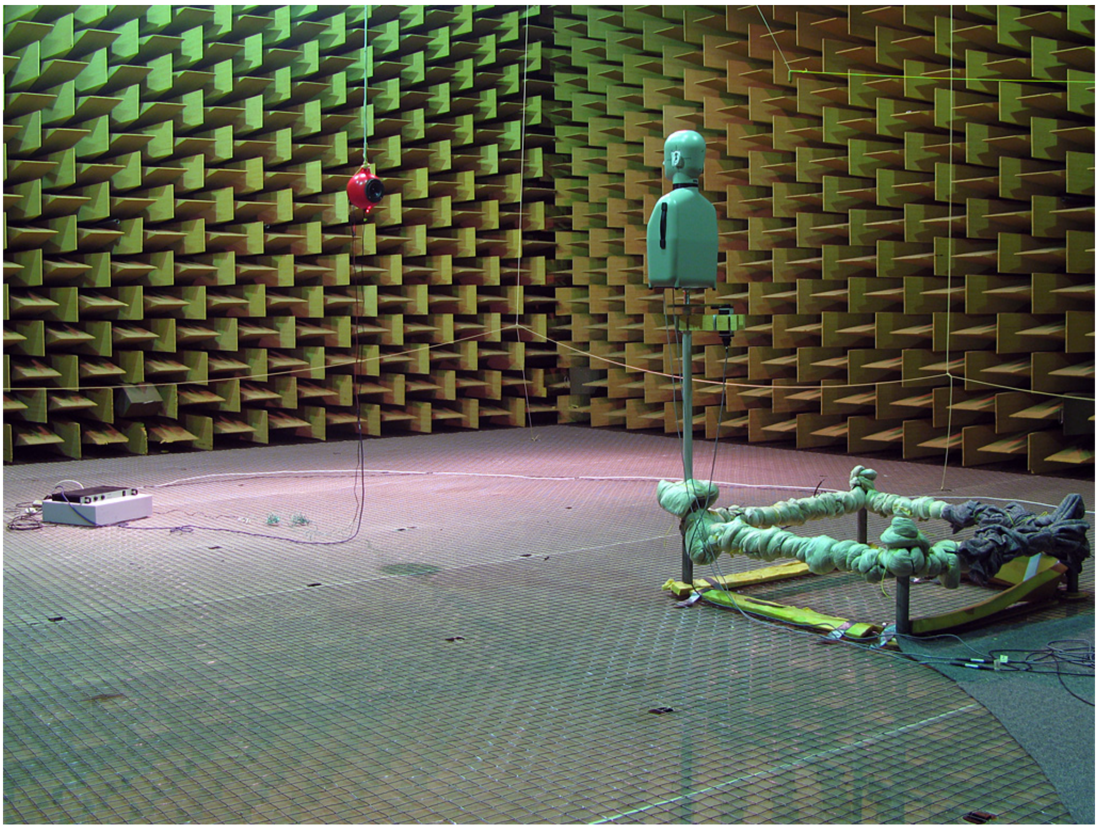

Figure 3: *Brüel & Kjær Type 4128-C HATS model nr. 1 positioned in the anechoic chamber.*

In order for the manikin to rotate precisely around its axle, a plumb-line was hung over the head (shown on figure 42). The manikin was later rotated and adjusted, so that the plumb-line would remain at the center of the head. A laser projecting a line vertically onto the manikin's head was placed on top of the loudspeaker, in order for the loudspeaker to point directly to the manikin. For the manikin to always point exactly towards the loudspeaker, a test measurement was done. The alignment between the HATS and the loudspeaker was achieved by rotating the HATS until the impulse responses of both ears aligned in time when the loudspeaker was positioned in the frontal direction (0°). Figure 3 shows the setup in the anechoic chamber.

2.1.2 P_1 measurement at HATS reference point (HRP)

The dummy head and its stand was replaced with the Brüel & Kjær Type 4192 free-field microphone, with the diaphragm positioned where the center of head was. The plumb-line could be used again for precisely placing the microphone's diaphragm at the correct distance. The laser on the loudspeaker was used to point directly at the microphone's diaphragm, in order to help adjusting the position. The microphone was subjected to the same measurement stimuli as the manikins.

2.2 Diffuse-field measurements

The diffuse-field measurements were made in one of DTU's reverberation chambers ("room 005"), at five different positions in the room, i.e., HRTFs for each manikin were measured for each position. Prior to the measurements, it was verified that the atmospheric conditions of ambient pressure, temperature and relative humidity was within the tolerances specified in sec. 5 of IEC 60318-7[1]. The manikins were all placed at the same position in the room, while the loudspeaker was moved to the different positions. The room's dimensions are 7,85 m x 6,25 m x 4,95 m (length, width, height)[6]. Figure 4 shows the position in the reverberation chamber where the loudspeaker was placed.

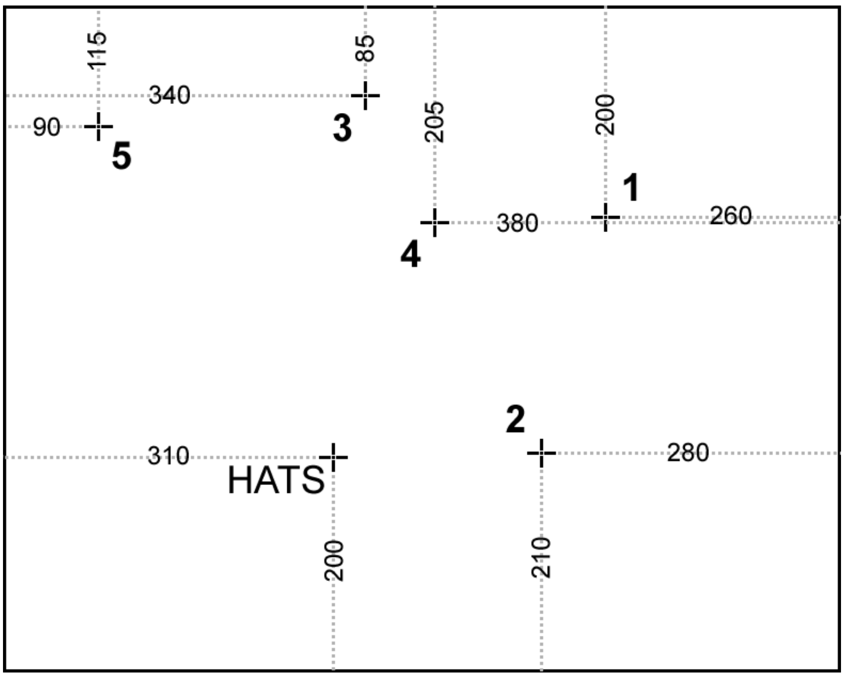

Figure 4: *The five measurement positions in the reverberation chamber.*

The same type of noise measurement as in the anechoic chamber was made, but this time using the Tannoy active loudspeaker as the sound source, and using only pink noise. When positioning each manikin in the room, three lasers were used in order to keep the position of the center of head consistent. As one monaural measurement was made for each position, each manikin's center of head had to be placed at the same spot. Two lasers were pointing at both ears, and

the line laser was pointing vertically along the manikin's head, in order to keep the same looking direction each time. Figure 5 shows the Brüel & Kjær Type 4128-C HATS model nr. 1 along with the sound source and the line laser.
For each position, the sound field was also measured in order to verify that it was diffuse according to ISO-4869-1[3]. With the manikin absent, the array with four Brüel & Kjær 4938 Pressure-field microphones was placed in such a way that the center of the array was at the center of the manikin's head. The frequency response from each microphone should not deviate more than 2,5 dB from each other, at each center frequency in 1/3rd octave bands, according to ISO-4869-1.

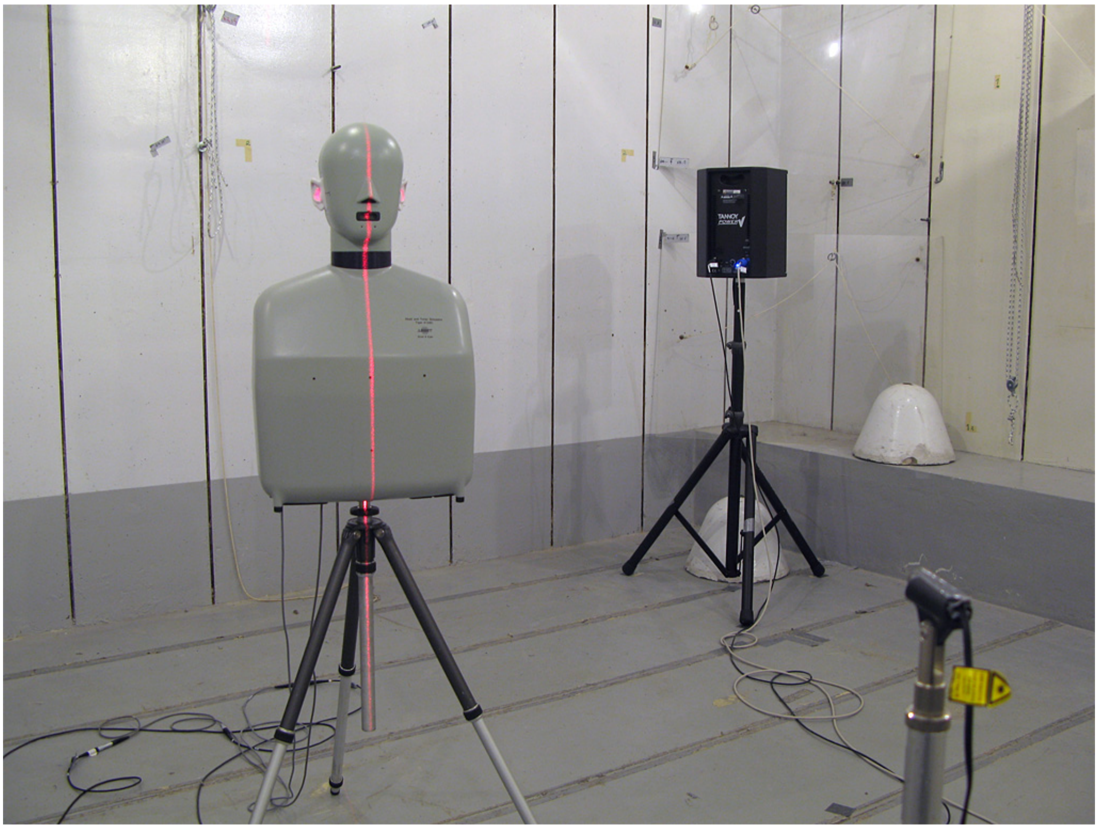

Figure 5: *Brüel & Kjær Type 4128-C HATS model nr. 1 positioned in the reverberation chamber.*

2.3 Calculating the HRTFs

Calculation of the HRTFs was done using MATLAB to process the raw recordings. Instead of directly using P_1 and P_2, the frequency response functions were calculated between the recorded pressure signals and the voltage input to the loudspeaker. The derived frequency responses substituted P_1 and P_2 in Eq. 1 in order to calculate the corresponding HRTF. The HRTF is then converted to Head Related Impulse Response function (HRIR) by taking the inverse FFT. A time window of 784 samples corresponding to 12 ms was applied to the HRIR in order to remove the possible effect of reflections in the measurement setup, in the anechoic chamber. The nature of the diffuse field measurement makes it unnecessary to apply a window, as P_1 and P_2 consist of sound reflected many times in the room. The final HRTF was calculated by doing an FFT of the windowed HRIR and subsequently applying a 1/12th or 1/3rd octave synthesis. The latter was calculated by taking the mean of all values in between a specified frequency band. As all the raw recordings were maintained, further processing of the data is possible.

3 Results

3.1 Verification of the sound field in the reverberation chamber

Figure 6 shows measurements of the sound field in the reverberation chamber at five positions. Results are shown in 1/3rd octave bands. Each plot represents the frequency response of the omnidirectional sound-source measured with a microphone array, consisting of four Brüel & Kjær Type 4938 1/4" pressure-field microphones, mounted on a tripod. Each of them were at a distance of 15 cm from the center. Figure 43 shows the microphone array. It can be seen that all responses are within a 2,5 dB deviation from each other, thereby fulfilling the ISO-4869-1 standard for these types of measurements.

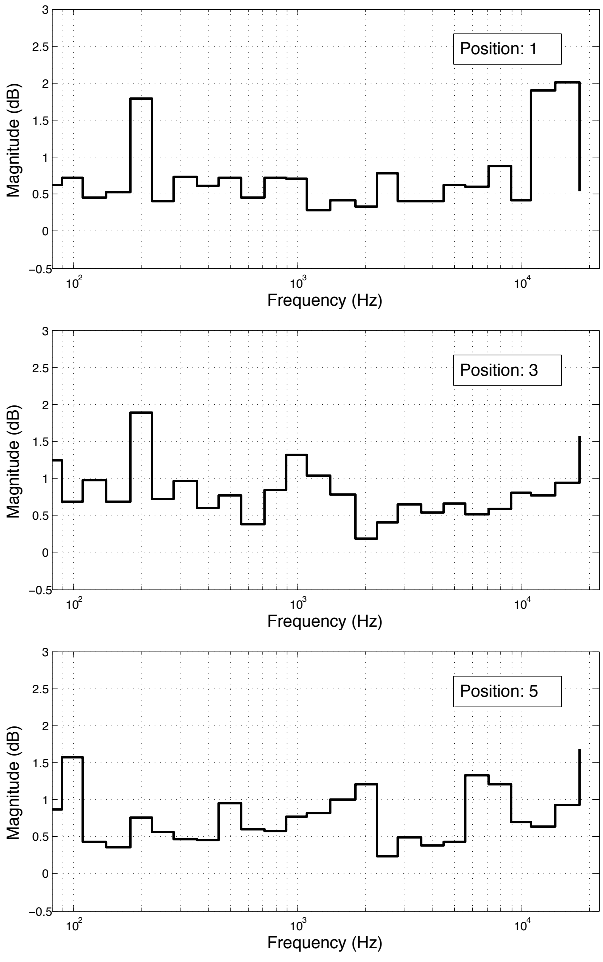

Figure 6: *Measurement of the sound field in the reverberation chamber. The values represent the largest difference between two of four pressure-field microphones.*

3.2 Reproducibility

Figure 7 shows a reproducibility test. A second measurement with the Brüel & Kjær Type 4128-C HATS model nr. 1 was made in the anechoic chamber, where the setup had been taken out from the room beforehand, and rebuilt again. The HRTF measurement in the frontal direction, i.e., at an azimuth angle of 0° was made and divided by the first measurement. Figure 7 shows the result of the division, and it can be seen that the deviation from the two measurements is no more than 0.4 dB from 100 Hz to 10 kHz, which is within the tolerances of the IEC-60318-7 standard.

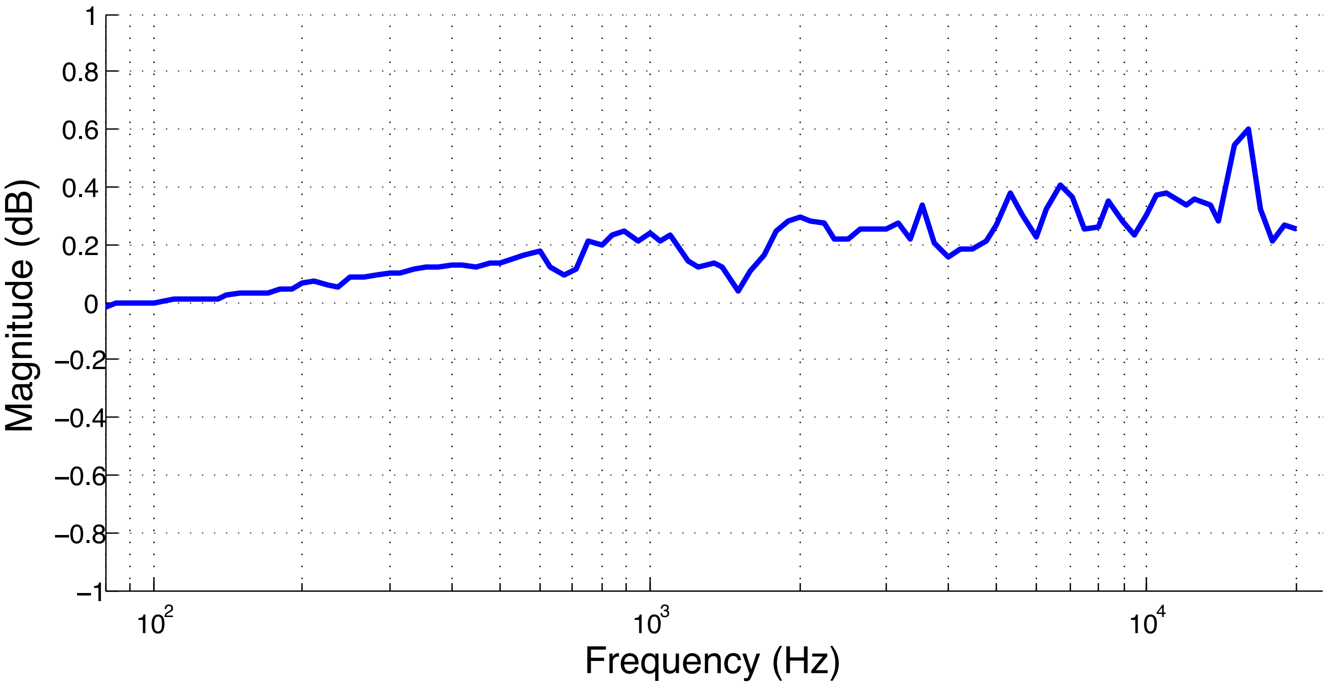

Figure 7: *Two HRTF measurements divided by each other to show deviation between the two, to illustrate reproducibility. HRTFs are from the Brüel & Kjær Type 4128-C HATS model nr. 1, in the frontal direction (azimuth of 0°)*

3.3 HRTFs in the free field

Figure 8 to 31 show HRTF measurement in the free field, for all manikins, using the random noise and sine sweep methods. The solid curve represents the HRTF, while the dotted lines are tolerances set by IEC 60318-7[1]. The left ear is presented in black, and right ear in grey.

It is important to note that the measurements are shown in 1/12th octave bands, while the tolerances are in 1/3rd octave bands, as per the present IEC 60318-7 standard. The 1/12th octave band representation should therefore not stay within the tolerances, as opposed to using 1/3rd octave bands, due to the increased precision.

From 200 Hz and up, the transmission is above 0 dB, which indicates a pressure buildup due to the reflections from the head and pinna and the gain is always highest at around 3kHz. The transmission to the ear at 270° has the characteristics of a low-pass filter, with a cutoff at around 4 kHz, which is due to the shadowing effect of the head [5]. The HRTFs can be seen to converge towards 0 dB at low frequencies, as the wave-length at such frequencies are longer than the body's dimensions.

3.3.1 Random noise measurements

- **Brüel & Kjær Type 4128-C HATS model nr. 1**

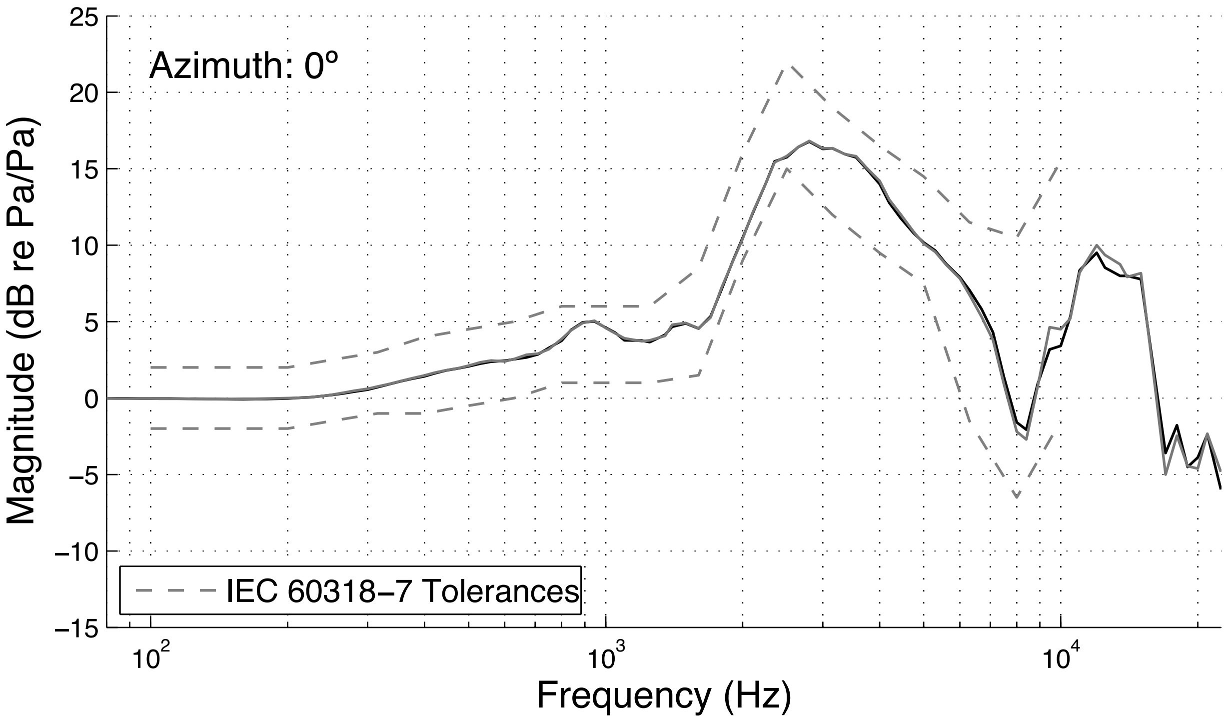

Figure 8: *Random noise HRTF measurement of Brüel & Kjær Type 4128-C HATS model nr. 1 at 0° azimuth. Black curve is left ear. 1/12th octave bands.*

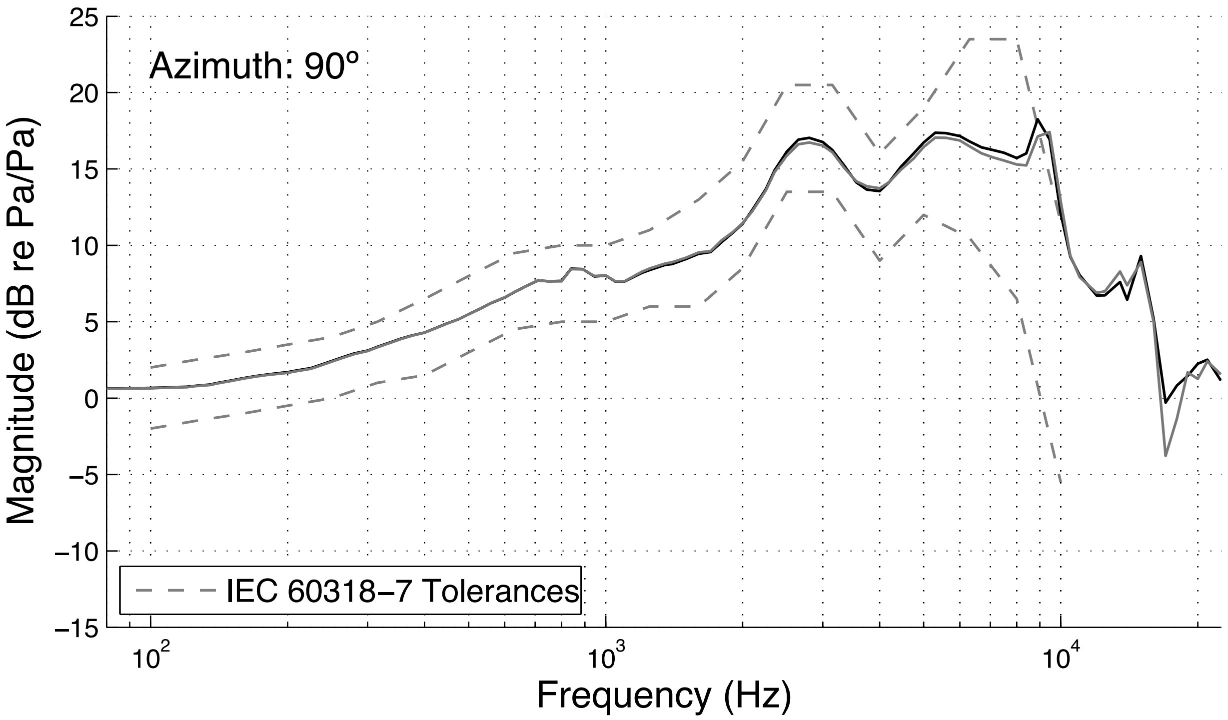

Figure 9: *Random noise HRTF measurement of Brüel & Kjær Type 4128-C HATS model nr. 1 at 90° azimuth. Black curve is left ear. 1/12th octave bands.*

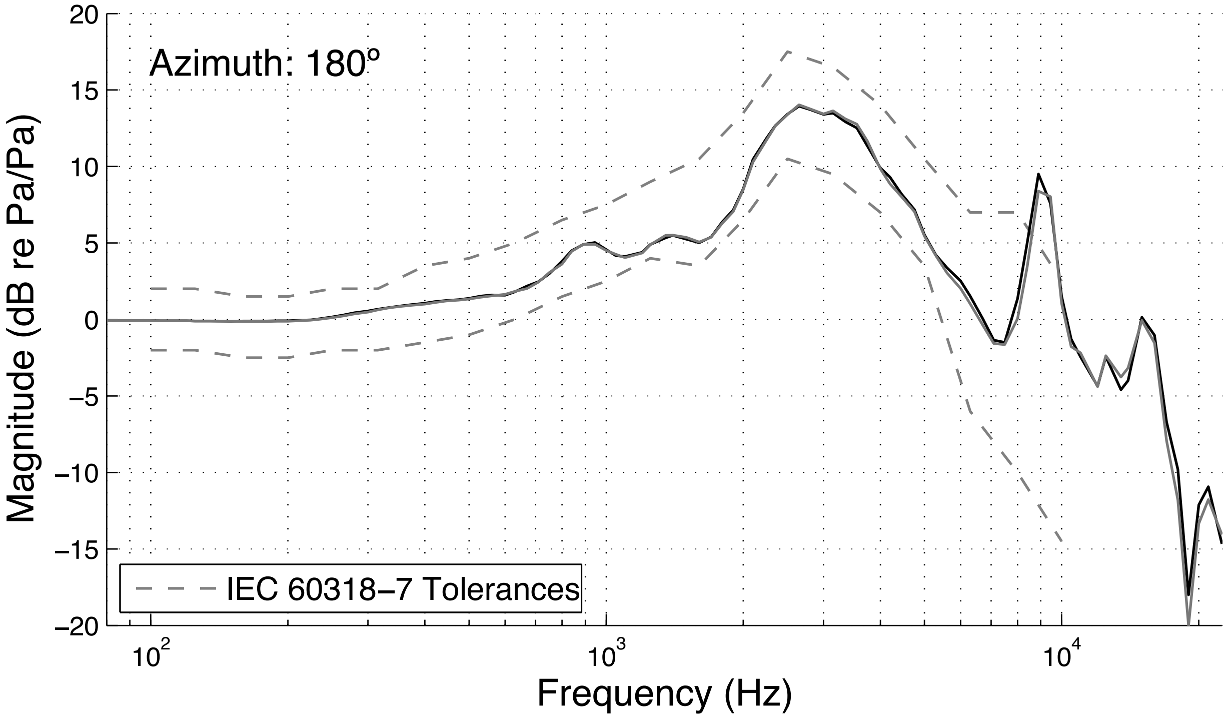

Figure 10: *Random noise HRTF measurement of Brüel & Kjær Type 4128-C HATS model nr. 1 at 180° azimuth. Black curve is left ear. 1/12th octave bands.*

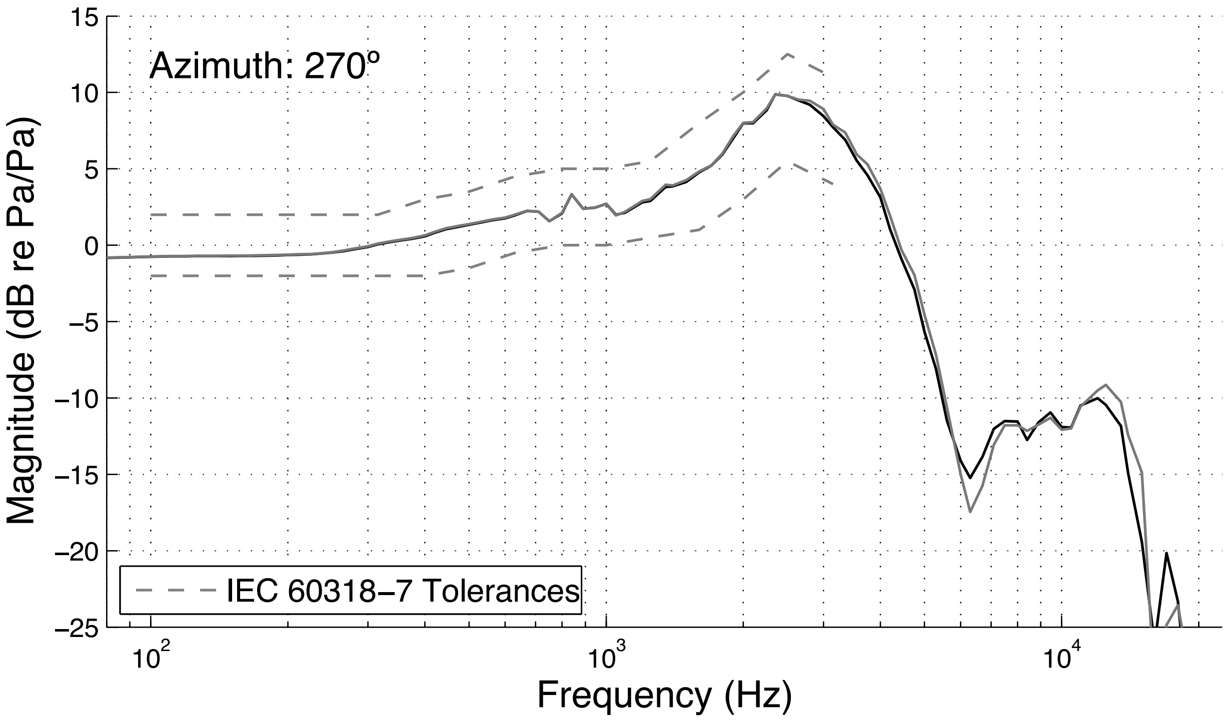

Figure 11: *Random noise HRTF measurement of Brüel & Kjær Type 4128-C HATS model nr. 1 at 270° azimuth. Black curve is left ear. 1/12th octave bands.*

• **G.R.A.S. KEMAR Type 45BM**

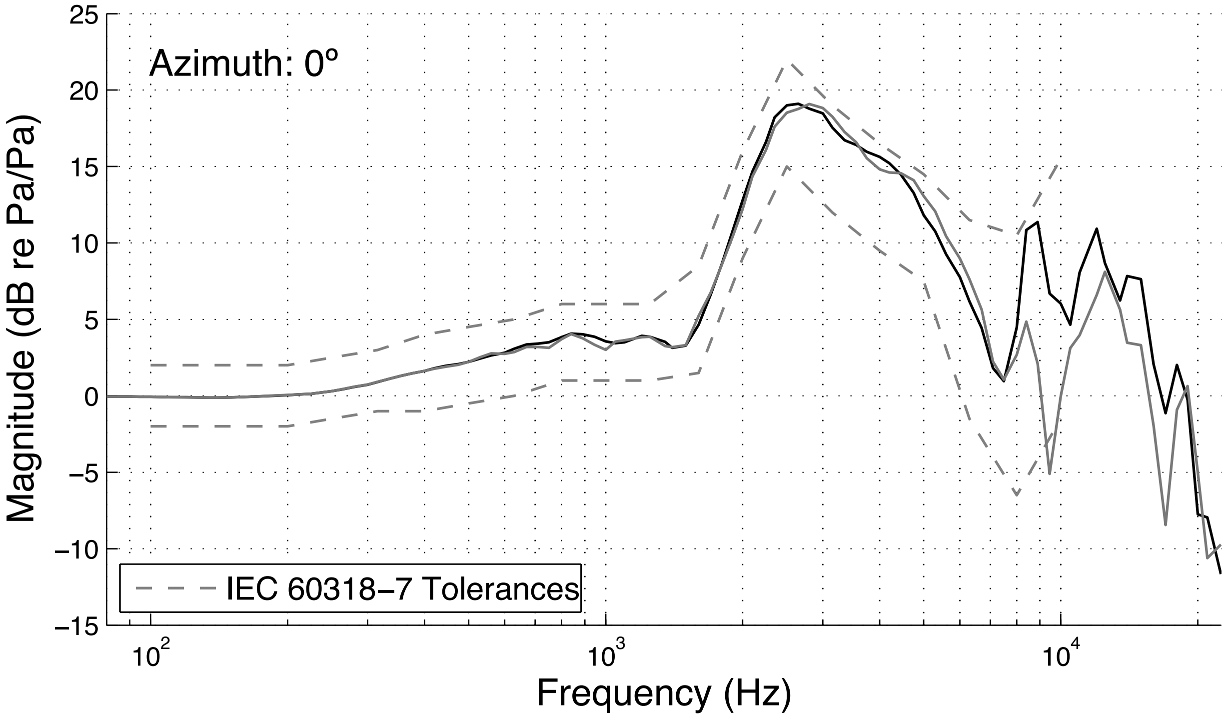

Figure 12: *Random noise HRTF measurement of G.R.A.S. KEMAR Type 45BM at 0° azimuth. Black curve is left ear. 1/12th octave bands.*

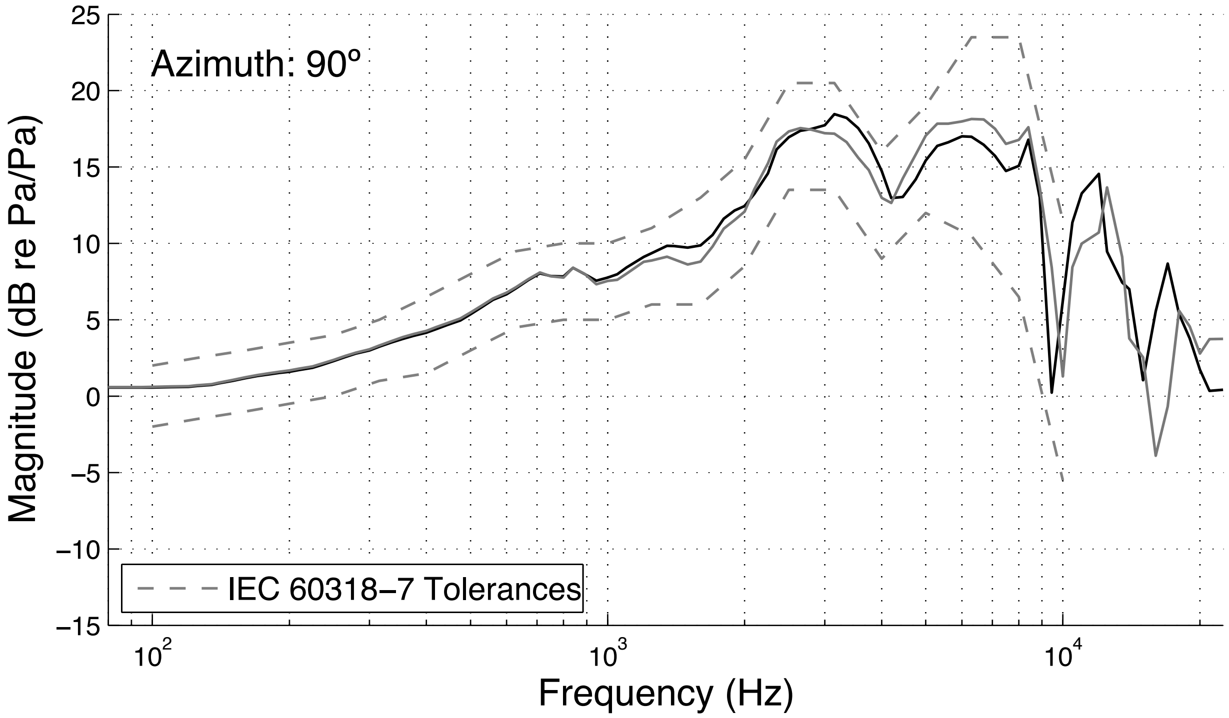

Figure 13: *Random noise HRTF measurement of G.R.A.S. KEMAR Type 45BM at 90° azimuth. Black curve is left ear. 1/12th octave bands.*

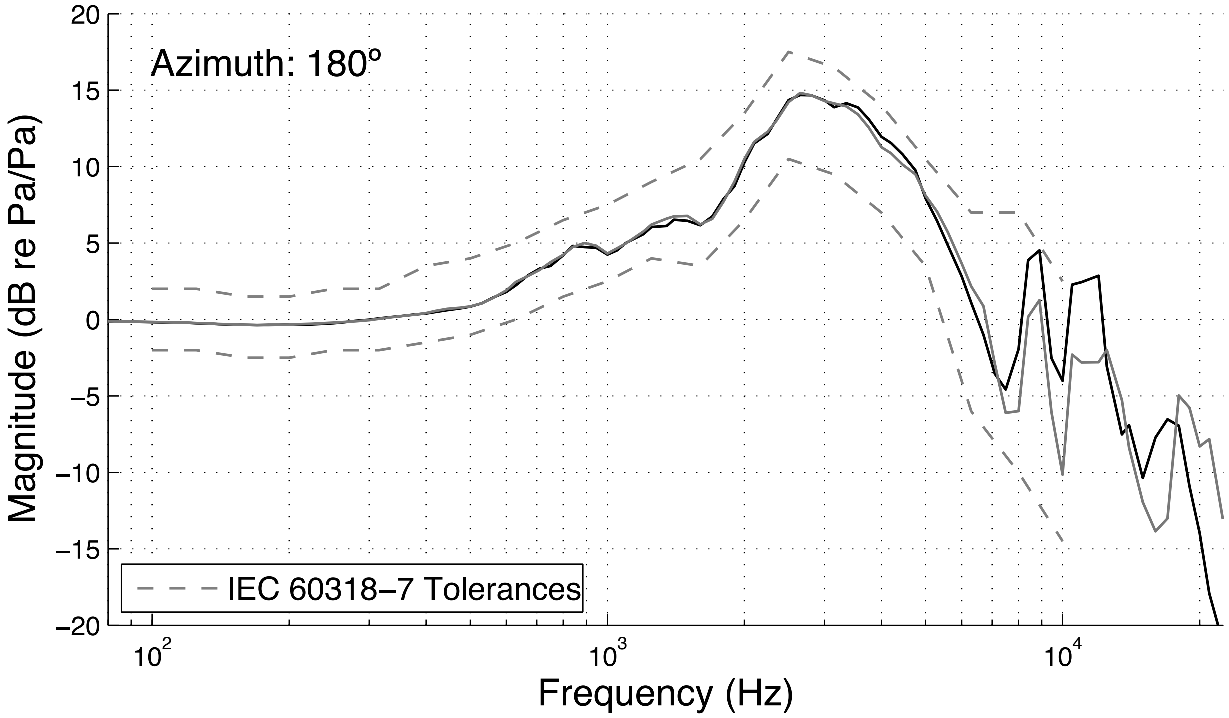

Figure 14: *Random noise HRTF measurement of G.R.A.S. KEMAR Type 45BM at 180° azimuth. Black curve is left ear. 1/12th octave bands.*

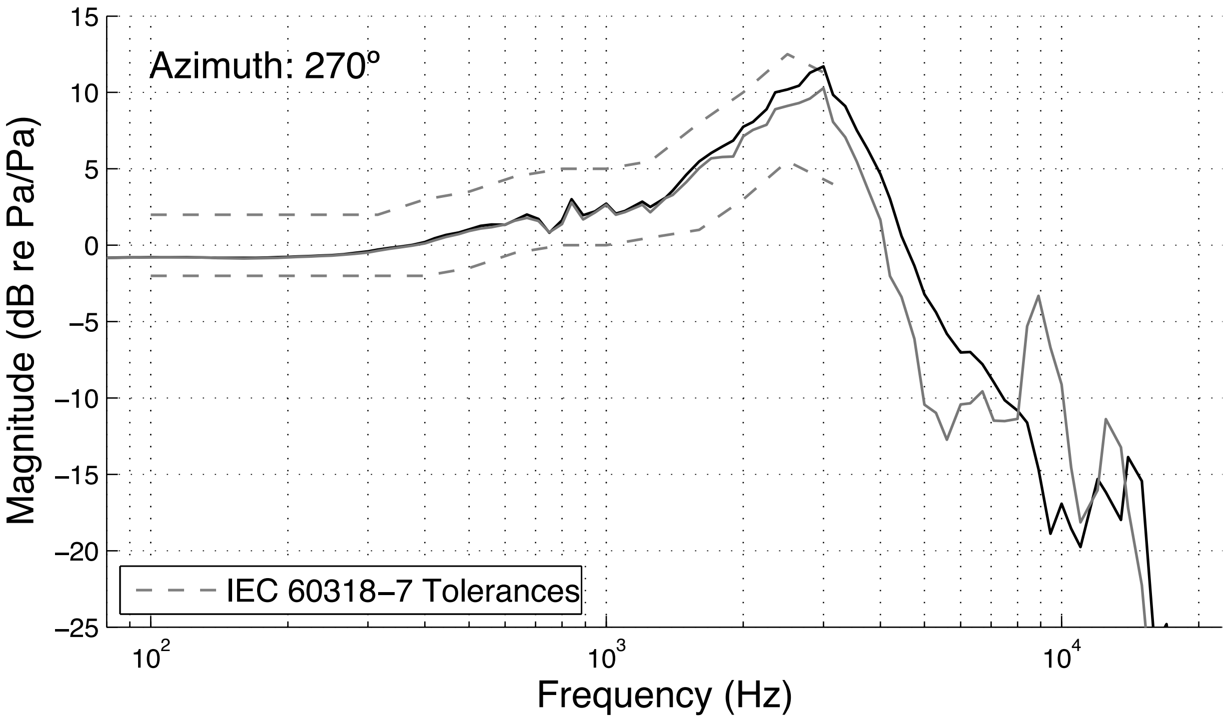

Figure 15: *Random noise HRTF measurement of G.R.A.S. KEMAR Type 45BM at 270° azimuth. Black curve is left ear. 1/12th octave bands.*

• **Head Acoustics HMS II.3**

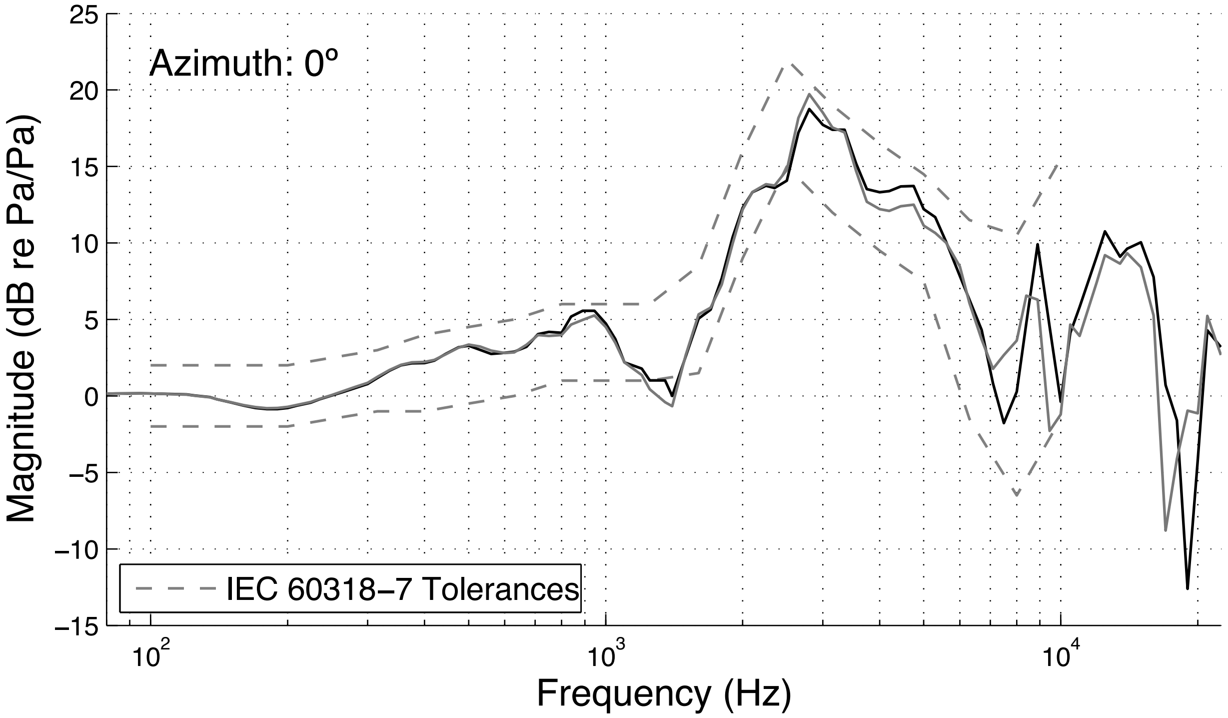

Figure 16: *Random noise HRTF measurement of Head Acoustics HMS II.3 at 0° azimuth. Black curve is left ear. 1/12th octave bands.*

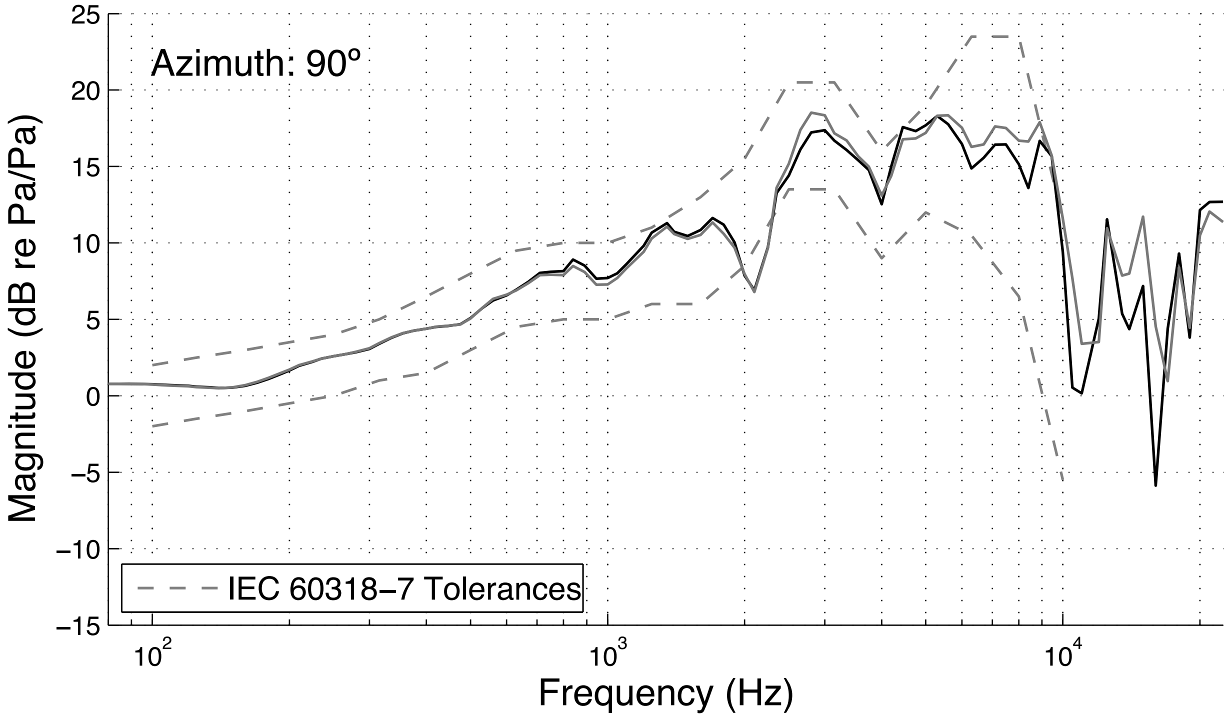

Figure 17: *Random noise HRTF measurement of Head Acoustics HMS II.3 at 90° azimuth. Black curve is left ear. 1/12th octave bands.*

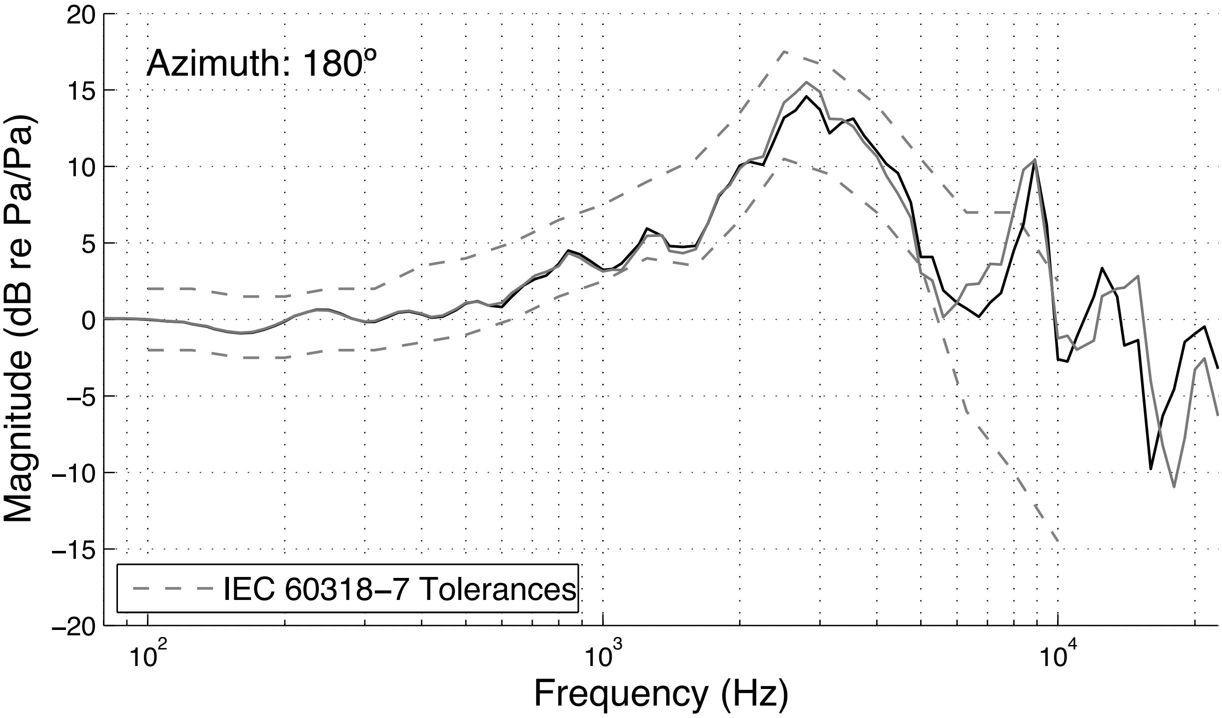

Figure 18: *Random noise HRTF measurement of Head Acoustics HMS II.3 at 180° azimuth. Black curve is left ear. 1/12th octave bands.*

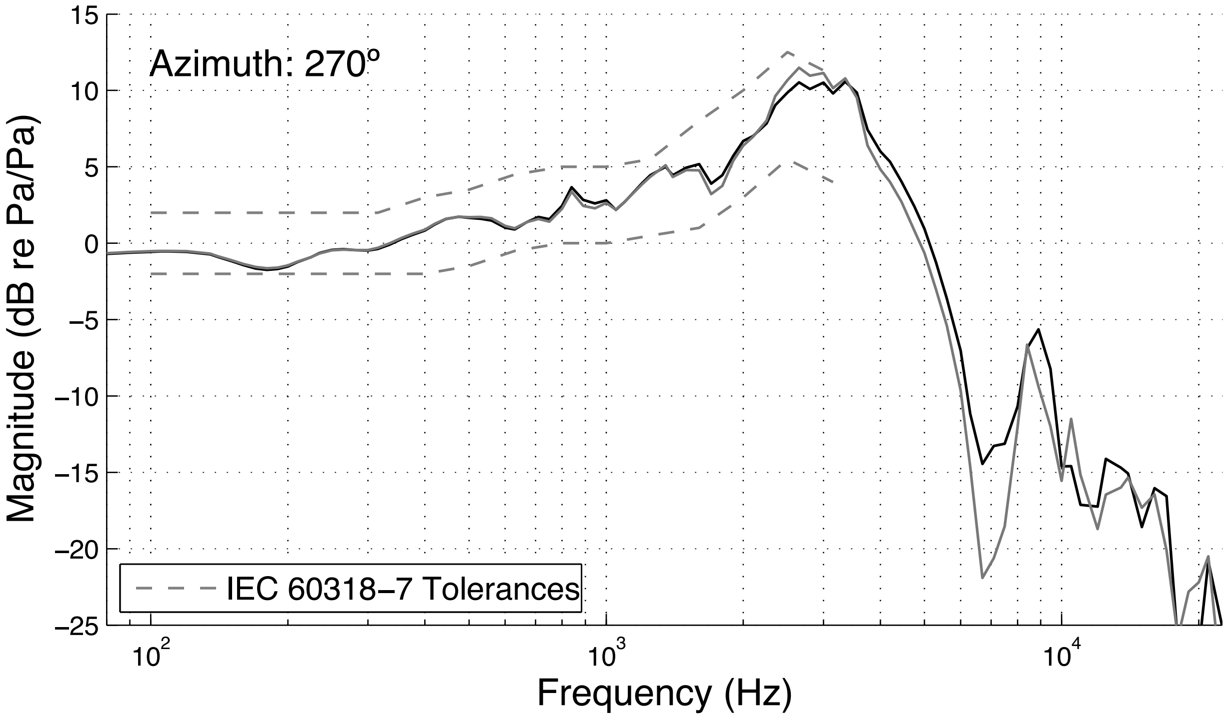

Figure 19: *Random noise HRTF measurement of Head Acoustics HMS II.3 at 270° azimuth. Black curve is left ear. 1/12th octave bands.*

3.3.2 Sine sweep measurements

- **Brüel & Kjær Type 4128-C HATS model nr. 1**

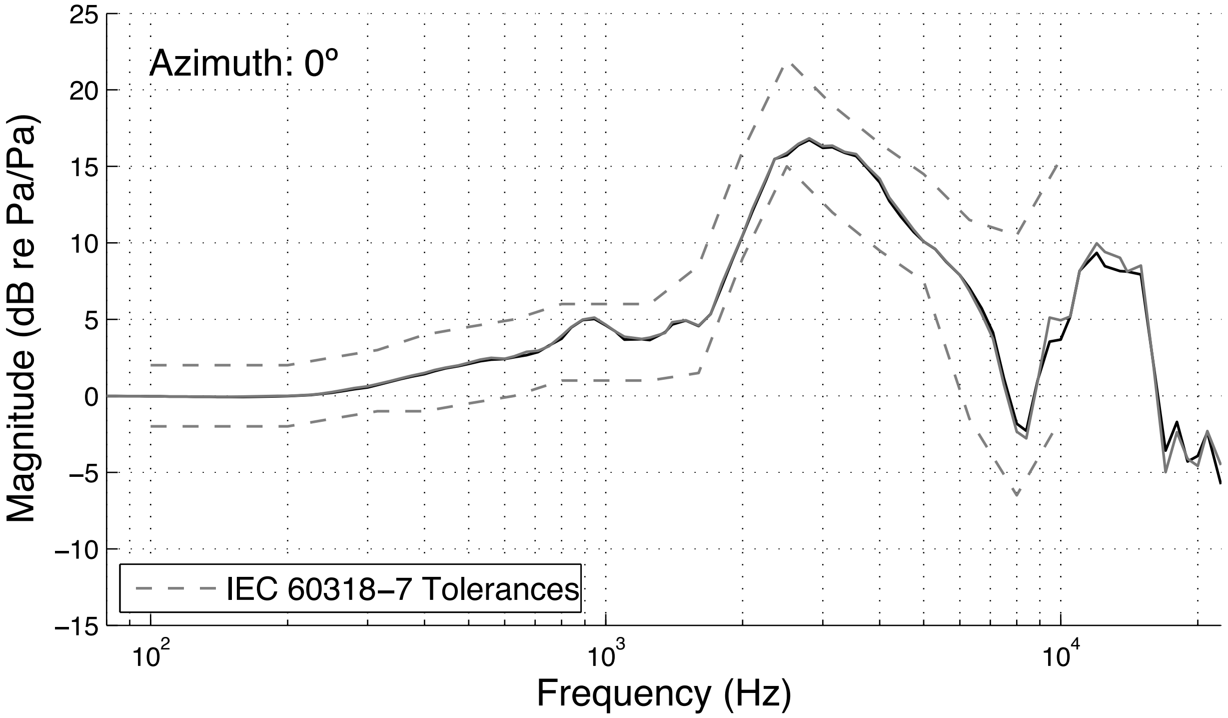

Figure 20: *Sine sweep HRTF measurement of Brüel & Kjær Type 4128-C HATS model nr. 1 at 0° azimuth. Black curve is left ear. 1/12th octave bands.*

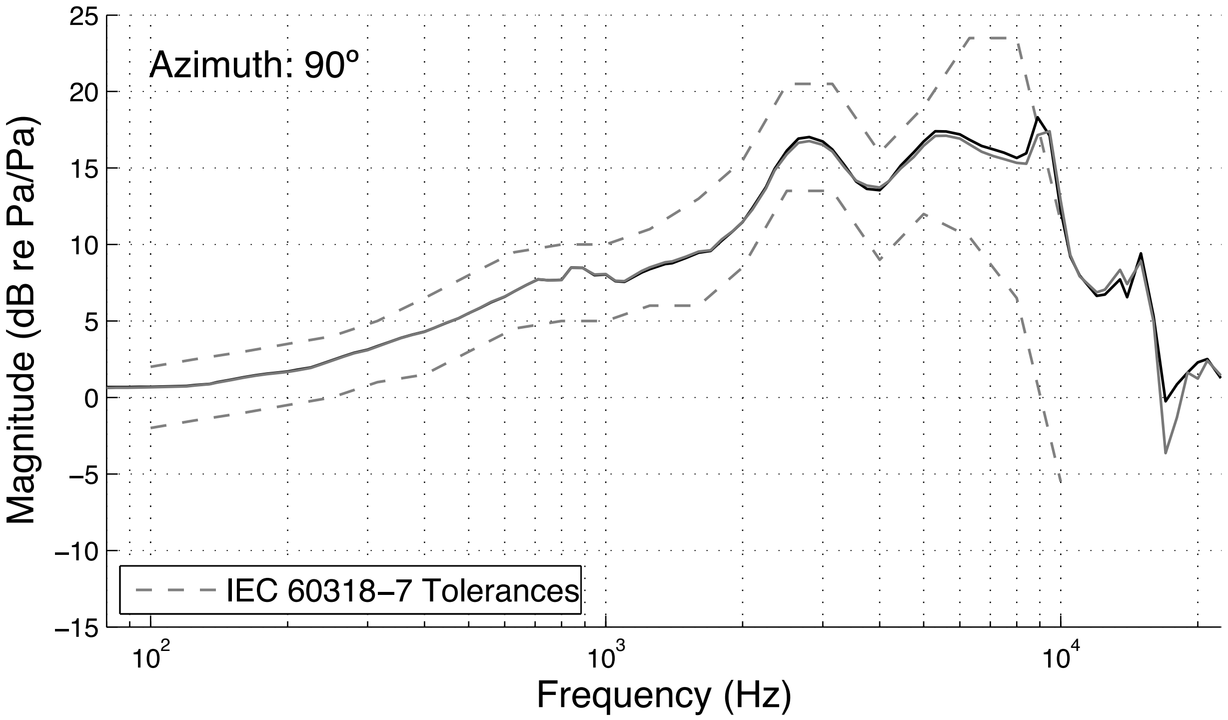

Figure 21: *Sine sweep HRTF measurement of Brüel & Kjær Type 4128-C HATS model nr. 1 at 90° azimuth. Black curve is left ear. 1/12th octave bands.*

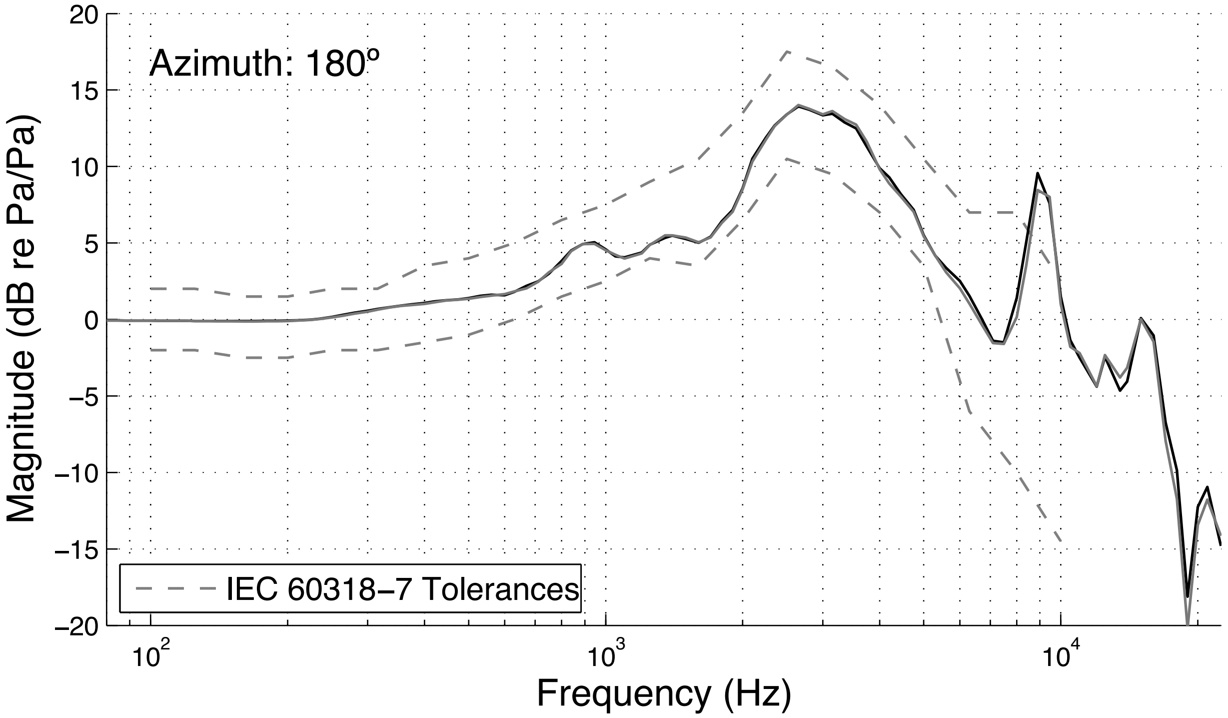

Figure 22: *Sine sweep HRTF measurement of Brüel & Kjær Type 4128-C HATS model nr. 1 at 180° azimuth. Black curve is left ear. 1/12th octave bands.*

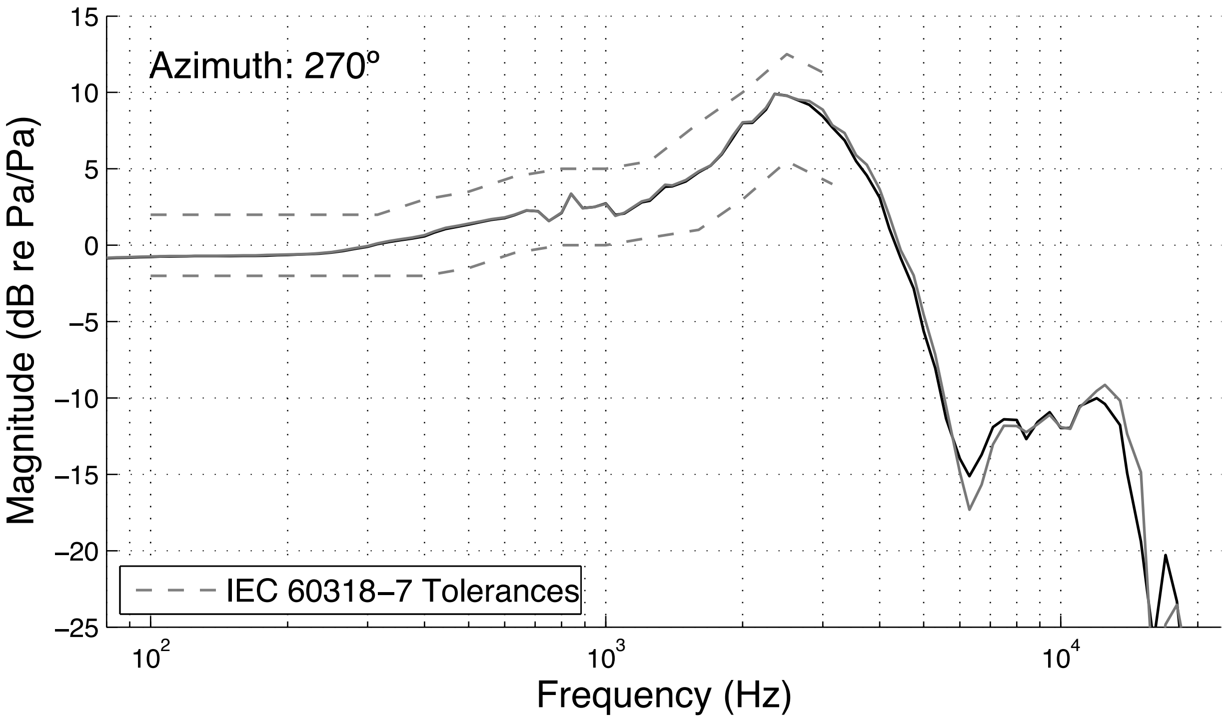

Figure 23: *Sine sweep HRTF measurement of Brüel & Kjær Type 4128-C HATS model nr. 1 at 270° azimuth. Black curve is left ear. 1/12th octave bands.*

• **G.R.A.S. KEMAR Type 45BM**

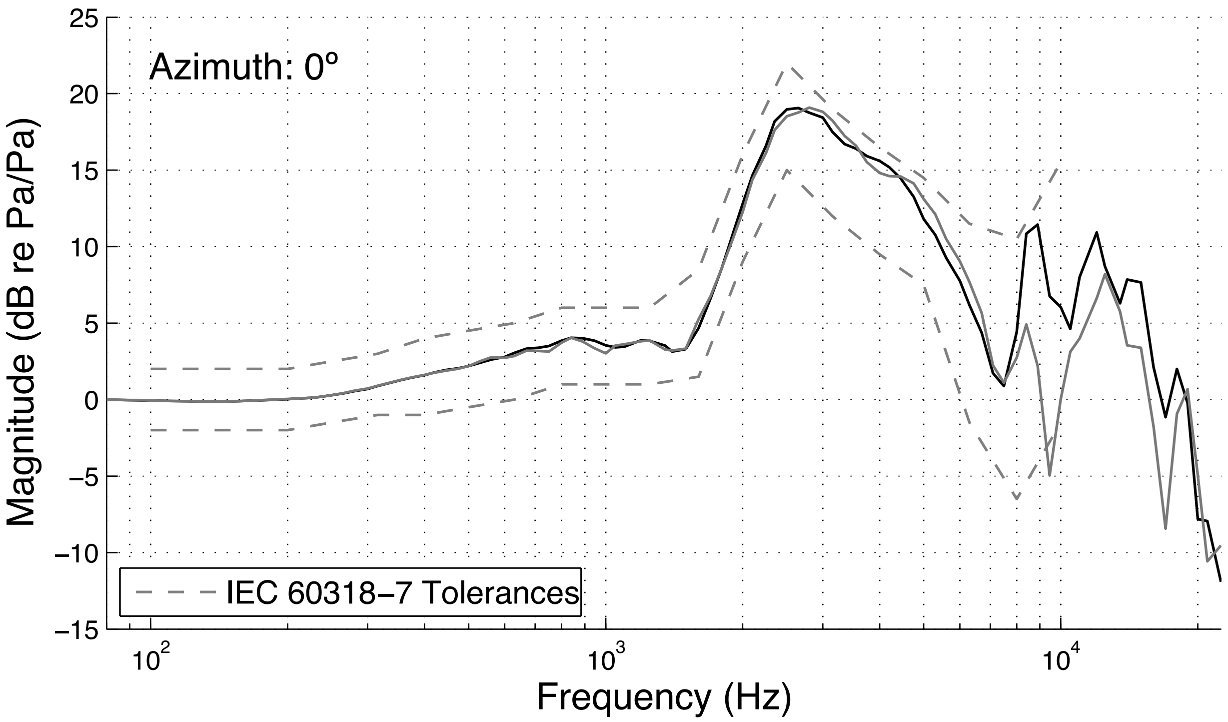

Figure 24: *Sine sweep HRTF measurement of G.R.A.S. KEMAR Type 45BM at 0° azimuth. Black curve is left ear. 1/12th octave bands.*

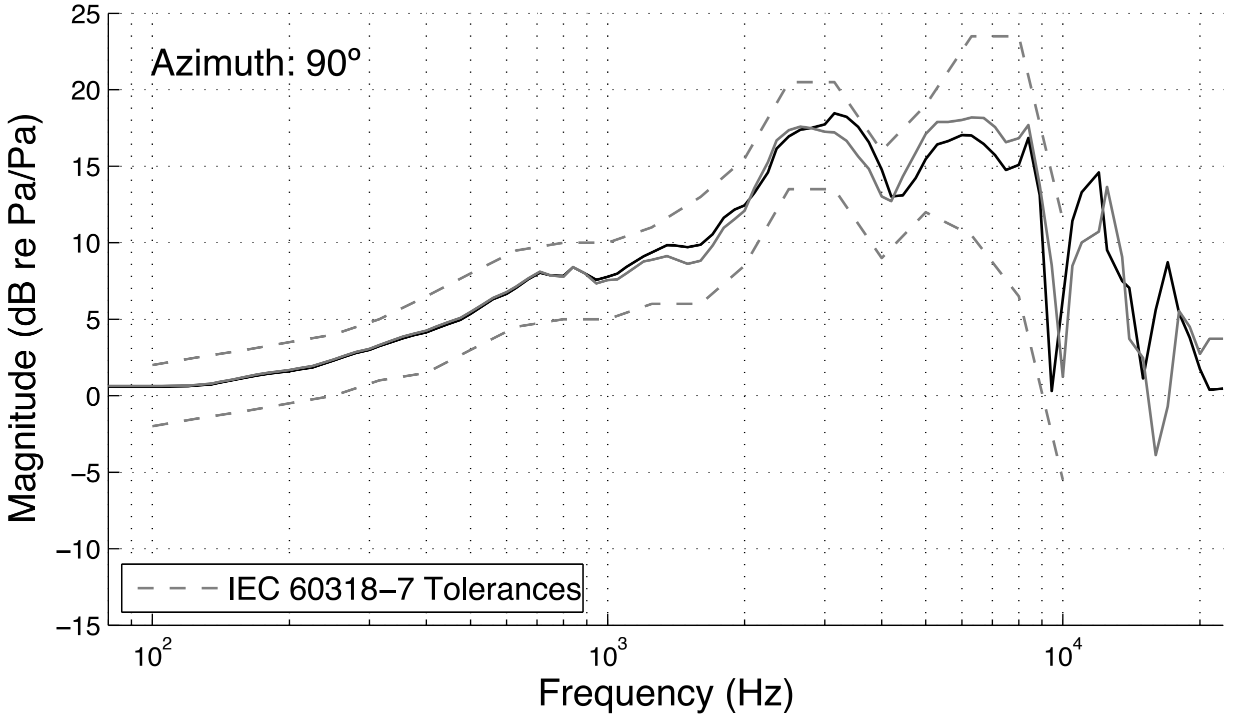

Figure 25: *Sine sweep HRTF measurement of G.R.A.S. KEMAR Type 45BM at 90° azimuth. Black curve is left ear. 1/12th octave bands.*

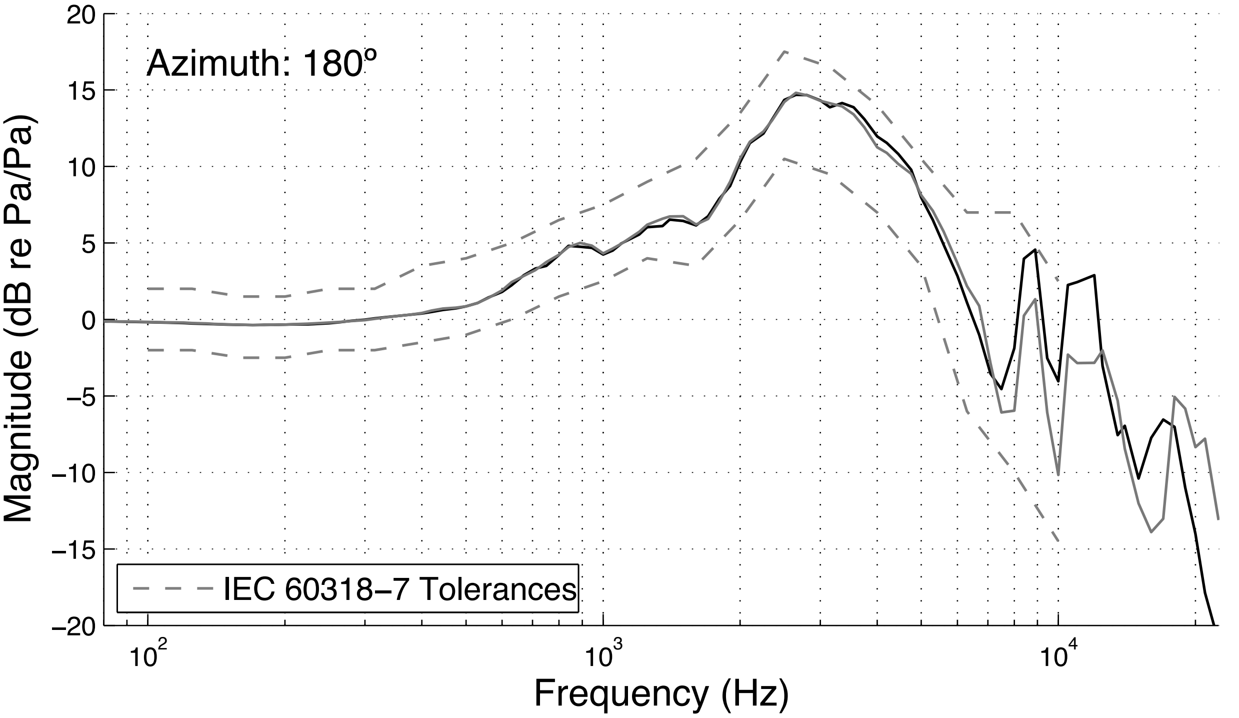

Figure 26: *Sine sweep HRTF measurement of G.R.A.S. KEMAR Type 45BM at 180° azimuth. Black curve is left ear. 1/12th octave bands.*

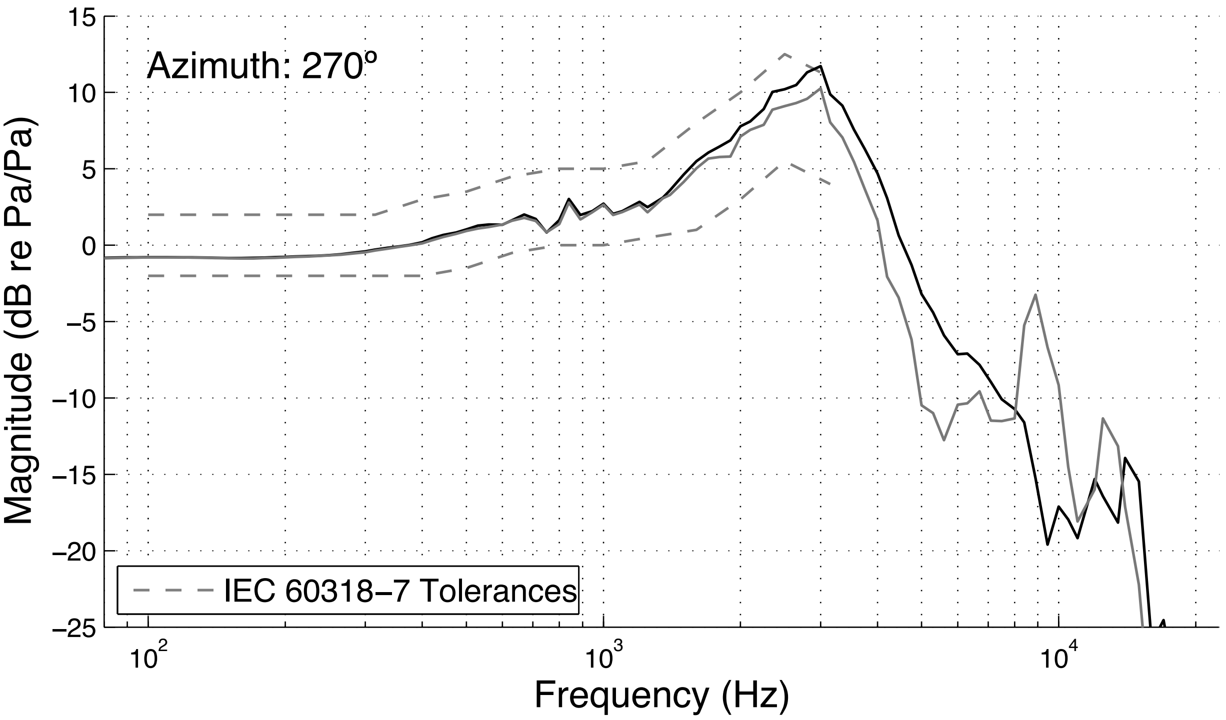

Figure 27: *Sine sweep HRTF measurement of G.R.A.S. KEMAR Type 45BM at 270° azimuth. Black curve is left ear. 1/12th octave bands.*

• **Head Acoustics HMS II.3**

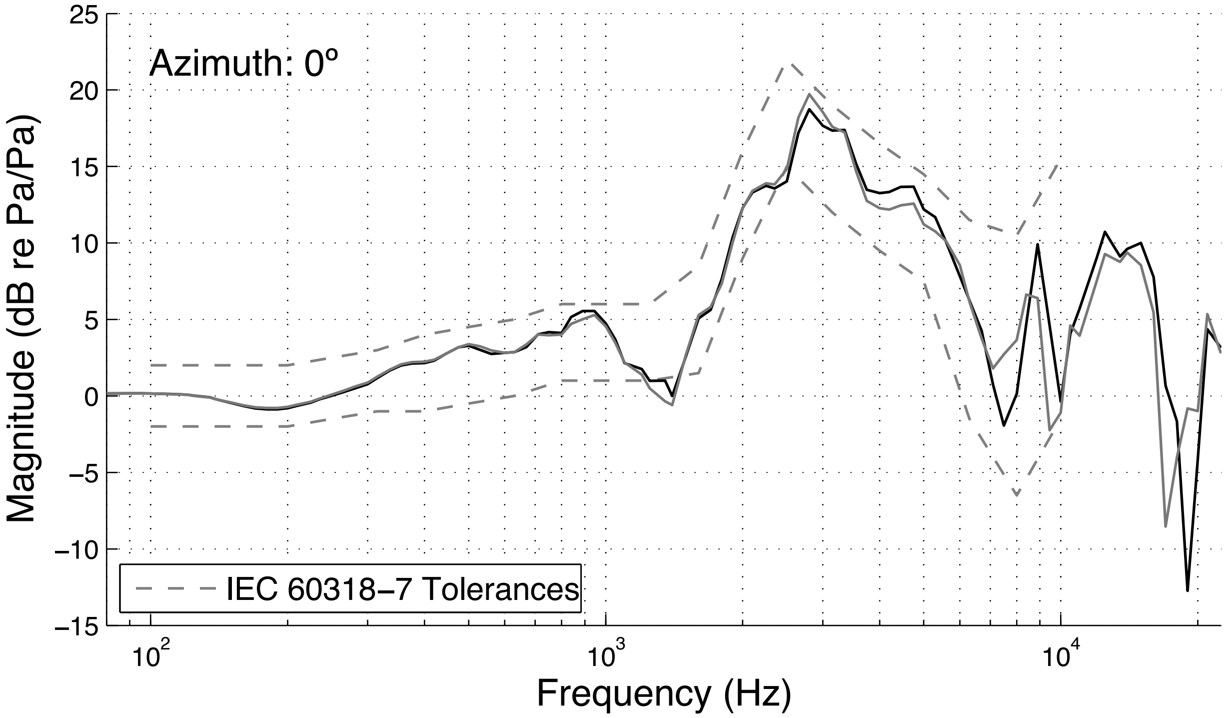

Figure 28: *Sine sweep HRTF measurement of Head Acoustics HMS II.3 at 0° azimuth. Black curve is left ear. 1/12th octave bands.*

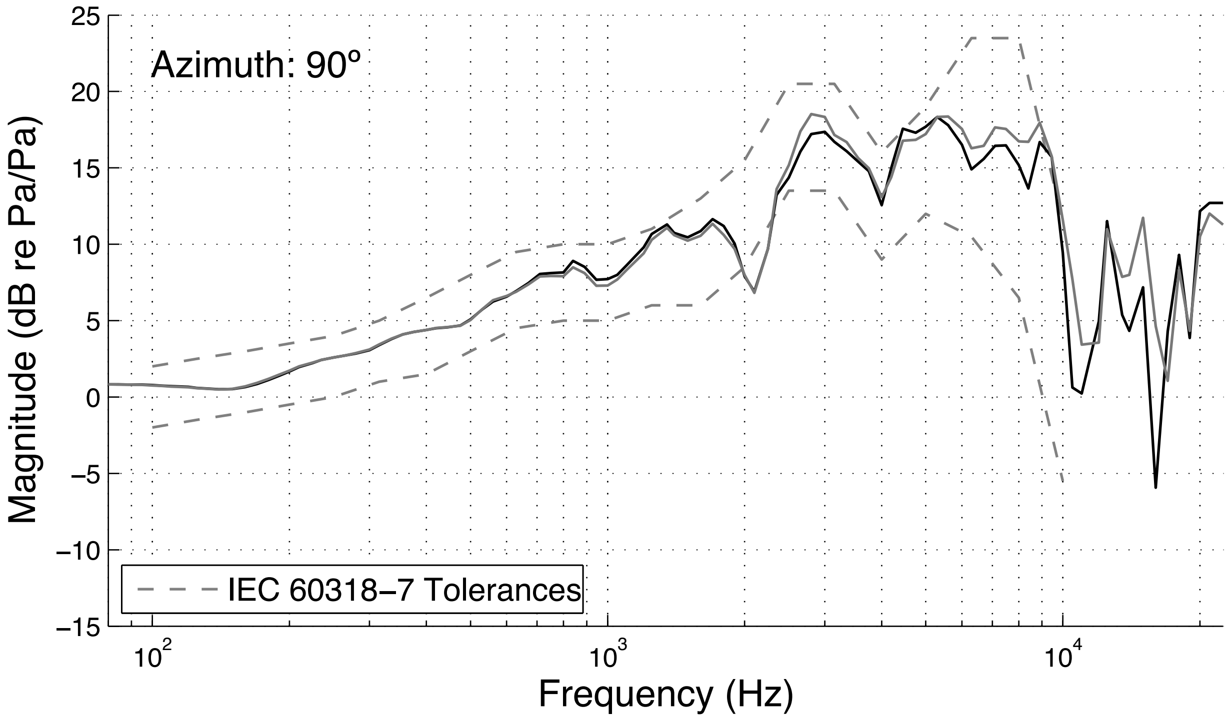

Figure 29: *Sine sweep HRTF measurement of Head Acoustics HMS II.3 at 90° azimuth. Black curve is left ear. 1/12th octave bands.*

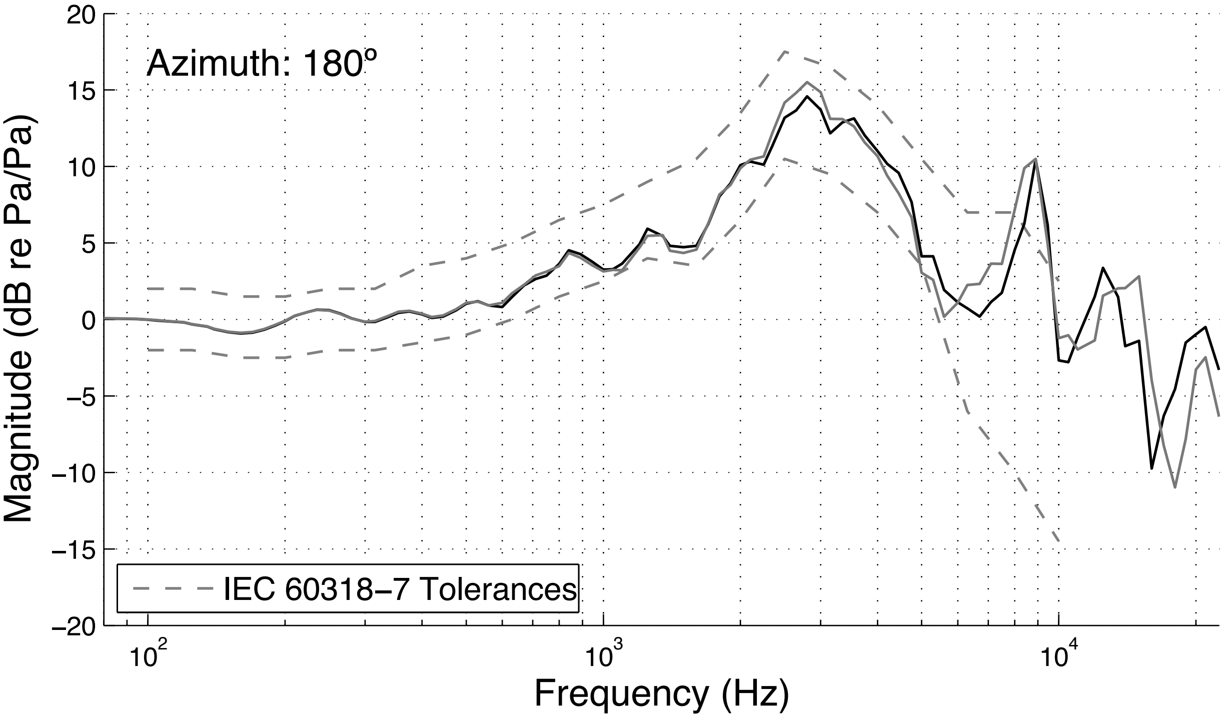

Figure 30: *Sine sweep HRTF measurement of Head Acoustics HMS II.3 at 180° azimuth. Black curve is left ear. 1/12th octave bands.*

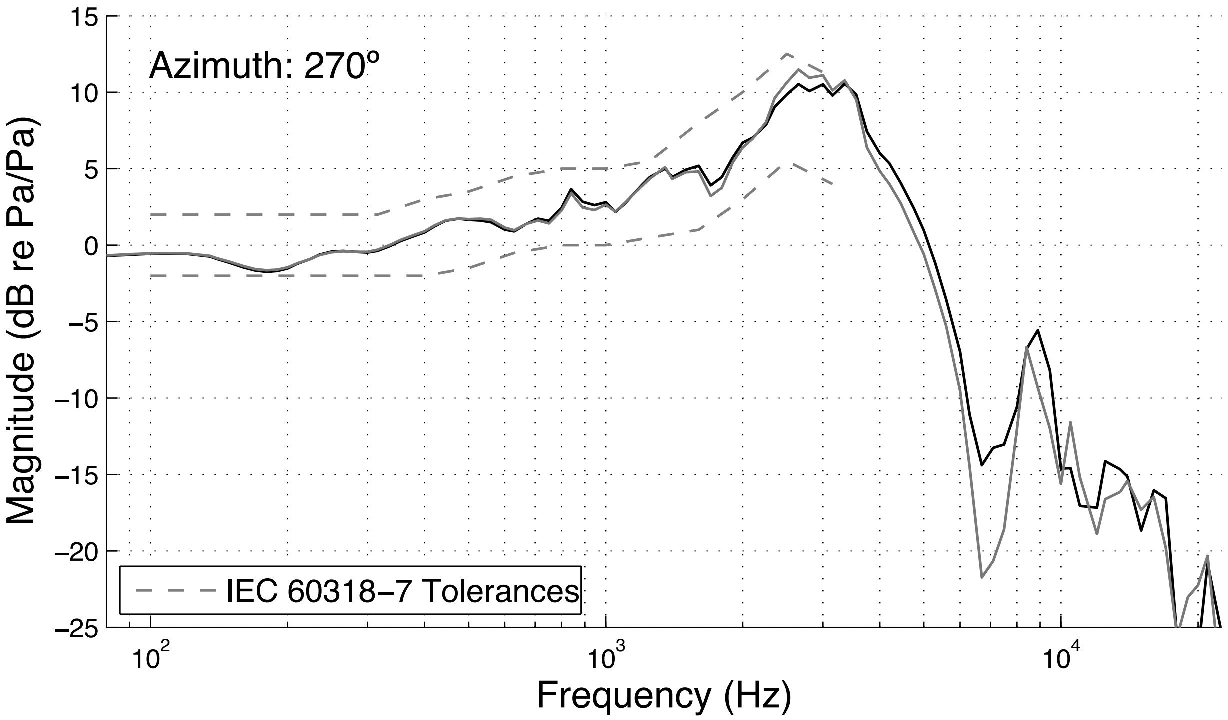

Figure 31: *Sine sweep HRTF measurement of Head Acoustics HMS II.3 at 270° azimuth. Black curve is left ear. 1/12th octave bands.*

3.4 HRTFs in the diffuse field

Figure 32 shows HRTF measurements in the diffuse field, for all manikins, made with pink noise. The solid curve represents the HRTF, while the dotted lines are tolerances set by ITU-T Rec. P.58[8]. All measurements and tolerances are shown in 1/3rd octave bands. The HRTFs are also an average of the five measured positions.

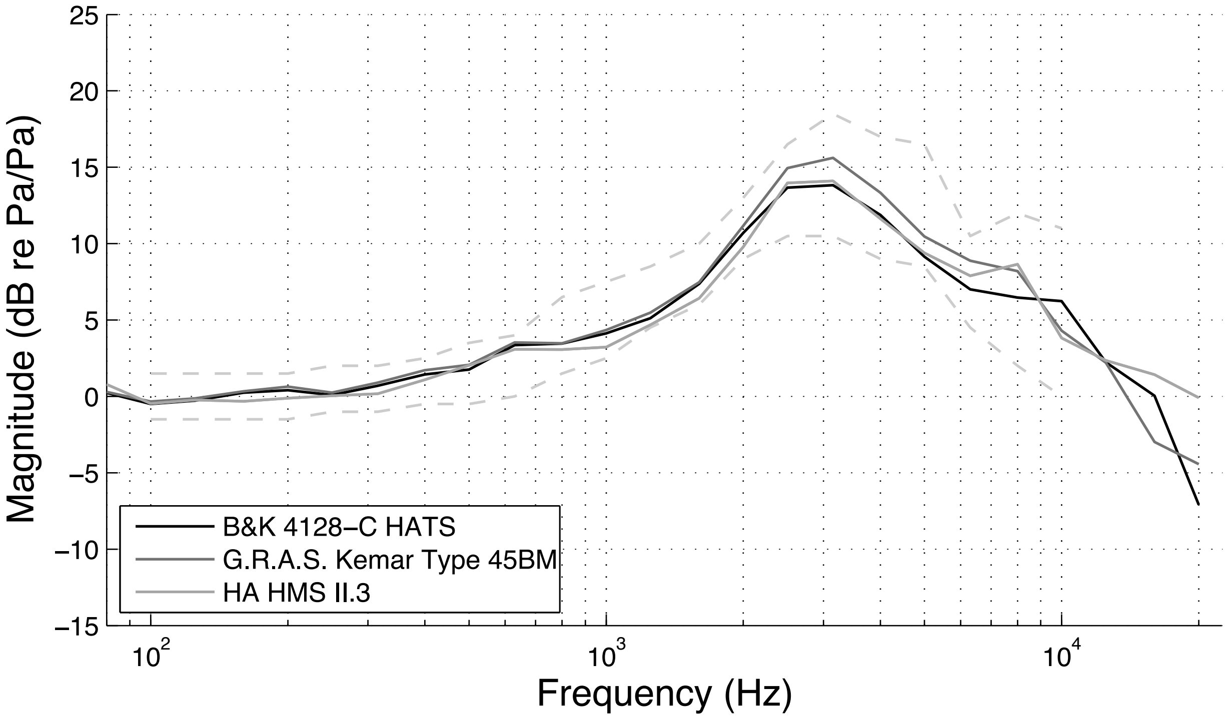

Figure 32: *Average of five positions for diffuse-field HRTF. ITU-T Rec. P.58 Tolerances in dashed lines. Right ear is presented. 1/3rd octave bands.*

4 Conclusions

Measurement of HRTFs of Brüel & Kjær Type 4128-C HATS, G.R.A.S. KEMAR Type 45BM, and Head Acoustics HMS II.3 Head and Torso Simulators were made in DTU's anechoic and reverberation chambers. All results for free- and diffuse-field conditions were shown along with IEC 60318-7[1] and ITU-T Rec. P.58[8] tolerances respectively. By means of an advanced setup using a controllable motor it was possible to obtain HRTF measurements with high accuracy and repeatability. Results were presented from measurements made with the use of two excitation signals, namely pink noise, and sine sweep. The HRTFs were calculated by doing an FFT of the windowed HRIR and subsequently applying a 1/12th or 1/3rd octave synthesis. As all the raw recordings are available, it is possible to process the data for further representations. It is the intention to examine different HRTF measurement methods further in a later study.

5 Appendix

5.1 Comparison of two Brüel & Kjær 4128-C HATS

Results are shown from the sine sweep method, in 1/12th octave bands.

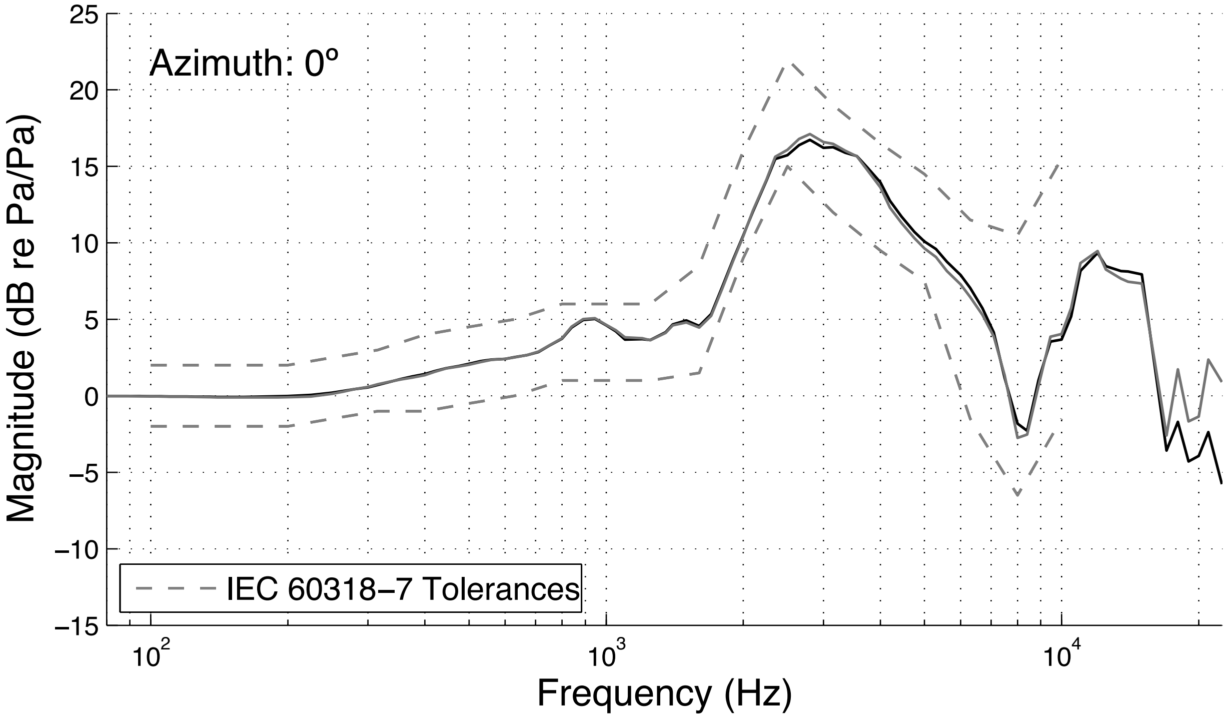

Figure 33: *HRTF of the two Brüel & Kjær 4128-C HATS at 0° azimuth. Left ear is presented. Black curve shows Brüel & Kjær Type 4128-C HATS model nr. 1.*

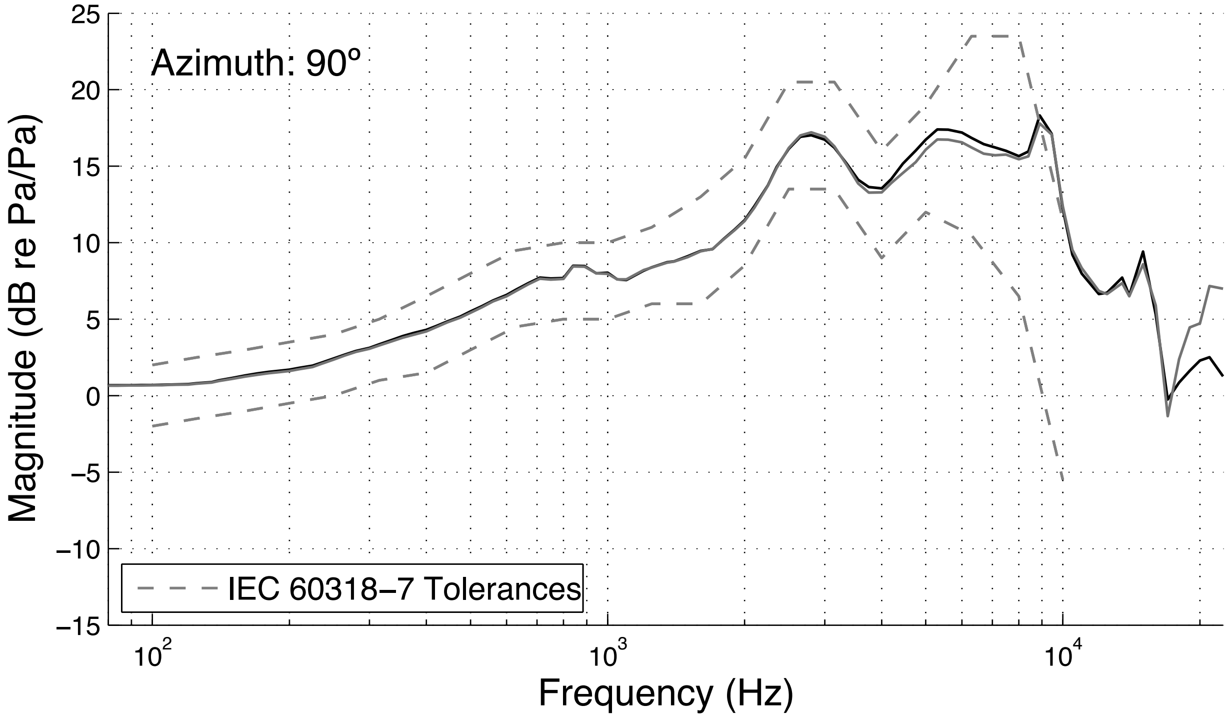

Figure 34: *HRTF of the two Brüel & Kjær 4128-C HATS at 90° azimuth. Left ear is presented. Black curve shows Brüel & Kjær Type 4128-C HATS model nr. 1.*

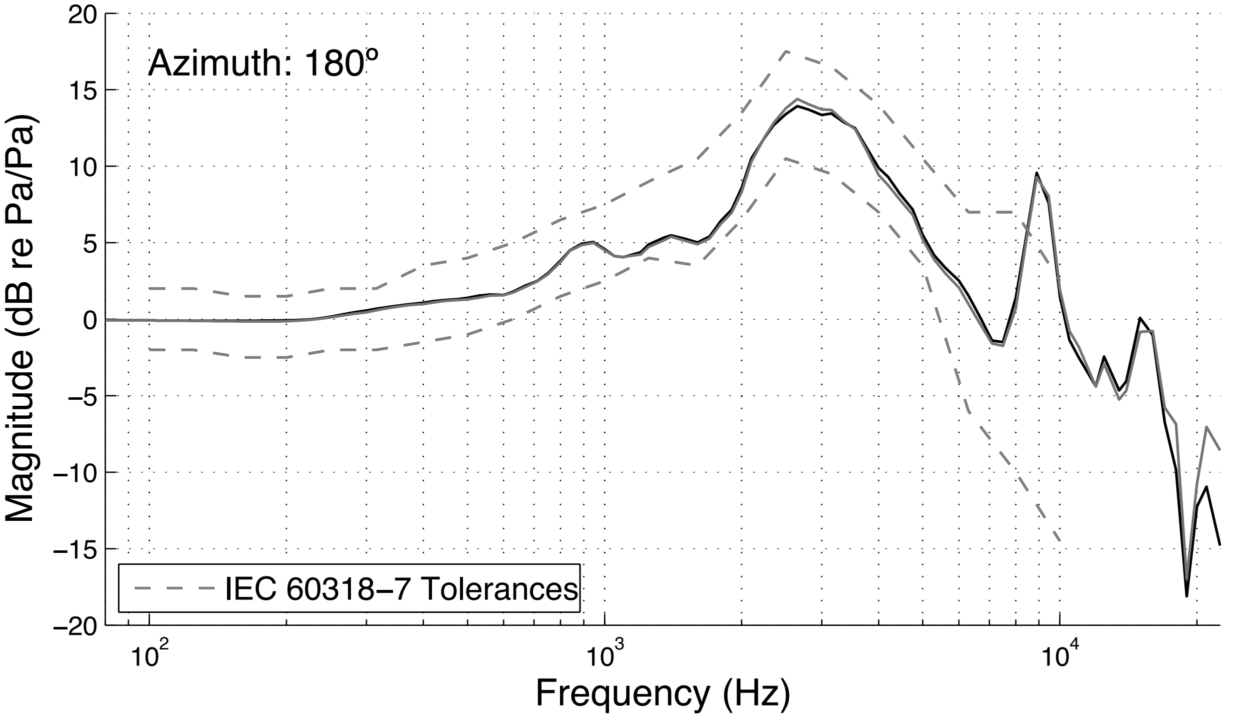

Figure 35: *HRTF of the two Brüel & Kjær 4128-C HATS at 180° azimuth. Left ear is presented. Black curve shows Brüel & Kjær Type 4128-C HATS model nr. 1.*

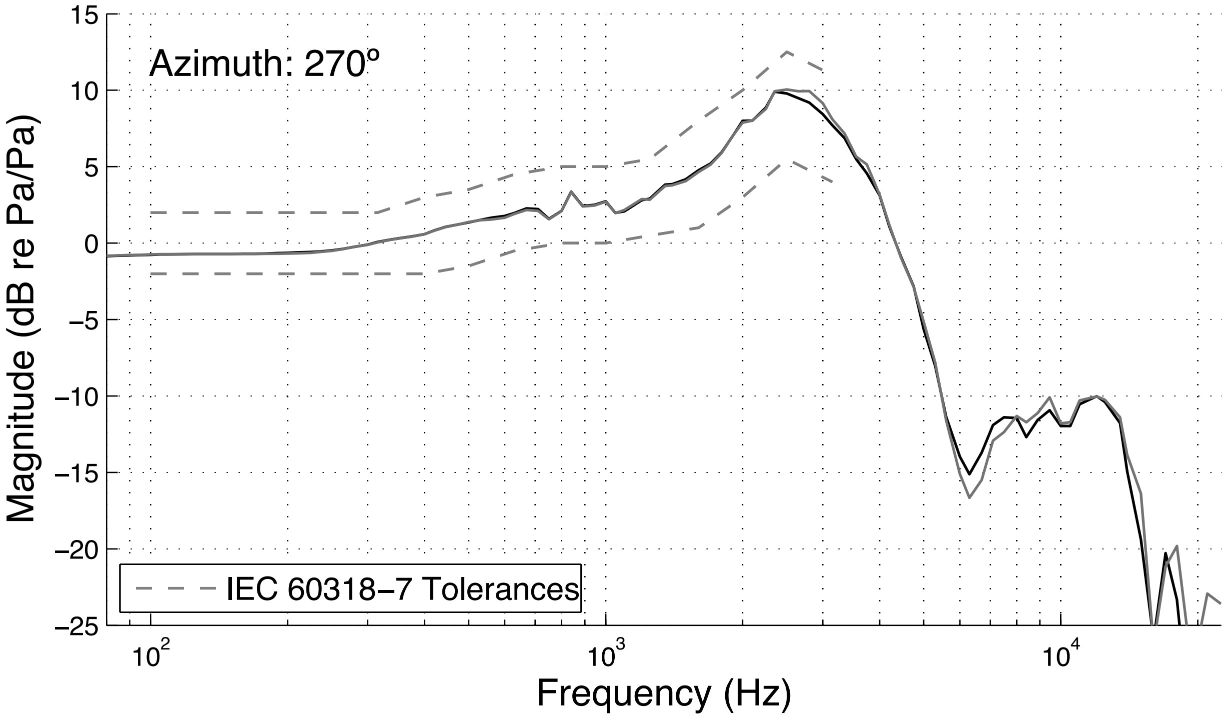

Figure 36: *HRTF of the two Brüel & Kjær 4128-C HATS at 270° azimuth. Left ear is presented. Black curve shows Brüel & Kjær Type 4128-C HATS model nr. 1.*

5.2 All HATS presented in same plots

Results are shown from the sine sweep method, in 1/12th octave bands.

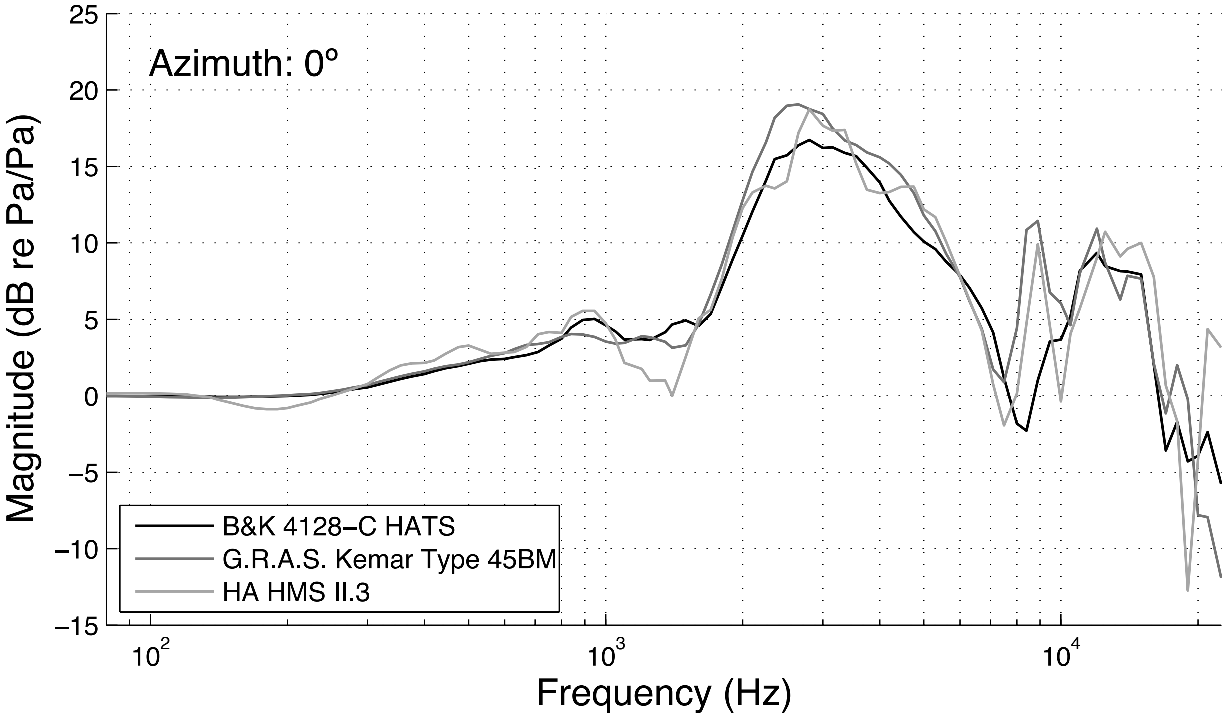

Figure 37: *Free-field HRTF of all HATS at 0° azimuth. Left ear is presented.*

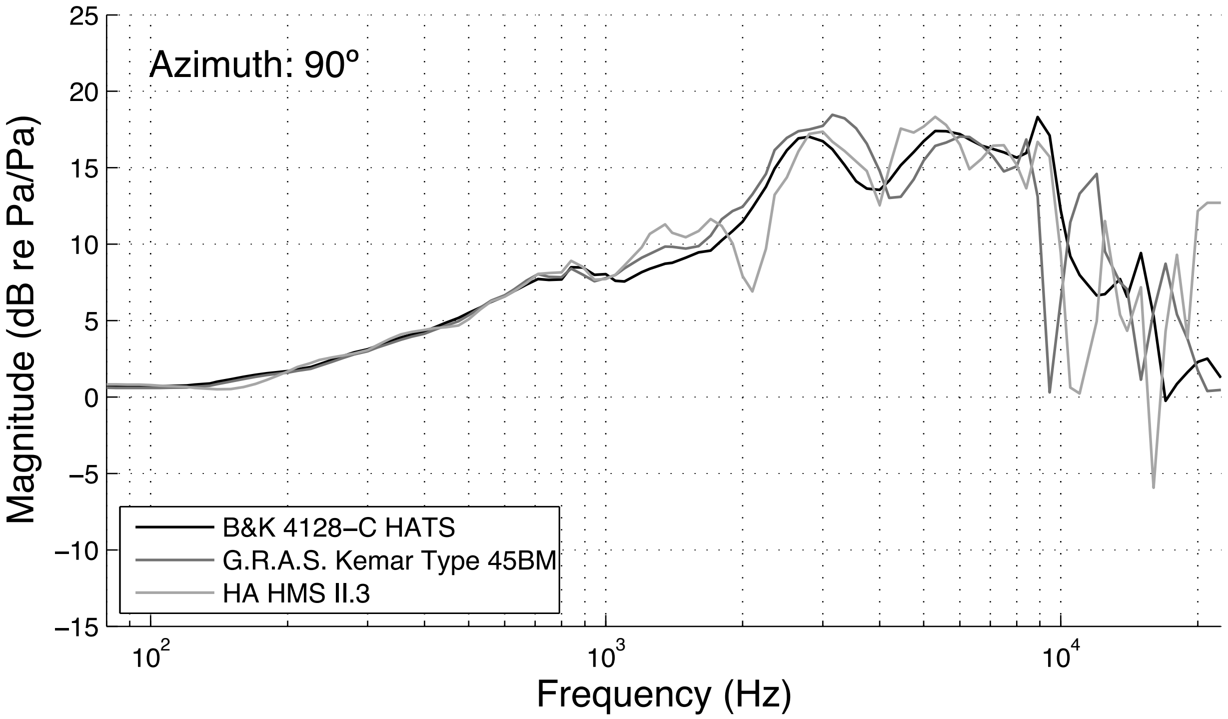

Figure 38: *Free-field HRTF of all HATS at 90° azimuth. Left ear is presented.*

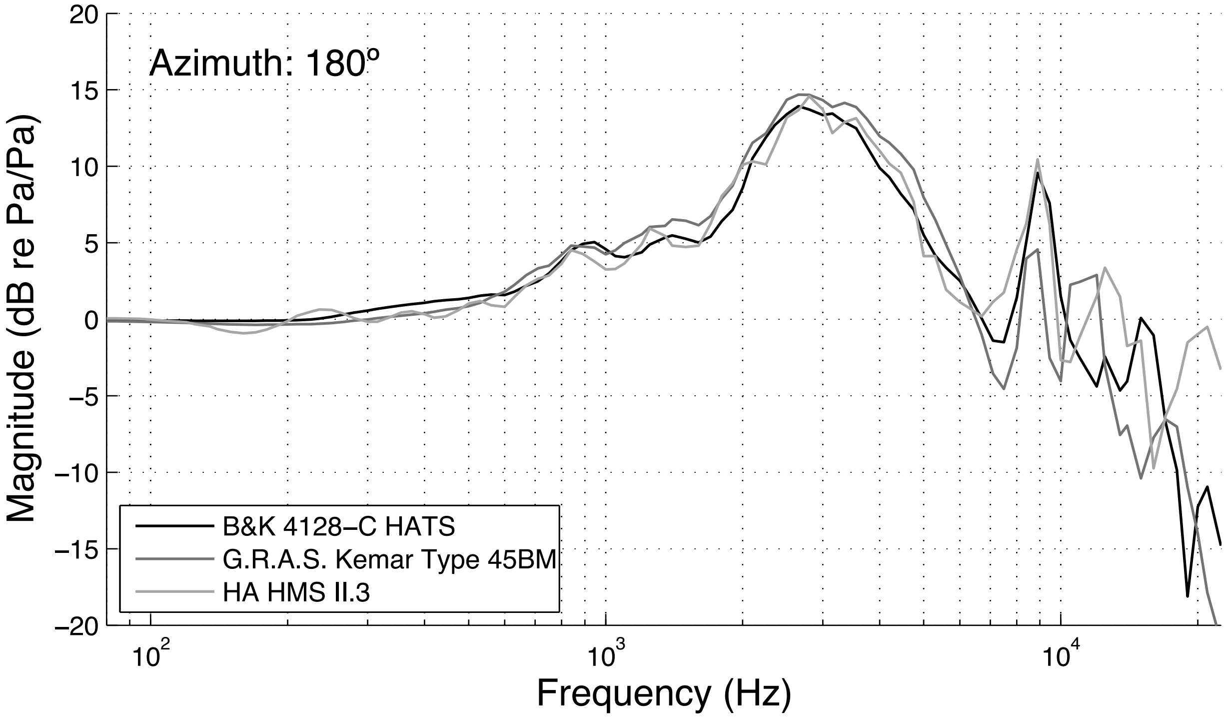

Figure 39: *Free-field HRTF of all HATS at 180° azimuth. Left ear is presented.*

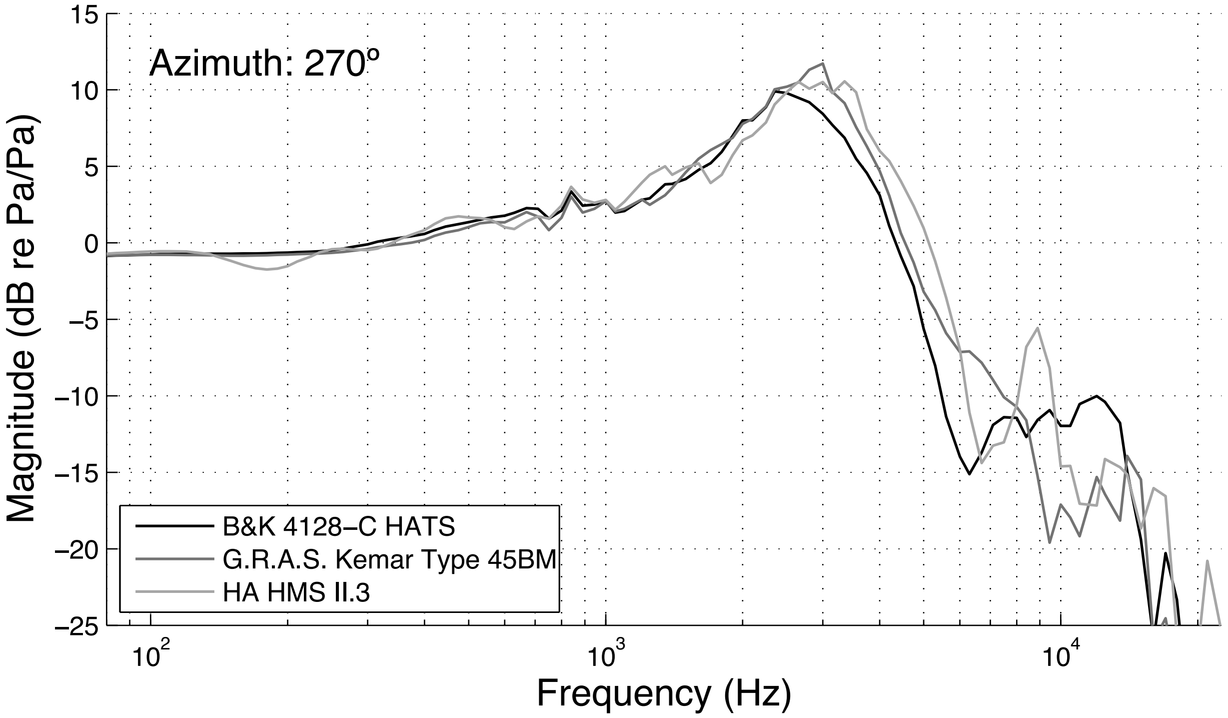

Figure 40: *Free-field HRTF of all HATS at 270° azimuth. Left ear is presented.*

5.3 Pictures of the setup

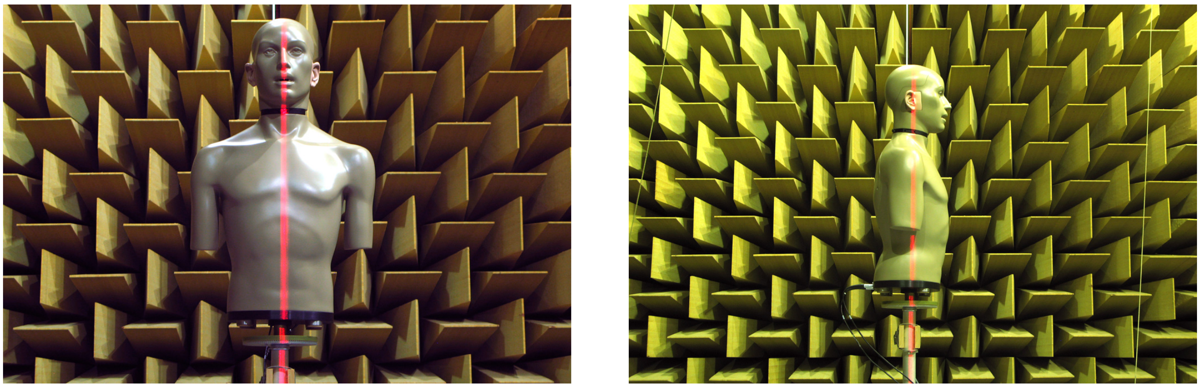

Figure 41: *The G.R.A.S. KEMAR here, is shown in the anechoic chamber, along with the line laser that helped with positioning.*

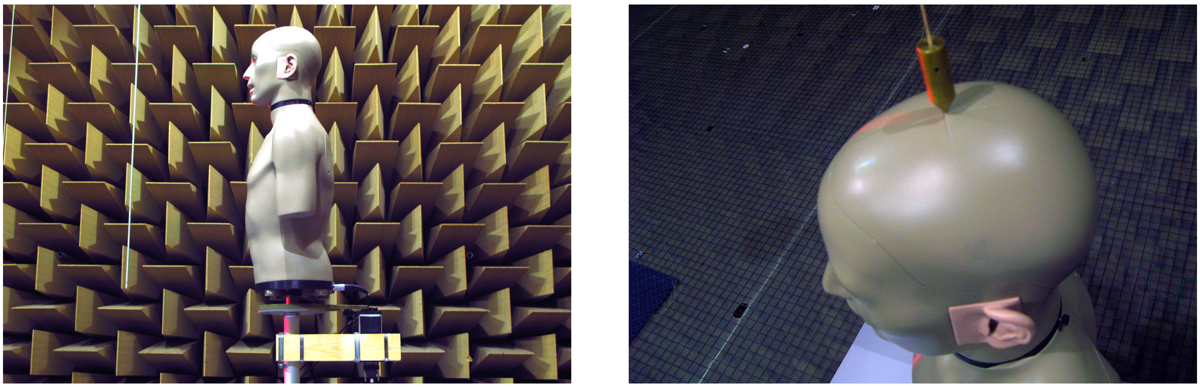

Figure 42: *On the left is shown how the motor was attached to the pole, and driving the rotation with a belt. On the right, the plumb line is pointing at the center of head to ensure that the manikin rotated along a vertical axis.*

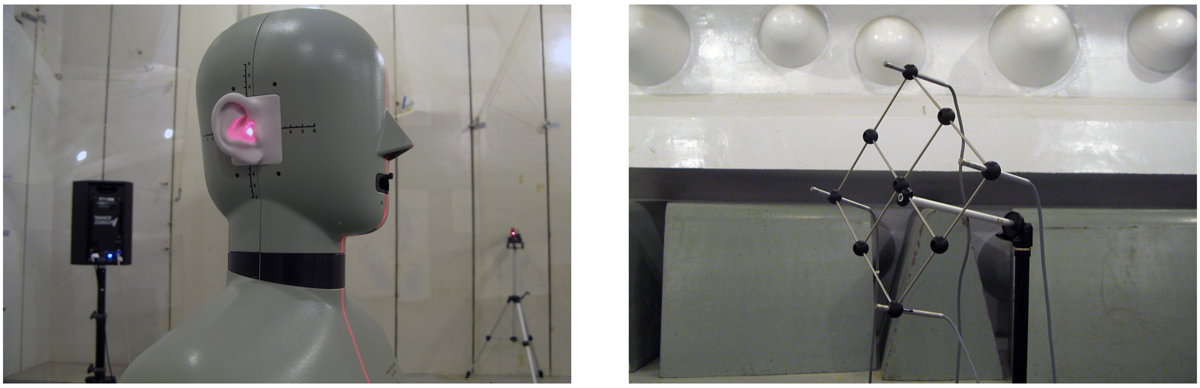

Figure 43: *The setup in the reverberation chamber is shown on the left picture, along with the Brüel & Kjær Type 4128-C, the loudspeaker and lasers that helped with positioning. The microphone array to measure the sound field is shown on the right.*

Figure 44: *From left to right, Brüel & Kjær Type 4128-C, Head Acoustics HMS II.3 and G.R.A.S. KEMAR Type 45BM*

Figure 45: *Right and left pinnae from Brüel & Kjær Type 4128-C HATS. Type numbers are DZ-9769 and DZ-9770 respectively.*

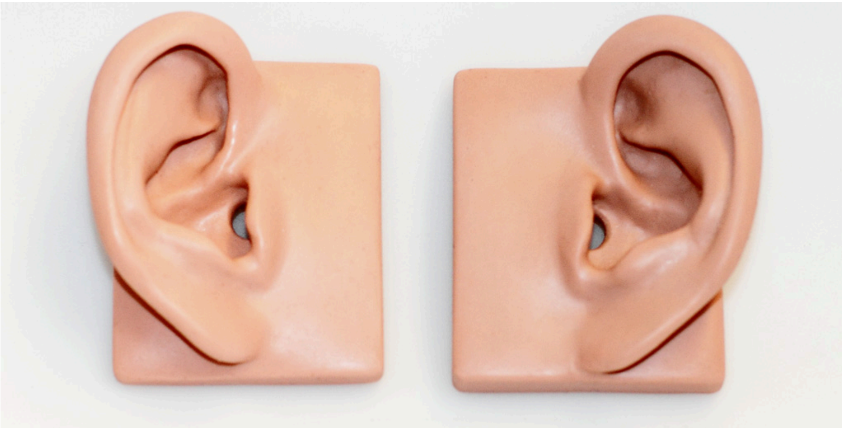

Figure 46: *Right and left pinnae from G.R.A.S. KEMAR Type 45BM. Type numbers are KB0065 and KB0066 respectively.*

Figure 47: *Right and left pinnae from Head Acoustics HMS II.3. Right/Left Pinna according to ITU-T P.57 Type 3.3, anatomically shaped.*

5.4 Tables for free-field measurement results

Results are shown from the sine sweep method, in 1/12th octave bands.

Freq. (Hz)	Ampli. (dB)	Freq. (Hz)	Ampli. (dB)	Freq. (Hz)	Ampli. (dB)
100	-0.03	600	2.42	3550	15.67
105	-0.03	630	2.53	3750	14.92
110	-0.04	670	2.66	4000	13.95
120	-0.04	710	2.86	4200	12.75
125	-0.05	750	3.28	4450	11.72
135	-0.06	800	3.74	4750	10.72
140	-0.07	840	4.46	5000	10.09
150	-0.07	890	4.95	5300	9.60
160	-0.07	945	5.03	5600	8.76
170	-0.06	1000	4.61	6000	7.89
180	-0.05	1050	4.21	6300	7.04
190	-0.04	1100	3.68	6700	5.73
200	-0.02	1200	3.71	7100	4.15
210	0.01	1250	3.65	7500	1.16
225	0.05	1350	4.15	8000	-1.82
235	0.11	1400	4.67	8400	-2.28
250	0.21	1500	4.92	8900	1.02
265	0.31	1600	4.57	9450	3.54
280	0.43	1700	5.34	10000	3.68
300	0.55	1800	7.14	10500	5.20
315	0.72	1900	8.93	11000	8.17
335	0.92	2000	10.48	12000	9.34
355	1.10	2100	12.05	12500	8.47
375	1.26	2250	14.09	13500	8.15
400	1.42	2350	15.48	14000	8.13
420	1.61	2500	15.73	15000	7.93
445	1.80	2650	16.39	16000	2.02
475	1.95	2800	16.74	17000	-3.57
500	2.09	3000	16.21	18000	-1.70
530	2.26	3150	16.26	19000	-4.29
560	2.38	3350	15.89	20000	-3.92

Table 1: *HRTF at 0° azimuth angle, left ear - Brüel & Kjær Type 4128 HATS*

Freq. (Hz)	Ampli. (dB)	Freq. (Hz)	Ampli. (dB)	Freq. (Hz)	Ampli. (dB)
100	0.70	600	6.58	3550	14.11
105	0.71	630	6.93	3750	13.63
110	0.73	670	7.35	4000	13.55
120	0.75	710	7.72	4200	14.17
125	0.81	750	7.66	4450	15.16
135	0.89	800	7.69	4750	16.03
140	1.00	840	8.49	5000	16.73
150	1.16	890	8.47	5300	17.40
160	1.32	945	7.99	5600	17.39
170	1.46	1000	8.04	6000	17.20
180	1.56	1050	7.60	6300	16.85
190	1.63	1100	7.57	6700	16.44
200	1.70	1200	8.17	7100	16.23
210	1.81	1250	8.39	7500	16.01
225	1.96	1350	8.73	8000	15.66
235	2.16	1400	8.77	8400	15.96
250	2.43	1500	9.11	8900	18.31
265	2.69	1600	9.46	9450	17.12
280	2.92	1700	9.58	10000	12.22
300	3.12	1800	10.25	10500	9.22
315	3.35	1900	10.85	11000	7.97
335	3.63	2000	11.47	12000	6.65
355	3.90	2100	12.38	12500	6.73
375	4.10	2250	13.76	13500	7.73
400	4.30	2350	14.95	14000	6.56
420	4.55	2500	16.14	15000	9.42
445	4.86	2650	16.92	16000	5.31
475	5.18	2800	17.03	17000	-0.25
500	5.51	3000	16.74	18000	0.85
530	5.86	3150	16.21	19000	1.63
560	6.22	3350	15.17	20000	2.30

Table 2: *HRTF at 90° azimuth angle, left ear - Brüel & Kjær Type 4128 HATS*

Freq. (Hz)	Ampli. (dB)	Freq. (Hz)	Ampli. (dB)	Freq. (Hz)	Ampli. (dB)
100	-0.08	600	1.58	3550	12.49
105	-0.08	630	1.81	3750	11.30
110	-0.09	670	2.19	4000	9.89
120	-0.09	710	2.48	4200	9.29
125	-0.10	750	3.00	4450	8.19
135	-0.10	800	3.82	4750	7.16
140	-0.11	840	4.51	5000	5.51
150	-0.11	890	4.92	5300	4.18
160	-0.10	945	5.05	5600	3.38
170	-0.10	1000	4.57	6000	2.52
180	-0.09	1050	4.13	6300	1.54
190	-0.09	1100	4.06	6700	0.06
200	-0.08	1200	4.37	7100	-1.39
210	-0.06	1250	4.89	7500	-1.50
225	-0.02	1350	5.34	8000	1.40
235	0.05	1400	5.48	8400	5.07
250	0.16	1500	5.26	8900	9.57
265	0.30	1600	5.02	9450	7.58
280	0.44	1700	5.40	10000	1.51
300	0.56	1800	6.41	10500	-1.36
315	0.68	1900	7.16	11000	-2.50
335	0.80	2000	8.57	12000	-4.40
355	0.90	2100	10.51	12500	-2.44
375	0.99	2250	11.90	13500	-4.66
400	1.08	2350	12.69	14000	-4.06
420	1.17	2500	13.41	15000	0.08
445	1.25	2650	13.94	16000	-1.05
475	1.30	2800	13.72	17000	-6.74
500	1.39	3000	13.35	18000	-9.86
530	1.54	3150	13.45	19000	-18.12
560	1.61	3350	12.89	20000	-12.25

Table 3: *HRTF at 180° azimuth angle, left ear - Brüel & Kjær Type 4128 HATS*

Freq. (Hz)	Ampli. (dB)	Freq. (Hz)	Ampli. (dB)	Freq. (Hz)	Ampli. (dB)
100	-0.76	600	1.77	3550	5.50
105	-0.74	630	1.96	3750	4.56
110	-0.73	670	2.26	4000	3.11
120	-0.72	710	2.22	4200	1.10
125	-0.72	750	1.59	4450	-0.86
135	-0.71	800	2.11	4750	-2.84
140	-0.71	840	3.36	5000	-5.63
150	-0.71	890	2.42	5300	-8.03
160	-0.70	945	2.51	5600	-11.35
170	-0.69	1000	2.74	6000	-13.97
180	-0.68	1050	1.98	6300	-15.12
190	-0.66	1100	2.08	6700	-13.71
200	-0.64	1200	2.80	7100	-11.90
210	-0.61	1250	2.91	7500	-11.40
225	-0.58	1350	3.83	8000	-11.44
235	-0.54	1400	3.86	8400	-12.69
250	-0.47	1500	4.17	8900	-11.57
265	-0.37	1600	4.77	9450	-10.93
280	-0.24	1700	5.20	10000	-11.96
300	-0.10	1800	5.94	10500	-11.97
315	0.07	1900	7.00	11000	-10.54
335	0.23	2000	8.00	12000	-10.02
355	0.34	2100	8.01	12500	-10.39
375	0.43	2250	8.87	13500	-11.77
400	0.59	2350	9.90	14000	-14.92
420	0.83	2500	9.79	15000	-19.39
445	1.07	2650	9.48	16000	-25.98
475	1.23	2800	9.20	17000	-20.28
500	1.36	3000	8.43	18000	-23.32
530	1.51	3150	7.71	19000	-30.13
560	1.66	3350	6.87	20000	-28.83

Table 4: *HRTF at 270° azimuth angle, left ear - Brüel & Kjær Type 4128 HATS*

Freq. (Hz)	Ampli. (dB)	Freq. (Hz)	Ampli. (dB)	Freq. (Hz)	Ampli. (dB)
100	-0.06	600	2.79	3550	16.39
105	-0.08	630	3.06	3750	15.93
110	-0.09	670	3.33	4000	15.60
120	-0.10	710	3.39	4200	15.20
125	-0.12	750	3.50	4450	14.46
135	-0.13	800	3.84	4750	13.25
140	-0.13	840	4.05	5000	11.81
150	-0.12	890	4.02	5300	10.78
160	-0.10	945	3.85	5600	9.28
170	-0.06	1000	3.54	6000	7.76
180	-0.03	1050	3.41	6300	6.18
190	0.00	1100	3.45	6700	4.38
200	0.03	1200	3.90	7100	1.73
210	0.07	1250	3.84	7500	0.89
225	0.11	1350	3.53	8000	4.44
235	0.18	1400	3.15	8400	10.85
250	0.28	1500	3.31	8900	11.44
265	0.41	1600	4.68	9450	6.75
280	0.55	1700	6.63	10000	6.05
300	0.70	1800	8.60	10500	4.63
315	0.88	1900	10.79	11000	8.02
335	1.09	2000	12.80	12000	10.93
355	1.28	2100	14.66	12500	8.71
375	1.44	2250	16.59	13500	6.29
400	1.59	2350	18.19	14000	7.85
420	1.78	2500	18.98	15000	7.66
445	1.94	2650	19.07	16000	2.11
475	2.06	2800	18.76	17000	-1.15
500	2.19	3000	18.43	18000	2.01
530	2.41	3150	17.51	19000	-0.24
560	2.62	3350	16.71	20000	-7.82

Table 5: *HRTF at 0° azimuth angle, left ear - G.R.A.S. KEMAR Type 45BM*

Freq. (Hz)	Ampli. (dB)	Freq. (Hz)	Ampli. (dB)	Freq. (Hz)	Ampli. (dB)
100	0.59	600	6.66	3550	17.57
105	0.60	630	7.06	3750	16.58
110	0.61	670	7.62	4000	14.79
120	0.63	710	8.04	4200	13.03
125	0.67	750	7.87	4450	13.09
135	0.74	800	7.83	4750	14.23
140	0.85	840	8.40	5000	15.48
150	1.01	890	8.00	5300	16.43
160	1.18	945	7.57	5600	16.65
170	1.32	1000	7.78	6000	17.04
180	1.44	1050	7.98	6300	17.01
190	1.53	1100	8.41	6700	16.46
200	1.60	1200	9.11	7100	15.73
210	1.71	1250	9.37	7500	14.76
225	1.85	1350	9.85	8000	15.10
235	2.03	1400	9.82	8400	16.85
250	2.29	1500	9.71	8900	13.12
265	2.55	1600	9.87	9450	0.31
280	2.79	1700	10.56	10000	6.34
300	3.00	1800	11.63	10500	11.42
315	3.23	1900	12.16	11000	13.30
335	3.51	2000	12.45	12000	14.60
355	3.76	2100	13.26	12500	9.52
375	3.95	2250	14.59	13500	7.50
400	4.14	2350	16.16	14000	7.05
420	4.39	2500	16.95	15000	1.13
445	4.66	2650	17.39	16000	5.61
475	4.96	2800	17.50	17000	8.72
500	5.36	3000	17.74	18000	5.41
530	5.85	3150	18.47	19000	3.80
560	6.31	3350	18.23	20000	1.75

Table 6: *HRTF at 90° azimuth angle, left ear - G.R.A.S. KEMAR Type 45BM*

Freq. (Hz)	Ampli. (dB)	Freq. (Hz)	Ampli. (dB)	Freq. (Hz)	Ampli. (dB)
100	-0.17	600	1.80	3550	13.87
105	-0.19	630	2.24	3750	13.11
110	-0.21	670	2.90	4000	11.96
120	-0.23	710	3.32	4200	11.55
125	-0.26	750	3.50	4450	10.82
135	-0.28	800	4.21	4750	9.78
140	-0.31	840	4.81	5000	7.97
150	-0.34	890	4.76	5300	6.51
160	-0.36	945	4.69	5600	4.88
170	-0.36	1000	4.24	6000	2.85
180	-0.35	1050	4.51	6300	1.11
190	-0.34	1100	4.99	6700	-1.00
200	-0.34	1200	5.56	7100	-3.54
210	-0.33	1250	6.03	7500	-4.55
225	-0.31	1350	6.10	8000	-1.88
235	-0.29	1400	6.52	8400	3.96
250	-0.24	1500	6.44	8900	4.56
265	-0.17	1600	6.15	9450	-2.53
280	-0.09	1700	6.75	10000	-4.05
300	-0.01	1800	7.88	10500	2.25
315	0.07	1900	8.73	11000	2.45
335	0.16	2000	10.28	12000	2.90
355	0.24	2100	11.53	12500	-3.03
375	0.31	2250	12.16	13500	-7.56
400	0.39	2350	13.08	14000	-6.95
420	0.50	2500	14.36	15000	-10.40
445	0.62	2650	14.69	16000	-7.74
475	0.73	2800	14.68	17000	-6.54
500	0.85	3000	14.33	18000	-7.02
530	1.08	3150	13.87	19000	-10.99
560	1.44	3350	14.14	20000	-14.02

Table 7: *HRTF at 180° azimuth angle, left ear - G.R.A.S. KEMAR Type 45BM*

Freq. (Hz)	Ampli. (dB)	Freq. (Hz)	Ampli. (dB)	Freq. (Hz)	Ampli. (dB)
100	-0.79	600	1.34	3550	7.56
105	-0.79	630	1.63	3750	6.32
110	-0.79	670	2.01	4000	4.70
120	-0.79	710	1.72	4200	3.09
125	-0.80	750	0.83	4450	0.64
135	-0.82	800	1.65	4750	-1.30
140	-0.83	840	3.03	5000	-3.20
150	-0.84	890	1.98	5300	-4.40
160	-0.84	945	2.22	5600	-5.90
170	-0.83	1000	2.72	6000	-7.14
180	-0.81	1050	2.06	6300	-7.09
190	-0.79	1100	2.22	6700	-7.84
200	-0.76	1200	2.84	7100	-8.95
210	-0.74	1250	2.49	7500	-10.09
225	-0.72	1350	3.12	8000	-10.73
235	-0.69	1400	3.60	8400	-11.60
250	-0.65	1500	4.62	8900	-15.26
265	-0.59	1600	5.50	9450	-19.60
280	-0.50	1700	6.06	10000	-17.11
300	-0.41	1800	6.46	10500	-17.96
315	-0.29	1900	6.86	11000	-19.18
335	-0.17	2000	7.78	12000	-15.30
355	-0.08	2100	8.10	12500	-16.43
375	0.02	2250	8.92	13500	-18.16
400	0.20	2350	10.03	14000	-13.93
420	0.45	2500	10.22	15000	-15.46
445	0.67	2650	10.48	16000	-26.02
475	0.83	2800	11.31	17000	-24.54
500	1.03	3000	11.73	18000	-28.36
530	1.28	3150	9.88	19000	-36.65
560	1.36	3350	9.14	20000	-32.72

Table 8: *HRTF at 270° azimuth angle, left ear - G.R.A.S. KEMAR Type 45BM*

Freq. (Hz)	Ampli. (dB)	Freq. (Hz)	Ampli. (dB)	Freq. (Hz)	Ampli. (dB)
100	0.16	600	2.81	3550	15.18
105	0.15	630	2.87	3750	13.48
110	0.12	670	3.19	4000	13.25
120	0.09	710	4.02	4200	13.33
125	0.01	750	4.17	4450	13.66
135	-0.09	800	4.11	4750	13.69
140	-0.23	840	5.16	5000	12.19
150	-0.45	890	5.56	5300	11.69
160	-0.66	945	5.56	5600	10.06
170	-0.81	1000	4.73	6000	7.82
180	-0.88	1050	3.70	6300	6.26
190	-0.87	1100	2.15	6700	4.25
200	-0.79	1200	1.76	7100	0.75
210	-0.64	1250	0.99	7500	-1.93
225	-0.44	1350	1.00	8000	0.15
235	-0.23	1400	-0.01	8400	4.73
250	0.02	1500	2.56	8900	9.92
265	0.25	1600	5.07	9450	4.59
280	0.48	1700	5.62	10000	-0.37
300	0.77	1800	7.65	10500	4.05
315	1.17	1900	10.36	11000	5.71
335	1.65	2000	12.28	12000	9.02
355	1.99	2100	13.30	12500	10.73
375	2.13	2250	13.73	13500	9.11
400	2.15	2350	13.56	14000	9.60
420	2.31	2500	14.03	15000	10.00
445	2.75	2650	17.20	16000	7.78
475	3.18	2800	18.73	17000	0.67
500	3.29	3000	17.66	18000	-1.66
530	3.01	3150	17.35	19000	-12.74
560	2.74	3350	17.38	20000	-4.13

Table 9: *HRTF at 0° azimuth angle, left ear - Head Acoustics HMS II.3*

Freq. (Hz)	Ampli. (dB)	Freq. (Hz)	Ampli. (dB)	Freq. (Hz)	Ampli. (dB)
100	0.78	600	6.58	3550	15.40
105	0.74	630	6.94	3750	14.79
110	0.71	670	7.46	4000	12.56
120	0.67	710	8.05	4200	14.98
125	0.60	750	8.11	4450	17.57
135	0.54	800	8.16	4750	17.31
140	0.51	840	8.91	5000	17.70
150	0.53	890	8.52	5300	18.33
160	0.65	945	7.68	5600	17.80
170	0.86	1000	7.72	6000	16.51
180	1.12	1050	7.99	6300	14.90
190	1.40	1100	8.60	6700	15.58
200	1.66	1200	9.80	7100	16.44
210	1.97	1250	10.68	7500	16.47
225	2.23	1350	11.30	8000	15.18
235	2.43	1400	10.74	8400	13.65
250	2.59	1500	10.46	8900	16.68
265	2.71	1600	10.85	9450	15.72
280	2.85	1700	11.64	10000	9.44
300	3.06	1800	11.20	10500	0.62
315	3.40	1900	10.05	11000	0.24
335	3.79	2000	7.90	12000	4.96
355	4.09	2100	6.91	12500	11.52
375	4.27	2250	9.69	13500	5.38
400	4.39	2350	13.23	14000	4.33
420	4.50	2500	14.37	15000	7.18
445	4.57	2650	16.07	16000	-5.94
475	4.68	2800	17.22	17000	4.30
500	5.09	3000	17.36	18000	9.30
530	5.73	3150	16.70	19000	3.87
560	6.25	3350	16.09	20000	12.17

Table 10: *HRTF at 90° azimuth angle, left ear - Head Acoustics HMS II.3*

Freq. (Hz)	Ampli. (dB)	Freq. (Hz)	Ampli. (dB)	Freq. (Hz)	Ampli. (dB)
100	-0.02	600	0.81	3550	13.14
105	-0.07	630	1.46	3750	12.04
110	-0.12	670	2.23	4000	11.00
120	-0.19	710	2.65	4200	10.18
125	-0.32	750	2.86	4450	9.57
135	-0.47	800	3.63	4750	7.68
140	-0.64	840	4.52	5000	4.13
150	-0.83	890	4.27	5300	4.13
160	-0.91	945	3.78	5600	1.93
170	-0.86	1000	3.25	6000	1.12
180	-0.67	1050	3.28	6300	0.72
190	-0.41	1100	3.64	6700	0.18
200	-0.12	1200	4.91	7100	1.13
210	0.23	1250	5.94	7500	1.75
225	0.50	1350	5.46	8000	4.55
235	0.64	1400	4.81	8400	6.26
250	0.62	1500	4.73	8900	10.45
265	0.39	1600	4.81	9450	6.19
280	0.07	1700	6.25	10000	-2.67
300	-0.17	1800	8.06	10500	-2.80
315	-0.16	1900	8.88	11000	-1.16
335	0.13	2000	10.08	12000	1.50
355	0.44	2100	10.33	12500	3.37
375	0.52	2250	10.12	13500	1.47
400	0.33	2350	11.35	14000	-1.75
420	0.11	2500	13.19	15000	-1.40
445	0.19	2650	13.67	16000	-9.75
475	0.59	2800	14.58	17000	-6.30
500	1.04	3000	13.71	18000	-4.54
530	1.19	3150	12.17	19000	-1.52
560	0.92	3350	12.88	20000	-0.97

Table 11: *HRTF at 180° azimuth angle, left ear - Head Acoustics HMS II.3*

Freq. (Hz)	Ampli. (dB)	Freq. (Hz)	Ampli. (dB)	Freq. (Hz)	Ampli. (dB)
100	-0.57	600	1.02	3550	9.85
105	-0.55	630	0.91	3750	7.43
110	-0.55	670	1.40	4000	6.01
120	-0.57	710	1.73	4200	5.35
125	-0.63	750	1.58	4450	4.04
135	-0.73	800	2.45	4750	2.42
140	-0.90	840	3.67	5000	0.97
150	-1.17	890	2.84	5300	-1.20
160	-1.45	945	2.62	5600	-3.58
170	-1.66	1000	2.81	6000	-6.96
180	-1.74	1050	2.16	6300	-11.09
190	-1.69	1100	2.70	6700	-14.39
200	-1.52	1200	3.92	7100	-13.25
210	-1.23	1250	4.46	7500	-13.05
225	-0.90	1350	5.01	8000	-10.58
235	-0.62	1400	4.45	8400	-6.80
250	-0.42	1500	4.94	8900	-5.56
265	-0.38	1600	5.19	9450	-8.18
280	-0.44	1700	3.92	10000	-14.61
300	-0.48	1800	4.45	10500	-14.58
315	-0.37	1900	5.73	11000	-17.05
335	-0.07	2000	6.70	12000	-17.17
355	0.27	2100	7.03	12500	-14.13
375	0.54	2250	7.86	13500	-14.67
400	0.83	2350	9.04	14000	-15.13
420	1.23	2500	9.86	15000	-18.67
445	1.60	2650	10.53	16000	-16.03
475	1.73	2800	10.07	17000	-16.56
500	1.66	3000	10.51	18000	-25.76
530	1.61	3150	9.79	19000	-33.09
560	1.49	3350	10.55	20000	-26.66

Table 12: *HRTF at 270° azimuth angle, left ear - Head Acoustics HMS II.3*

Value tables from noise measurements in the diffuse field, shown as 1/3th octave bands.

Freq. (Hz)	Ampli. (dB)
100	-0.49
125	-0.28
160	0.24
200	0.41
250	0.08
315	0.70
400	1.44
500	1.76
630	3.35
800	3.46
1000	4.13
1250	5.12
1600	7.36
2000	10.70
2500	13.66
3150	13.82
4000	11.88
5000	9.14
6300	7.01
8000	6.46
10000	6.23
12500	2.24
16000	0.04
20000	-7.10

Freq. (Hz)	Ampli. (dB)
100	-0.34
125	-0.13
160	0.33
200	0.63
250	0.24
315	0.90
400	1.71
500	2.06
630	3.54
800	3.47
1000	4.34
1250	5.48
1600	7.47
2000	11.16
2500	14.95
3150	15.61
4000	13.33
5000	10.45
6300	8.88
8000	8.19
10000	4.29
12500	2.20
16000	-3.00
20000	-5.13

Freq. (Hz)	Ampli. (dB)
100	-0.47
125	-0.23
160	-0.32
200	-0.12
250	0.03
315	0.17
400	1.08
500	2.03
630	3.08
800	3.06
1000	3.23
1250	4.68
1600	6.43
2000	9.79
2500	13.97
3150	14.10
4000	11.63
5000	9.39
6300	7.89
8000	8.65
10000	3.82
12500	2.36
16000	1.42
20000	-0.09

Table 13: *Measurements in the diffuse field, shown as 1/3th octave bands, right ear - Brüel & Kjær Type 4128 HATS, G.R.A.S. KEMAR Type 45BM and Head Acoustics HMS II.3 respectively*

References

[1] IEC/TS 60318-7 Ed. 1.0 / Electroacoustics - Simulators of human head and ear - Part 7: Head and torso simulator for acoustic measurements of air-conduction hearing aids" (Revision of IEC/TR 60959:1990).

[2] CEI IEC 959 First edition / Provisional head and torso simulator for acoustic measurements on air conduction hearing aids. Technical report, IEC, 4 1990.

[3] ISO-4869-1 / Acoustics – Hearing Protectors – Part 1: Subjective method for the measurement of sound attenuation, 12 1990.

[4] A. Farina. Simultaneous measurement of impulse response and distortion with a swept-sine technique. Journal of the Audio Engineering Society, 108th AES Convention, Paris, preprint 5093, 48:350, 2000.

[5] D. Hammershøi, H. Møller. Sound transmission to and within the human ear canal. Journal of the Acoustical Society of America, 100:408–427, 1996.

[6] F. Ingerslev, O.J. Pedersen, P.K. Møller and J. Kristensen. New rooms for acoustic measurements at the Danish Technical University. Acustica, 19:185–199, 1968.

[7] H. Møller. Fundamentals of binaural technology. Applied Acoustics, 36:171–218, 1992.

[8] ITU-T. Recommendation P.58 / Series P: Telephone Transmission Quality / Objective measuring apparatus / Head and Torso simulator for telephonometry.

[9] S. Müller, P. Massarani. Transfer-function measurement with sweeps. Journal of the Audio Engineering Society, 49:443–471, 2001.